NTNU – Trondheim
Norwegian University of
Science and Technology

Marine Cybernetics Vessel CS Saucer:

Design, construction and control

Tor Kvestad Idland

Master of Science in Engineering and ICT
Submission date: June 2015
Supervisor: Roger Skjetne, IMT
Co-supervisor: Andreas Reason Dahl, IMT

Norwegian University of Science and Technology
Department of Marine Technology

NTNU Trondheim
Norwegian University of Science and Technology
Department of Marine Technology

PROJECT DESCRIPTION SHEET

Name of the candidate: Tor Kvestad Idland

Field of study: Marine control engineering

Thesis title (Norwegian): Design, bygging, og automatisk styring av marine cybership "C/S Saucer".

Thesis title (English): Design, construction, and control of marine cybership "C/S Saucer"

Background
Components have been acquired to build a highly maneuverable and robust marine model vehicle in the NTNU Marine Cybernetics Laboratory (MC-Lab), to be called the "C/S Saucer". The intention is to develop a lab platform for students to be able to design, implement, and test a variety of nonlinear control algorithms on a marine surface-based platform highly affected by hydrodynamic loads.

The objective of this MSc project is to design and build the vehicle together with its control system, having the main basic functionality of necessary signal communication, a user interface, and basic manual control modes. In addition, the control design and simulation models, both HIL and non-HIL, should be established.

Work description
1) Perform a literature review, providing relevant references on:
   - Guidance and control of ocean vehicles.
   - Real-time control system software and hardware, in particular NI LabView and VeriStand, cRIO and myRIO.
   - Reports for control of cybership C/S Enterprise I, Cybership II, and Cybership III.

   Write a list with abbreviations and definitions of terms and concepts, explaining relevant concepts.

2) Design and construct the cybership "C/S Saucer" model, supervised by PhD cand. Andreas R. Dahl:
   - The design should account for different payloads.
   - Explain decisions with regards to hull form {kinematic, hydrostatic, hydrodynamic), component layout, etc.
   - Once the design is approved by your supervisor, construct the vessel. Document each construction step.

3) Present a control design model for C/S Saucer and establish its model parameters.
   - Perform system identification with tow-tank testing or some other sufficient method. Discuss the model with respect to intended hydrostatic and hydrodynamic properties.

4) Prepare the myRIO embedded controller for Hardware-in-The-Loop (HIL) simulation implementation. Develop and propose a suitable simulation model of the vessel.

5) Develop a guidance and control system for the cybership:
   - Interfacing IO for all relevant command and feedback signals.
   - Low-level control, such as individual thruster control or thruster mapping, and thrust allocation.
   - A user interface in LabView.
   - A manual thruster control mode.
   - A joystick control mode.

6) Propose a set of test cases for the different manual control modes and perform Matlab/Simulink simulations for the control system to verify correct behavior of the vehicle. Repeat then the test cases with HIL simulation or experimental trials and discuss the resulting responses.

7) Design a high-level dynamic positioning control algorithm, including necessary guidance functions. Experimentally test the closed-loop DP control system.

Tentatively:

8) Design a tentative path-following controller by use of waypoints. Design a user interface with functionality for waypoint selection and mission planning and deployment.

Guidelines

The scope of work may prove to be larger than initially anticipated. By the approval from the supervisor, described topics may be deleted or reduced in extent without consequences with regard to grading.

The candidate shall present his personal contribution to the resolution of problems within the scope of work. Theories and conclusions should be based on mathematical derivations and logic reasoning identifying the various steps in the deduction.

The report shall be organized in a rational manner to give a clear exposition of results, assessments, and conclusions. The text should be brief and to the point, with a clear language. The report shall be written in English (preferably US) and contain the following elements: Abstract, acknowledgements, table of contents, main body, conclusions with recommendations for further work, list of symbols and acronyms, references, and optional appendices. All figures, tables, and equations shall be numerated. The original contribution of the candidate and material taken from other sources shall be clearly identified. Work from other sources shall be properly acknowledged using quotations and a Harvard citation style (e.g. *natbib* Latex package). The work is expected to be conducted in an honest and ethical manner, without any sort of plagiarism and misconduct. Such practice is taken very seriously by the university and will have consequences. NTNU can use the results freely in research and teaching by proper referencing, unless otherwise agreed upon.

The thesis shall be submitted with a printed and electronic copy to 1) the main supervisor and 2) the external examiner, each copy signed by the candidate. The final revised version of this thesis description must be included. The report must appear in a bound volume or a binder according to the NTNU standard template. Computer code, pictures, videos, data series, and a PDF version of the report shall be included electronically.

Start date: 14 January 2015 **Due date:** As specified by the administration.

Supervisor: Prof. Roger Skjetne

Co-advisor: PhD candidate Andreas Reason Dahl.

_____

Roger Skjetne
Supervisor

Abstract

This thesis presents the design, construction and control systems development of the marine cybernetics vessel CS Saucer. CS Saucer is a fully actuated and highly controllable vessel with a spherically shaped hull, much like a flying saucer. The vessel is fitted with three azimuth thrusters which are driven by three Torpedo 800 motors. The embedded controller myRIO from National Instruments is used to control the vessel. The system is powered by a three cell 11.1V Lithium Polymer battery.

The hull of the vessel is constructed from three millimeter MDF sheeting, milled Divinycell foam and a woven carbon sheet fitted to the exterior of the vessel with epoxy. This results in a rigid and watertight hull with a low draft. The vessel has a detachable lid made of plexi glass that is secured to the top of the vessel with four butterfly screws.

The drag forces acting on the vessel have been analyzed through testing in the Marine Cybernetics Laboratory (MC Lab) at NTNU. The results have been used to derive the parameters for a dynamic model used in Hardware-in-the-loop testing and for future model based control design. The forces produced by each of the thrusters have been mapped and approximated with linear curve fitting. This approximated force mapping has been used in the implemented thrust allocation with fixed thruster angles.

Manual thruster control and manual force control of the vessel can be operated by the application on the host computer or directly from the Dashboard app from National Instruments available on Android and iOS devices. A dynamic positioning system has been implemented on the CS Saucer and tested in the MC Lab. The dynamic positioning system performs as desired when changing the setpoint for the vessel position. A tentative path following controller has also been implemented and tested on the vessel.

The completed CS Saucer is a fully functioning vessel and a stable and expandable platform for use in future demonstrations, projects and research at the MC Lab.

Sammendrag

Denne masteroppgaven presenterer design, konstruksjon og kontrollsystemutvikling av den marinkybernetiske farkosten CS Saucer. CS Saucer er en fullaktuert og høyst manøvrerbar farkost med et skrog formet som bunnen av en skål. Farkosten er utsyrt med tre azimuth thrustere som drives av tre Torpedo 800 motorer. Controlleren myRIO fra National Instruments brukes til å styre systemet. Sytemet drives av et tre-cellet, 11.1 Volts Lithium Polymer batteri.

Skroget er konstruert fra tre mm tykk finerplate, utfreset Divinycell konstruksonsskum og en vevet karbonduk som har blitt lagt på utsiden av skroget og mettet med epoxy. Resultatet er et vanntett skrog med lav dypgang. Farkosten har et avtagbart lokk som festes på skroget ved hjelp av fire vingemuttere.

Drag-kreftene som virker på skroget har blitt identifisert gjennom testing i Marin Kybernetikk Laben (MC Lab) ved NTNU. Resultatene har blitt brukt til å bestemme parameterene i en dynamisk modell av farkosten. Denne modellen kan brukes i blant annet Hardware-in-the-loop (HIL) testing og i modellbaserte kontrollsystemer. Kreftene som produseres av hver av thrusterene har blitt kartlagt og estimert med en lineær funksjon. Denne estimerte kraft-kartleggingen har blitt brukt i den implementerte thrust-allokasjonen med faste thruster-vinkler.

Manuell thruster kontroll og manuell kraft kontroll kan bli styrt både fra brukergrensesnittes på vert-datamaskinen, og fra National Instruments sin Dashboard app som er tilgjengelig på Android of iOS enheter. Dynamisk posisjonering har blitt implementert på farkosten og testet i MC Laben med gode resultater. En tentativ stifølger-kontroller har også blitt implementert og testet.

CS Saucer er en fullt fungerende farkost og en stabil og utvidbar platform for videre bruk i demonstrasjoner, prosjekter og forskning ved MC Laben.

Acknowledgments

Thank you to my supervisor Professor Roger Skjetne for his guidance and for allowing the resources needed to complete this thesis.

Thank you to my co-supervisor PhD Candidate Andreas Reason Dahl for offering up so much of his time to guide me this semester. He has made himself available whenever I have had questions and has been a fantastic resource providing both knowledge and support during the work with this thesis.

Thank you to Jostein Follestad for his help creating a 3D model of CS Saucer, something that simplified the design process and made it possible to mill the main part of the hull directly from the 3D model.

Thank you to Knut Arne Hegstad and Ole Erik Vinje at MARINTEK for their assistance in the construction phase of this thesis. Knut Arne has been very generous in allowing me to use the many material and personal resources that are available at MARINTEK. Ole Erik Vinje has helped me with a lot of the practical aspects of constructing such a vessel, and his knowledge and help has been invaluable.

Thank you to Trond Innset for his help in milling the main part of the vessel hull from leftover Divinycell H60 foam at MARINTEK.

Thank you to Theis Westergård for taking the time to educate and give advise on the subject of carbon coating.

Thank you to Senior Engineer Torgeir Wahl for patiently answering all my questions on anything electronics-related. He has also been a great source of knowledge when working in the MC Lab and with National Instruments hardware and Software.

Thank you to Mauro Candeloro for giving me a crash course in LabVIEW user interface development.

Thank you to Kristian Klausen for his advise and help with much of the electronics, and especially for lending out voltage converters on a short notice.

Thank you to Sigurd Holsen for accompanying me in the MC Lab on late evenings in order to fulfill the Health and safety requirements and for his advice and input on control theory.

Thank you to Eirik Valle and Fredrik Sandved for their help with some of the many practical aspects of the MC Lab.

Contents

List of Figures

List of Tables

Nomenclature

NTNU - Norwegian University of Science and Technology

DOF - Degrees of Freedom

ESC - Electronic speed controller

GPS - Global Positioning System

HIL - Hardware-in-the-loop

NED - North-East-Down reference frame denoted by $\{n\}$

LOS - Line of Sight

PID - Proportional-Integral-Derivative

DP - Dynamic positioning

MARINTEK - Norsk Marinteknisk Forskningsinstitutt AS

RC - Radio control

PWM - Pulse width modulation

QTM - Qualisys Track Manager

MC Lab - Marine cybernetics laboratory

Part I

Introduction

Chapter 1

Motivation and Background

Marine control spans over just about every aspect of a vessel. Automating tasks on a vessel can serve many purposes. In addition to the cost saving argument, automation leads to increased precision in menial and monotonous tasks. Automating dangerous tasks reduces the risk that will be a factor when involving human workers directly. Power systems, vessel position and heading, ballast tanks and emergency systems are some of the many aspects of marine operations that are automated in the modern era.

The idea for an over actuated, omni directional vessel was inspired by a short video taken of a research project at the Olin College of Engineering in Massachusetts [Wee, 2012]. The non conventional shape of the hull of such a marine vessel opens the possibilities for original projects in control theory and hydrodynamics, as well as serving as a platform where student can get experience with the practical aspects of control systems implementation. The initial design idea and list of components was formed by employees at the Department of Marine Technology at NTNU. As the idea for the CS Saucer was not directly based on an existing model vessel, the components were chosen and ordered individually.

1.1 NTNU Cybership Fleet

The Cybership fleet at NTNU provides students and employees with a platform to experiment with new technology and control solutions on small scale ship models as it is an easy accessible testing platform. The fleet gives tangible results for both students and scientific employees to solidify their theoretical work.

The fleet of model vessels at NTNU started with Cybership I, a 1:70 scaled model of a supply vessel. The fleet has since grown with Cybership II (2001), also a 1:70 scaled supply vessel, and Cybership III, a larger 1:30 scale model of a supply vessel [Dong, 2005]. The prefix "Cybership" (CS) has since been added to all new vessels in the fleet. The three cyberships have served as a platform for a wide variety of dynamic positioning systems.

The vessel CS Enterprise I was constructed as a model ship available to master and PhD students at NTNU [Skåtun, 2011]. The work performed on CS Enterprise I include, but is not limited to, dynamic positioning systems, maneuvering systems and path following, and navigation with virtual reality [Valle, 2015].

The CyberRig is a semi submersible 1:100 scaled model drilling rig used in student projects and research [Bjørneset, 2014].

1.2 CS Saucer

The CS Saucer adds a new and unorthodox shape to the fleet of fleet of vessels that have traditionally been modeled after full size ships. The CS Saucer adds possibilities for rapid response and motion in surge and sway, something that is difficult to obtain with a traditional ship hull. This opens up a wide range of possibilities for future projects with possible control solutions such as coordinated operations with aerial vehicles, amongst other things.

Chapter 2

Thesis Contributions

The main contribution of this thesis is a functioning and well documented marine cybernetics vessel that can serve as a platform for future research and student projects at NTNU. A software solution which can easily be extended with new operational modes and control solutions will simplify control system development on CS Saucer. The software solution implemented only in LabVIEW ensures a robust application with less time spent on dependency complications between several connected software solutions.

This thesis presents a stepwise and well documented process for constructing, assembling, and controlling a model marine vessel.

Through system identification and estimation of parameters, a dynamic model of the vessel will be defined. This model can be used and modified in future projects for model based control design and Hardware-in-the-loop (HIL) simulations. The logic needed to run a HIL model on the embedded controller has been implemented so that future users can easily continue the work with HIL testing.

This thesis aims to provide a tentative handbook for all practical aspects of the use of CS Saucer. It is the vision of the author of this thesis that this handbook will be integrated in the "Handbook of Marine HIL simulation and Marine cybernetics laboratories" [NTNU, 2015], and improved in the future as the CS Saucer is used in research and projects.

A video documenting the work done in this thesis and also demonstrating

some of the capabilities of CS Saucer has been created. This video aims to give a brief summary of the design and construction process in addition to serving as an inspiration for people that have ideas for projects that can be done with CS Saucer. This video can also be used for recruitment purposes to show the more practical side of an education that is often associated with a lot of theoretical work. The video has been uploaded to vimeo.com [Idland, 2015].

Chapter 3

Thesis Structure

Part II presents the design and construction phase of the vessel. This includes a step by step description of the hull construction process, as well as a the thorough description of the hardware used in the vessel and the assembly process.

Part III presents the low level control development done on the vessel. This includes actuator calibration and mapping from control input to actuator signals. This part also presents the thrust allocation implemented on the vessel.

Part IV presents the system identification and simulation work done on the vessel. This includes moment of inertia and added mass estimation, a dynamic equations, identification of system parameters, thruster force mapping, and a propose HIL simulation model.

Part V presents the high level control implemented on the vessel. This includes dynamic positioning and path following.

Part VI presents the software developed and implemented in this thesis. This includes software developed and implemented on both the host computer and the embedded controller.

Part VII presents the conclusions made and suggested further work on the vessel.

Appendix A presents datasheets for the main components of the vessel.

Appendix B presents a tentative handbook for the practical use of the vessel at the MC Lab.

Appendix C presents the digital attachments to this thesis.

Appendix D presents the drawings exported from the 3D-model of the vessel.

Part II

Design and Construction

Chapter 4

Hull

The vessel CS Saucer is a circular vessel with a shape much like a flying saucer. It is designed to be light weight, agile and very responsive. This makes the vessel ideal for future planned projects at NTNU. CS Saucer has been designed with the use of National Instruments (NI) myRIO in mind. However, it is also capable of housing the NI compactRIO which has been used in several previous projects at NTNU. The myRIO and compactRIO are embedded hardware devices produced by National Instruments. They are used as embedded controllers in all the vessels in the Cybership fleet at NTNU.

The vessel hull consists of three main parts, the bottom plate, a foam ring made of Divinycell H60, and a top ring made out of the same MDF material as the bottom plate. The foam ring will be glued on to the bottom plate and the top ring will be glue on top of the foam ring. A woven carbon fiber sheet is attached to the outside of the hull with epoxy. This ensures a hull that is rigid and watertight. A lid made out of plexi glass is placed on top of the vessel and screwed tight to ensure that the vessel is watertight. The complete assembly drawing exported from the 3D model of the vessel can be found in Appendix D.

4.1 Bottom Plate

The bottom plate of CS Saucer is designed to accomedate two different payload cases with different embedded controllers. The myRIO and the compactRIO. Of the two payload cases, the case with the compactRIO is the largest and therefore the constraint that the hull must be designed according to. In Figure 4.1, the placement of the compactRIO is shown. The compactRIO is placed in the middle of the hull with the three thrusters and motors surrounding it. Each thruster with its motor is represented with a single rectangle in the figure. This is done because the motor must stand in line with the thruster when connected.

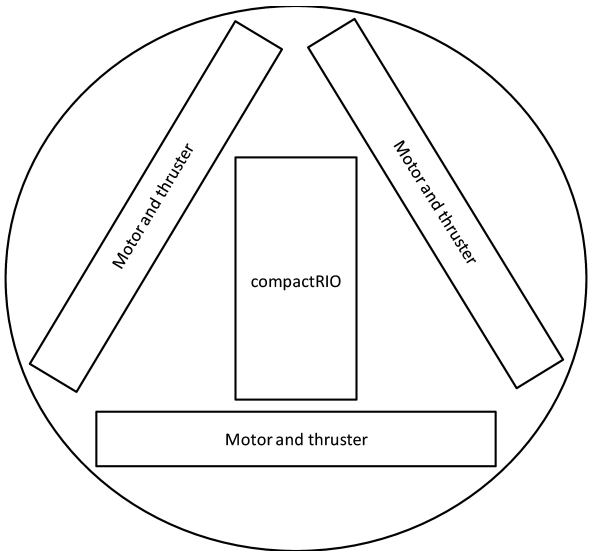

Figure 4.1: Thruster configuration for CS Saucer.

Both the motor and thruster have some clearance in the vertical direction. This means that the components can be safely fastened to the bottom plate while the ends stick out into the foam ring. By trimming the foam in these specific places it is possible to save space and make the diameter of the bottom plate smaller.

The radius of the bottom plate of the hull, r_2, is calculated as shown in Figure 4.2a. The dimensions of the compactRIO and the width of the rectangle containing the thruster and the motor are known, and thus r_2 is calculated

by finding the the length of the catheti. The longest cathetus is found by using the length of the compactRIO which is 185 mm and the width of the thruster and motor. The first cathetus is then calculated as

$$\frac{185}{2} + 57 = 149.5 \text{ mm} \tag{4.1}$$

The other cathetus is found using the length of the motor and thruster combined which is 260 mm. The second cathetus is then calculated as

$$\frac{260}{2} = 130 \text{ mm} \tag{4.2}$$

With the catheti calculated, the hypotenuse r_2 is then calculated using the Pythagorean theorem.

$$r_2 = \sqrt{149.5^2 + 130^2} \tag{4.3}$$
$$r_2 = 198.12 \text{ mm} \tag{4.4}$$

The distance from the center of the bottom plate to the center of each hole for the thrusters is calculated in much the same way. This is shown in Figure 4.2b. All three holes are the same distance from the center, 120 degrees apart. The hypotenuse r_1 is calculated as

$$r_1 = \sqrt{\left(\frac{185}{2} + \frac{57}{2}\right)^2 + \left(\frac{260}{2} - 65\right)^2} \tag{4.5}$$
$$r_1 = \sqrt{121^2 + 65^2} \tag{4.6}$$
$$r_1 = 137.35 \text{ mm} \tag{4.7}$$

where the length of the motor and thruster combined is 260 mm and the distance from the edge of the thruster to the thruster shaft is measured to be 65 mm.

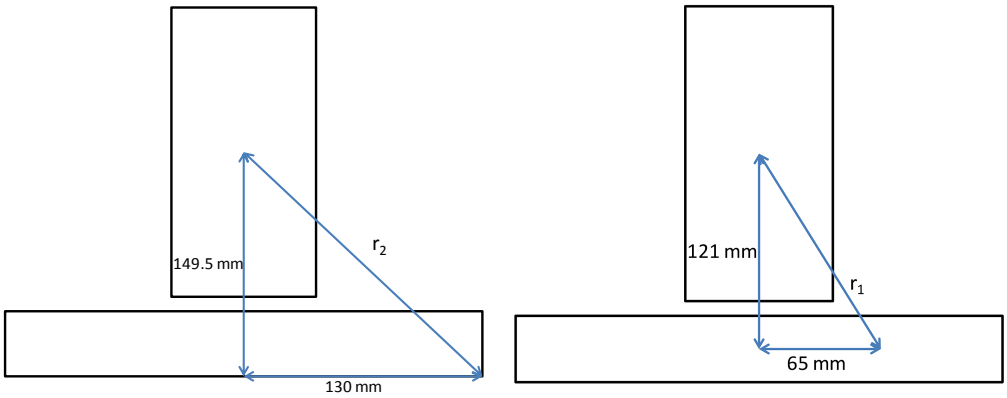

(a) Bottom plate radius r_2.

(b) Center to thruster radius r_1.

Figure 4.2: Radius r_2 and radius r_1 from the center of the bottom plate.

The holes in the bottom plate for the three thrusters are all the same size. The radius has been determined by measuring the diameter of the thrusters with a caliper. The diameter of the thrusters is 23 mm. In order to avoid friction between the rotating azimuth thrusters and the bottom plate of the ship, the diameter of the hole is set to 24 mm. This means that the radius r_3 is 12 mm. The final measurements for the bottom plate are shown in Figure 4.3.

4.2 Draft

To ensure that the draft of the vessel is satisfactory with both the compactRIO and the myRIO, an analysis of the different payloads has been performed. The draft of the vessel is the distance from the waterline to the bottom of the vessel. A vessel with a relative large draft will sit low in the water and this will affect the response of the vessel.

The mass of the components in the two different payloads can be seen in Table 4.1.

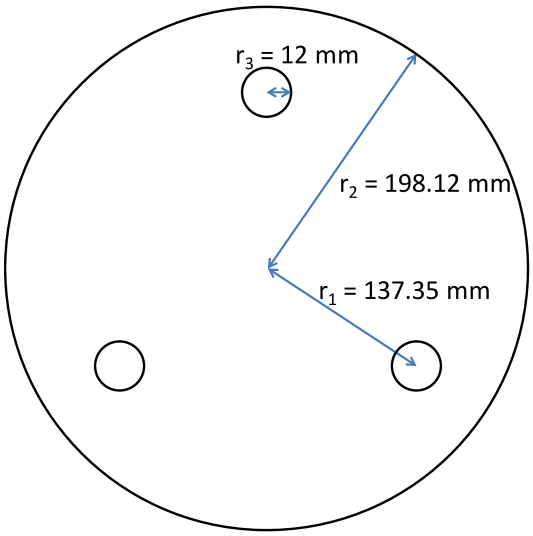

Figure 4.3: Final measurements for the bottom plate.

Component	myRIO [g]	compactRIO [g]
Azimuth truster (×3)	585	585
Motor (×3)	1737	1737
Servo motor (×3)	219	219
Servo motor control (×3)	159	159
myRio	196	
Battery	512	
compactRIO		1561
Raspberry PI		100
Sum	3408	4361

Table 4.1: Two different payload cases for the hull of the vessel.

The projected draft with the two different payloads can be calculated using the dimensions of the hull. The volume of the hull, simplified as a barge is

$$V = \pi\ 0.199^2\ 0.125$$
$$V = 0.01556\ m^3$$

The mass of the materials used to construct the hull of the vessel is estimated to be 450 grams. The total estimated mass for the two payloads is shown in Table 4.2.

	myRIO Configuration [g]	compactRIO Configuration [g]
Mass of components	3408	4361
Estimated mass of construction materials	450	450
Sum	3858	4811

Table 4.2: Estimated total mass of the vessel for the two payload cases.

The mass displaced by the vessel in the two payload cases means that the corresponding draft can be calculated as

$$\frac{\text{displaced mass}}{\text{density of water}} = \text{displaced volume} \tag{4.8}$$
$$\pi\ 0.199^2\ d = \text{displaced volume} \tag{4.9}$$

where d is the draft of the ship. For the myRIO case the mass displaced by the vessel is 3858 grams as shown in Table 4.2. The density of fresh water is approximately $1000\frac{kg}{m^3}$. The resulting displaced volume is calculated as shown in (4.8). By inserting this into (4.9) the draft d is found. The draft for the two payload cases is shown in Table 4.3.

Payload Configuration	Draft d [cm]
myRio Configuration	3.1
compactRIO Configuration	3.8

Table 4.3: Estimated draft of the vessel for the two payload cases.

4.3 Foam Ring

A circular foam ring serves as the main part of the vessel hull. This foam ring is glued to the bottom plate plate and coated with a carbon fiber sheet and epoxy. The foam ring was constructed of the material Divinycell H60, courtesy of Norsk Marinteknisk Forskningsinstitutt AS (MARINTEK). This material is frequently used by MARINTEK in the construction of ship models. The foam ring was be milled by MARINTEK according to the 3D model of CS Saucer. The work drawing exported from the 3D model used for milling is shown in Figure 4.4.

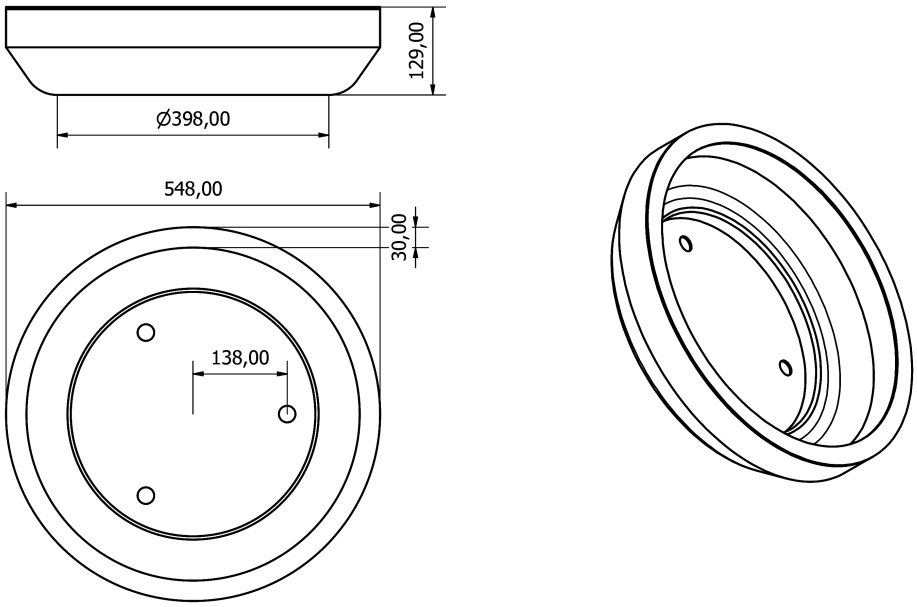

Figure 4.4: Work drawing of the foam ring with final measurements.

The finished milled foam ring can be seen in Figure 4.5.

Figure 4.5: Foam ring milled from Divinycell H60.

4.4 Top Ring

The top ring is glued on top of the foam ring. This ring is made of the same material as the bottom plate. It stiffens the construction and simplifies the fastening of the lid on top of the vessel. Four bolts are fastened to the top ring facing upwards. The purpose of these bolts is to secure the lid to the vessel. The design and dimensions of the top ring are shown in Figure 4.6.

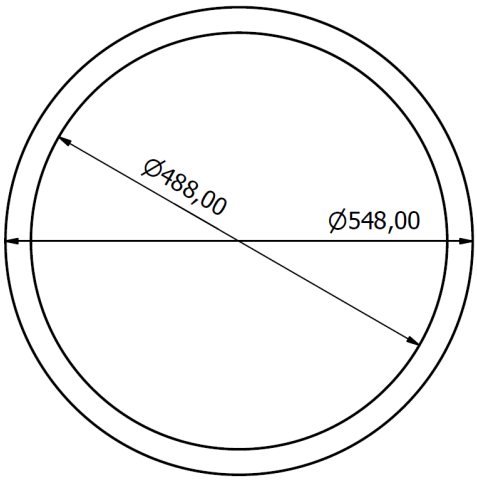

Figure 4.6: The top ring to be glued to the foam ring.

4.5 Top Lid

The top lid of the vessel is designed so that it is easy to remove and put back on when adjustments to the components inside must be made. The lid must be completely detachable so that it is easy to use new lids with different payloads in future projects. The lid should be water repellent, however it is not a design constraint that it should be completely watertight. To fasten the lid to the vessel, four bolts are permanently secured to the top ring of the vessel as shown in Figure 4.7. A rubber strip is glued on around the top ring. The lid has four holes placed corresponding to the bolts on the vessel. The lid can then be easily secured to the vessel with four butterfly screws.

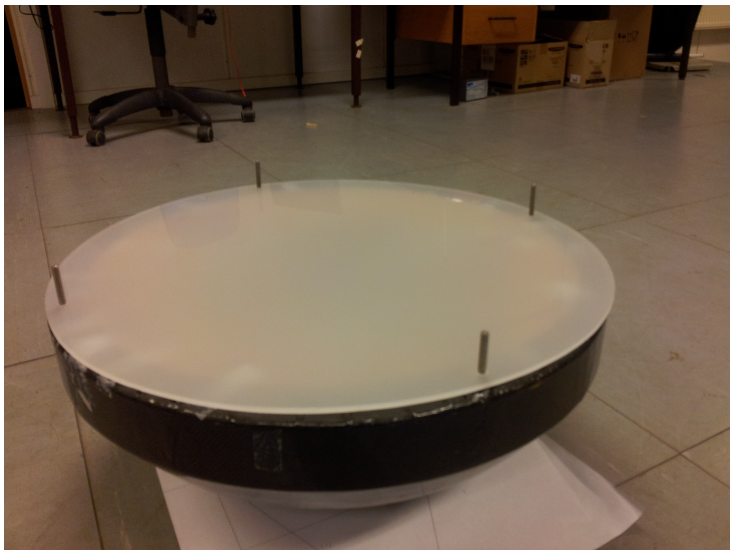

Figure 4.7: The plexi glass lid fitted on top of the vessel.

4.6 Carbon Coating

The outside of the hull is fitted with a flexible woven carbon fiber sheet. The sheet is hardened and fastened to the hull of the vessel with epoxy. Before applying the carbon fiber sheet the hull is sanded down and primed with a layer of epoxy. After the sheet is applied and saturated with epoxy, the hull is left to dry for 24 hours. The epoxy is then lightly sanded down to remove

bubbles that have formed and a new thin layer of epoxy is applied. This procedure has been done two times to ensure a nice finish to the carbon fiber and to ensure that the hull is watertight. The resulting carbon coated hull can be seen in Figure 4.8.

Figure 4.8: Vessel hull with exterior carbon coating.

Chapter 5

Hardware

5.1 Power

The system is powered by a single three cell 11.1V LiPo battery. The three servo motors require a 5V power connection. In order to convert the 11.1V power provided by the battery to 5V, a switching DC/DC converter is user together with a capacitor. The DC/DC Converter works at 98 % efficiency. A high efficiency converter means that the battery of the CS Saucer will last longer before it needs to be recharged. Using a linear regulator instead of a switching DC/DC converter would show a significant decrease in efficiency, especially when the difference between voltages increases. The capacitor is used to smooth out the output from the switching DC/DC converter. This further ensures a stable voltage output from the converter and reduces possible signal noise that can be generated by the switching converter. The data sheets for the DC/DC converter and the 5V capacitor can be found in Appendix A.4 and Appendix A.5, respectively.

The electronic speed controllers and motors in the CS Saucer have proved particularly vulnerable to the voltage transients in the circuit. This caused very jumpy and unreliable performance of the three thrusters. This challenge was solved with three capacitors eliminating voltage transients in the power leading to the three electronic speed controllers and in turn the motors. The capacitors must be able to handle more than 12V and at least 10000 μF(Microfarad).

With the capacitors included in the circuit the layout of the grid from the power source is as shown in Figure 5.1.

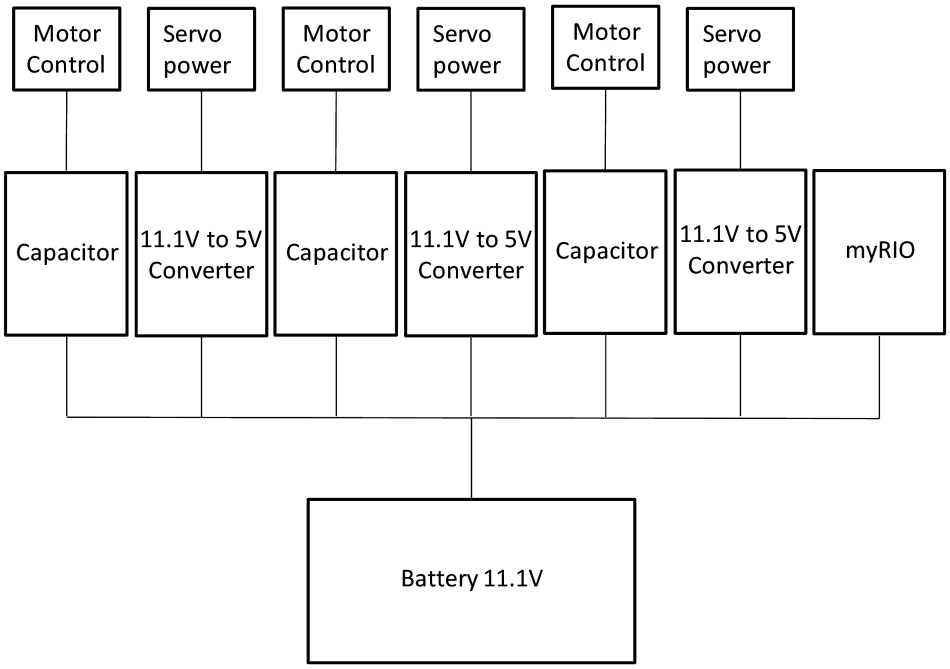

Figure 5.1: Connection grid from the power source on CS Saucer.

5.1.1 Traxxas 6400

The power source used on the CS Saucer is a Traxxas 640 mAh battery. It is capable of delivering 160 Ampere continuously. The battery is a three cell Lithium Polymer (LiPo) battery which means that the three cells of 3.7V combined form a 11.1 battery. It is highly recommended that the battery is always supervised while being charged because of its high flammability. The battery should also be charged using both the Traxxas plug and the balancing plug which is connected to the battery by four small wires. The

balancing plug ensures that the three cells of the battery are evenly charged, something that is very important in a Lipo battery.

5.2 myRIO Embedded Controller

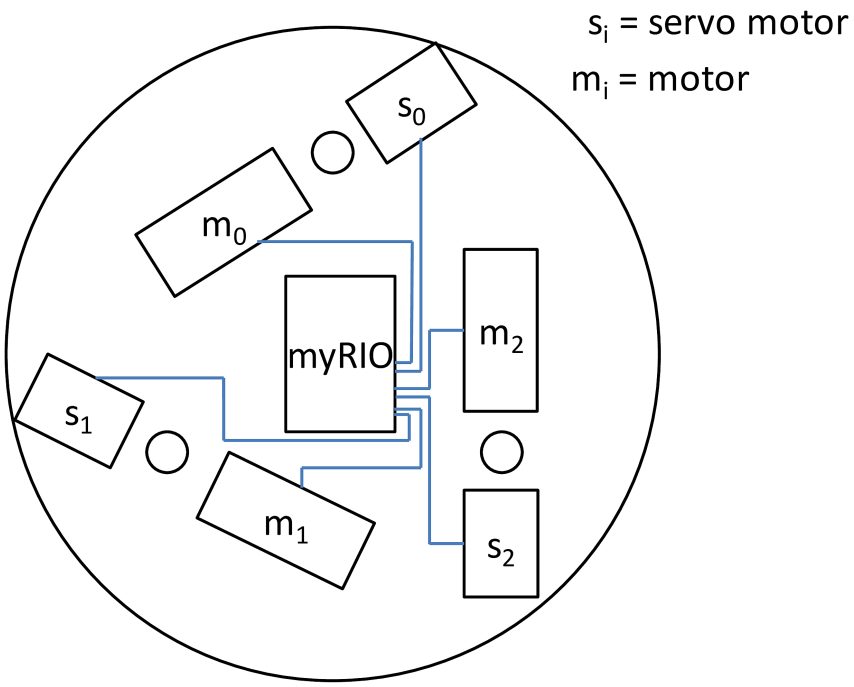

Figure 5.2: Visualization of the PWM signal flow.

The myRIO from National Instruments is a compact and re-programmable FPGA target. It serves as the embedded controller for the CS Saucer. The myRIO with its default FPGA personality is capable of driving 8 PWM signals simultaneously, in addition to multiple digital and analog connections. The FPGA personality of the myRIO can be programmed to fit sepecific needs that are not covered by the default personality. In the case of the CS Saucer the default FPGA personality is sufficient since the CS Saucer

requires six PWM signal outs from the myRIO. The PWM signals used in the CS Saucer and their respective pinouts and signals are shown in Table 5.1. An overview of the PWM signal flow can be sen in Figure 5.2.

myRIO connector pin	Signal identification
A/PWM0(pin 27)	u_{PWM_0}
A/PWM1(pin 29)	u_{PWM_1}
A/PWM2(pin 31)	u_{PWM_2}
B/PWM0(pin 27)	α_{PWM_0}
B/PWM1(pin 29)	α_{PWM_1}
B/PWM2(pin 31)	α_{PWM_2}

Table 5.1: PWM signal wires connected to the myRIO.

Where u is the force signal to the thrusters and α is the heading signal sent to the servos rotating the thrusters. The wires used for all the PWM signals are shielded cables. This is to eliminate the possibility of noise from the components of the CS Saucer disturbing the PWM signals. The MPX connector pinouts of the myRIO are shown in Figure 5.3.

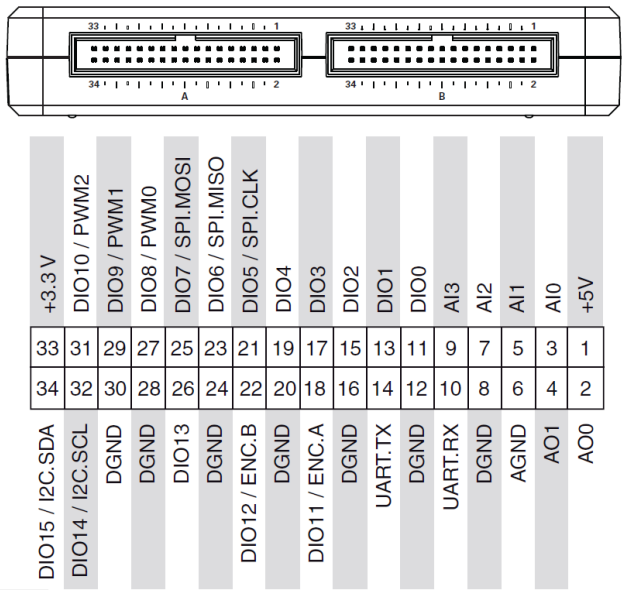

Figure 5.3: myRIO MPX connector pinouts.

A PWM signal consist of a frequency and a duty cycle. The frequency for the servo motors and ESCs used in this thesis is set to a constant frequency of 50 Hz. The duty cycle is then the only parameter controlled in order to generate the PWM signal. The duty cycle can be set in the range $dc = [0, 1]$. A duty cycle of 0.5 means that the signal will be "on" for 50 % of the period. This example is illustrated in Figure 5.4.

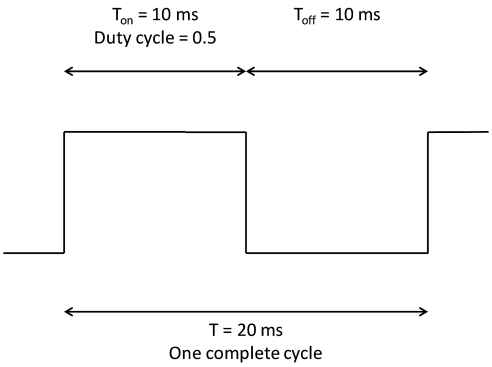

Figure 5.4: Example of a PWM signal with $frequency = 50\ Hz$ and $duty\ cycle = 0.5$.

5.3 Thruster

5.3.1 Graupner DS8311 Servo

The Graupner DS8311 Servo motor is used to control the angle of the thruster and in turn the heading of CS Saucer. The servo itself rotates about 150 degrees. A gear connects the servo to the azimuth gear on the thruster. The connecting gear is twice as large as the gear it connects to. This means that the 150 degrees of rotation of the servo translates into about 300 degrees of

rotation of the thruster itself. The DS8311 servo requires a 5V power signal and a PWM signal to control the position of the thruster. More detailed specifications on the DS8311 servo can be found in Appendix A.2.

5.3.2 Marine 30 ESC

The Marine 30 Electronic Speed Controller (ESC) is used to control the DC motors driving the thruster propellers. It has several programmable modes such as forwards only mode and different modes for different battery types. The speed controller normally requires a 5V power signal and a PWM signal to control the speed of the motor in addition to the 12 power required to run the motor. This is intended for Radio control (RC) applications where the radio receiver does not have a power. However, for multiple speed controllers used simultaneously and since the myRIO has it's own 11.1V power line from the battery, none of the 5V power cables to the electronic speed controllers need to be connected. More documentation on the Marine 30 speed controller can be found in Appendix A.1.

5.3.3 Torpedo 800

The Torpedo 800 is a brushed DC motor. One of these motors is attached to each of the thrusters where it drives the propeller. The Torpedo 800 can operate with voltages from 6 to 12 Volts. The motors has been elevated with wooden blocks so that the shaft of the motor line up with the shaft of the thruster. The motors are fastened to the wooden blocks will bolts and nuts. The wooden blocks are in turn fastened to the bottom plate of CS Saucer with screws that have been screwed in from the underside of the vessel.

A suppression filter set has been soldered to each of the three DC motors on CS Saucer. Each set consists of three ceramic capacitors which will suppress sudden voltage spikes and unwanted noise created by the the motor. The capacitors are soldered to the motor as shown in Figure 5.5. In the case of the Torpedo 800 motor, the two upper capacitors would not fasten to the can of the motor. The two capacitors were instead joined and connected to a wire leading down to one of the fastening holes of the motor were it was

easily soldered on. This solution serves the same purpose as the one outlined in Figure 5.5, albeit a bit less elegant.

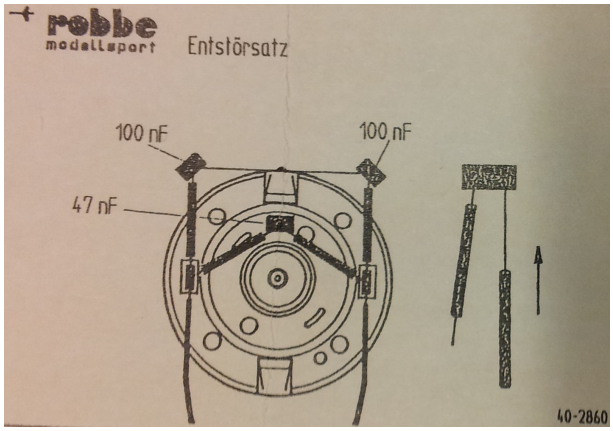

Figure 5.5: Recommended mounting of the suppression filter set.

5.3.4 Graupner Schottel drive unit II

The Graupner thrusters are azimuth thrusters. The thrusters have been bolted to the bottom plate of the vessel so that they can be replaced if needed. The thrusters have been coated with a silicone seal to create a watertight seal between the thrusters and the bottom plate of the vessel. The Thrusters have been disassembled and lubricated through the two designated holes on each thruster before they were assembled and mounted on CS Saucer. It is very important that the thrusters are not run for more than one minute when out of water.

The forward direction of CS Saucer is defined through one of the thrusters so that it has one forward thruster on line with the X-axis in the body frame $\{b\}$ of the vessel. The other two thrusters are then situated symmetrically on each side of the X-axis to the rear of the vessel. If these thrusters both rotate clockwise, the torque of the propellers will cause the vessel to be dragged to the starboard side. If the propellers rotate opposite ways, the two propellers will cancel each other out and the vessel will move straighter. The rear propeller on the starboard side has therefore been changed to a pushing propeller that will create forwards thrust when run counter clockwise. The

two rear propellers both run outwards when seen from the stern of the vessel. The port propeller runs counter clockwise and the starboard propeller runs clockwise. This is illustrated in Figure 5.6.

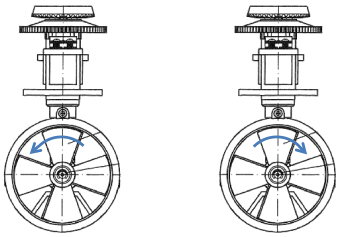

Figure 5.6: Counter rotating rear propellers. This Figure is modified from the thruster datasheet in Appendix A.3.

More information on the Graupner thrusters can be found in Appendix A.3.

Part III

Low Level Control

Chapter 6

Actuator Calibration

6.1 ESC Calibration

In order to calibrate a Marine 30 speed controller, the neutral PWM signal of the controller must first be found. The PWM signal consist of a frequency and a duty cycle. The duty cycle together with the frequency decides the pulse width or the "on time" of a given signal. For the Marine 30 speed controller the frequency is set to a constant of 50 Hz which gives a period of 20 ms. Based on the calibrations done in this thesis, the neutral PWM signal for the Marine 30 speed controller lies somewhere in the duty cycle range $[0, 0.1]$. The neutral signal is indicated on the speed controller itself by all three LEDs lighting solidly.

- Once the neutral signal is found, apply this signal to the controller and reboot it by switching the power off and on.
- In the first few seconds of the controller rebooting all three LEDs will flash. Press the button on the controller during this window to enter calibration mode.
- If the correct neutral signal is sent to the controller, the green LED will light solidly.
- Now set the duty cycle you want as your full forwards signal. Then switch back to the neutral PWM signal. The maximum forwards signal

has now been set and the red LED will light solidly.

- Now set your desired full reverse signal and then switch back to the neutral signal as before. All three LEDs will now light solidly to indicate the neutral position and the controller is calibrated.

The current calibration of the three speed controllers on CS Saucer is shown in Table 6.1.

ESC mode	Duty Cycle	LED indication RGB
Full forwards	0.0940	GB
Neutral	0.0685	RGB
Full backwards	0.0430	RB

Table 6.1: Current calibration of ECSs with corresponding LED indications. All ECSs run on the $frequency = 50\ Hz$.

6.2 Servo Motor calibration

In order to get the same amount of rotation in both directions the neutral position of the servo must coincide with the neutral position of the thruster. For the CS Saucer, the neutral position of the thrusters is defined as parallel to the x axis of the body fixed coordinate system and directed in the positive direction. The gear that connects the servo to the thruster must be detached and the servo manually set in the neutral position. With the servo motor in its neutral position, the gear is then reattached. Creating a paper template with three parallel lines proved to be the best solution for lining the thrusters up as precisely as possible. The calibration of the servo motors can be seen in Table 6.2.

A mapping between the desired thruster angle α_i and the duty cycle sent to the servo motor u_{α_i} has been developed. In order to measure the maximum rotation of the thrusters the paper template described earlier was used. By setting the thruster to its maximum angle $\alpha_{i_{max}}$, the thruster position of the thruster can be marked down on the template and the resulting angle measured. This procedure and the paper template are shown in Figure 6.1.

The maximum rotation of the thrusters is found to be $\alpha_i = [-114^o,\ 114^o]$. Converted to radians, the mapping can then be defined as

$$u_{\alpha_i} = \frac{\alpha_i}{1.9897} \cdot 0.0345 + 0.0745 \tag{6.1}$$

Servo Position	Duty Cycle
Maximum rotation left	0.1090
Neutral	0.0745
Maximum rotation right	0.0400

Table 6.2: Current calibration of servos on CS Saucer. All servos run on the $frequency = 50\ Hz$.

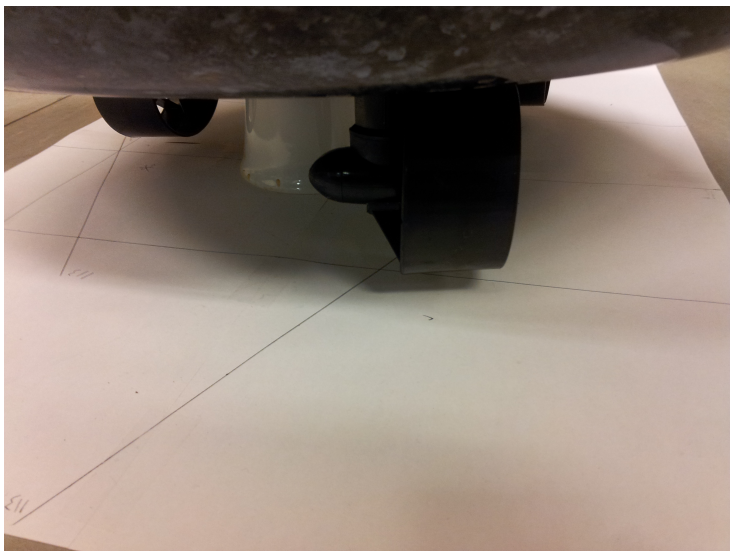

Figure 6.1: Paper template used to determine the maximum rotation of the thrusters.

6.3 Control Input to Actuator Signals

The sub VI "U2PWM" handles the mapping from the control input to the PWM signals sent to the actuators. The input to the sub VI are the two

vectors

$$u = [u_0, u_1, u_2] \in [-1, 1] \tag{6.2}$$
$$\alpha = [\alpha_0, \alpha_1, \alpha_2] \in [-\pi, \pi] \tag{6.3}$$

The output from the sub VI are the two vectors with PWM signals

$$u_{\text{PWM}} = [u_{\text{PWM}_0}, u_{\text{PWM}_1}, u_{\text{PWM}_2}] \in [0.0430, 0.0940] \tag{6.4}$$
$$\alpha_{\text{PWM}} = [\alpha_{\text{PWM}_0}, \alpha_{\text{PWM}_1}, \alpha_{\text{PWM}_2}] \in [0.0400, 0.1090] \tag{6.5}$$

where the control inputs are mapped so that the following relationships are satisfied

$$[-1, 1] \rightarrow [0.0430, 0.0940] \tag{6.6}$$
$$[-\pi, \pi] \rightarrow [0.0400, 0.1090] \tag{6.7}$$

The PWM signals are then fed to the actuators through their corresponding pinouts listed in Table 5.1.

Chapter 7

Thrust Allocation

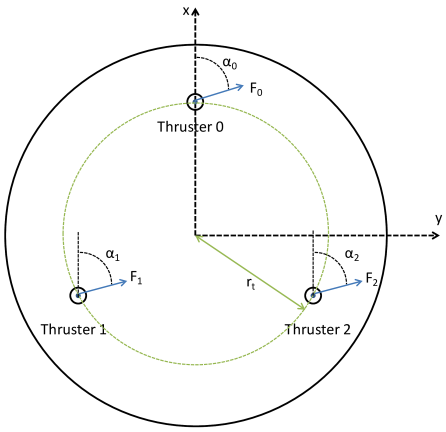

Figure 7.1: Thruster configuration for CS Saucer.

The force created by each thruster is defined as $F_i = K_i u_i$, where u_i is the control input and K_i is a force coefficient. The aggregated forces and moments from all the thrusters in Figure 7.1 can be represented as

$$\tau = \begin{bmatrix} X \\ Y \\ N \end{bmatrix}$$

where X and Y are the forces in surge and sway, respectively, and N is the moment in yaw. With the radius r_t seen in figure 7.1, τ can be expressed as

$$\tau = T(\alpha)Ku \tag{7.1}$$

where $T(\alpha)$ is the thrust configuration matrix and K is a gain matrix, $K = K^T$. In the case of rotational thrusters like on CS Saucer, the thrust configuration matrix will depend on the rotational angle α of the azimuth thrusters as seen in (7.2).

$$T(\alpha) = \begin{bmatrix} \cos(\alpha_0) & \cos(\alpha_1) & \cos(\alpha_2) \\ \sin(\alpha_0) & \sin(\alpha_1) & \sin(\alpha_2) \\ \sin(\alpha_0)r_t & \sin(\alpha_1 + \frac{2\pi}{3})r_t & \sin(\alpha_2 - \frac{2\pi}{3})r_t \end{bmatrix} \tag{7.2}$$

Using this matrix results in a non linear problem when solving for u. An alternative representation of the thrust configuration matrix is to decompose the forces from the thrusters. This means that the force F_i will be represented in the thrust configuration matrix as F_{i_x} and F_{i_y}. The decomposition of the forces is illustrated in figure 7.2 The matrix T is then defined independently

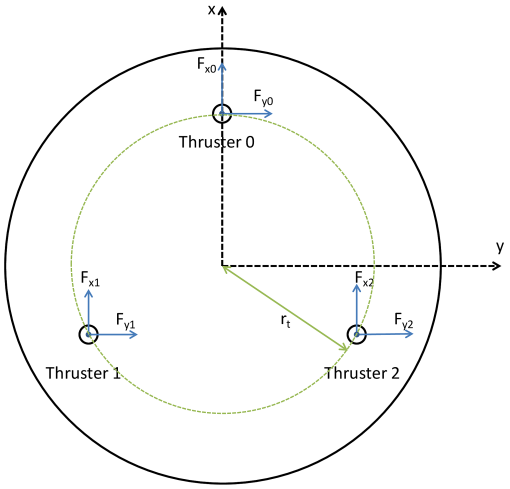

Figure 7.2: Decomposed thrust forces on CS Saucer.

of the azimuth angle α as

$$T = \begin{bmatrix} 1 & 0 & 1 & 0 & 1 & 0 \\ 0 & 1 & 0 & 1 & 0 & 1 \\ 0 & r_t & \cos(\frac{\pi}{6})r_t & -\sin(\frac{\pi}{6})r_t & -\cos(\frac{\pi}{6})r_t & -\sin(\frac{\pi}{6})r_t \end{bmatrix} \tag{7.3}$$

The equation for the forces and moments (7.1) can then be expressed with the extended vector u_e as

$$\tau = TKu_e \tag{7.4}$$

$$\begin{bmatrix} X \\ Y \\ N \end{bmatrix} = \begin{bmatrix} 1 & 0 & 1 & 0 & 1 & 0 \\ 0 & 1 & 0 & 1 & 0 & 1 \\ 0 & r_t & l_x & -l_y & -l_x & -l_y \end{bmatrix} \begin{bmatrix} K_{0_x} & & & & & \\ & K_{0_y} & & & & \\ & & K_{1_x} & & & \\ & & & K_{1_y} & & \\ & & & & K_{2_x} & \\ & & & & & K_{2_y} \end{bmatrix} \begin{bmatrix} u_{0_x} \\ u_{0_y} \\ u_{1_x} \\ u_{1_y} \\ u_{2_x} \\ u_{2_y} \end{bmatrix} \tag{7.5}$$

where $l_x = \cos(\frac{\pi}{6})r_t$ and $l_y = \sin(\frac{\pi}{6})r_t$. The extended vector u_e is created by decomposing the force created by each thruster so that u_e corresponds to the thrust configuration matrix T.

$$u_e = Lu \tag{7.6}$$

$$u_e = \begin{bmatrix} \cos(\alpha_0) & 0 & 0 \\ \sin(\alpha_0) & 0 & 0 \\ 0 & \cos(\alpha_1) & 0 \\ 0 & \sin(\alpha_1) & 0 \\ 0 & 0 & \cos(\alpha_2) \\ 0 & 0 & \sin(\alpha_2) \end{bmatrix} \begin{bmatrix} u_0 \\ u_1 \\ u_2 \end{bmatrix} \tag{7.7}$$

As explained in [Fossen, 2011, sec. 12.3] solving the thrust allocation for a vessel with azimuth thrusters poses a non convex optimization problem. Since optimization theory is out of the scope of this thesis, fixed thruster angles have been used in the DP thrust allocation in this thesis. This solution with numerical results is explained in detail in the next section.

7.1 Thrust Allocation with Fixed Azimuth Angles

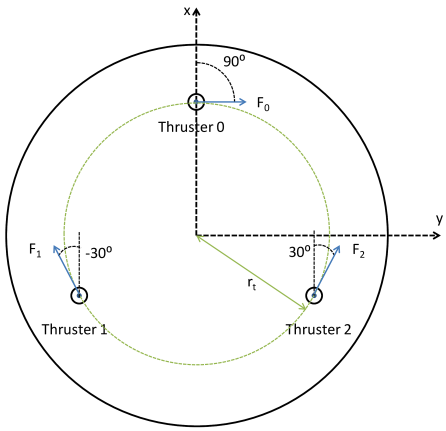

Figure 7.3: Thruster configuration with fixed azimuth angles.

The thruster configuration for CS Saucer in DP is shown in Figure 7.3. The two rear thrusters are directed 30 degrees out from the x axis of the body coordinate system while the bow thruster acts along the y axis of the vessel giving no thrust contribution in surge. This thrust configuration is completely symmetrical around the center of the vessel as the force vectors of the three thrusters form a triangle with its center at the center of the vessel. The equation for the forces and moments acting in surge, sway and yaw can the be expressed as

$$\tau = TKu \tag{7.8}$$

$$\begin{bmatrix} X \\ Y \\ N \end{bmatrix} = \begin{bmatrix} 0 & \cos(\frac{\pi}{6}) & \cos(\frac{\pi}{6}) \\ 1 & -\sin(\frac{\pi}{6}) & \sin(\frac{\pi}{6}) \\ r_t & l & -l \end{bmatrix} \begin{bmatrix} K_0 & & \\ & K_1 & \\ & & K_2 \end{bmatrix} \begin{bmatrix} u_0 \\ u_1 \\ u_2 \end{bmatrix} \tag{7.9}$$

where $l = \cos(\frac{\pi}{6})r_t$, $r_t = 0.135\ cm$ and T is the thrust configuration matrix.

The gain matrix K has been designed based on the experimental data from Chapter 12 where the force produced by each thruster in surge and sway has been measured and approximated using linear curve fitting. The resulting

numerical gain for the three thrusters in negative and positive direction are listed in Table 7.1.

Thruster command and sign	K gain
$+u_0$	$K_0 = 5.8491$
$-u_0$	$K_0 = 5.2602$
$+u_1$	$K_1 = 5.5333$
$-u_1$	$K_1 = 5.3632$
$+u_2$	$K_2 = 5.6558$
$-u_2$	$K_2 = 5.3716$

Table 7.1: Gain matrix K for positive and negative thrust commands.

The dynamic gain matrix K was implemented in LabVIEW with a MathScript Node using the code shown in Listing 7.1. The implemented logic check whether the different thrusters are commanded force in either the positive or negative direction. The gain matrix K is then formed with the appropriate gains.

Listing 7.1: Implemented thrust allocation.

```
function u = thrustAlloc(tau)
  r_t = 0.135;
  l = cos(pi/6)*r_t;
  c30 = cos(pi/6);
  s30 = sin(pi/6);
  T = [0     cos(pi/6)      cos(pi/6);
       1     sin(-pi/6)     sin(pi/6);
       r_t   l              -l ];
  uTemp = T'*tau';
  K0 = 1;
  K1 = 1;
  K2 = 1;
  K0_pos = 5.9491;
  K0_neg = 5.0602;
  K1_pos = 7.0;
  K1_neg = 5.3632;
  K2_pos = 5.6558;
```

```
18    K2_neg = 6.2816;
19    if(uTemp(1) > 0)
20            K0 = K0_pos;
21    elseif(uTemp(1) < 0)
22            K0 = K0_neg;
23    end
24    if(uTemp(2) > 0)
25            K1 = K1_pos;
26    elseif(uTemp(2) < 0)
27            K1 = K1_neg;
28    end
29    if(uTemp(3) > 0)
30            K2 = K2_pos;
31    elseif(uTemp(3) < 0)
32            K2 = K2_neg;
33    end
34    Kdg = [K0 K1 K2];
35    K = diag(Kdg)
36    TKL = T*K;
37    LKT = inv(TKL);
38    u = LKT*tau';
39 end
```

The output vector u from the thrust allocation module is sent together with the constant thruster angle vector α to the "u2PWM" module described in Chapter 6.3. The two vectors sent from the thrust allocation module are then

$$u = [u_0, u_1, u_2] \tag{7.10}$$
$$\alpha = [\alpha_0, \alpha_1, \alpha_2] \tag{7.11}$$
$$= [1.5708, -0.5236, 0.5236] \tag{7.12}$$

where (7.12) is the fixed thruster configuration shown in Figure 7.3, expressed in radians in {b}.

This thrust allocation was tested in the test setup used in Chapter 11. The validity of the system was tested by measuring the forces created by the vessel in surge and sway when run in manual force control mode.

Figure 7.4 and 7.5 shows the force measurements taken in negative and positive surge, respectively. As seen in the figures, the force measured in sway for both negative and positive commanded surge force is very low, and decreasing as the commanded surge force increases. This can be explained by the linear approximation made to design the gain matrix K. A more detailed explanation with additional plots can be found in Chapter 12.

Figure 7.6 and 7.7 shows the force measurements taken in negative and positive sway, respectively. The measured surge force is low, validating the implemented thrust allocation. The measured surge forces are higher that the measured sway forces were with surge force commanded. Because of the angles of the thrusters in relation to the body fixed coordinate system and the linear approximation of the thruster force it is expected that a force command in sway will bleed some force to the surge direction. Overall these results are still considered to be good enough to validate the thrust allocation implemented on CS Saucer.

The gains listed in Table 7.1 have been adjusted during manual force control operation. Due to the low drag resistance forces acting on the vessel, small inaccuracies in the thrust allocation will rapidly compound to a large error which causes course instability in both surge and sway motion. In order to obtain a more stable performance from the vessel, the gains in the K matrix have been manually tuned while the ship has been deployed in manual force control mode. Although the results were not perfect, the adjustment lead to a more stable heading in surge motion, something that will improve accuracy in dynamic positioning.

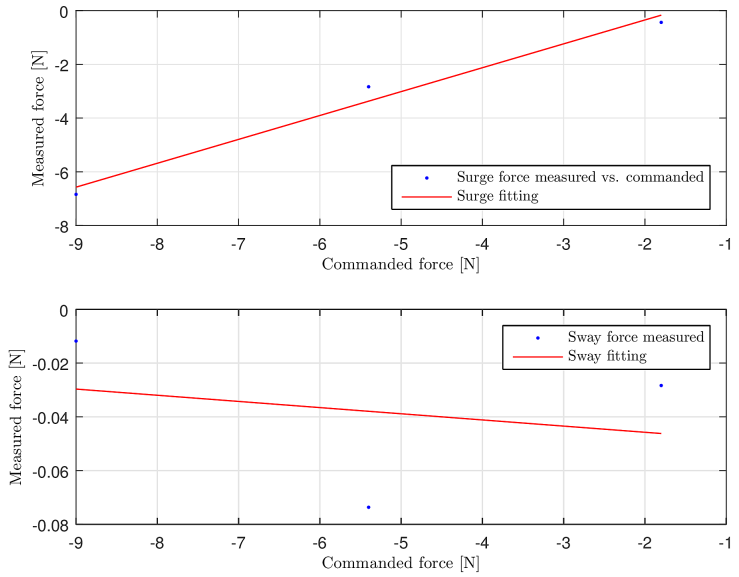

Figure 7.4: Forces measured in surge and sway while commanding negative surge force to the vessel.

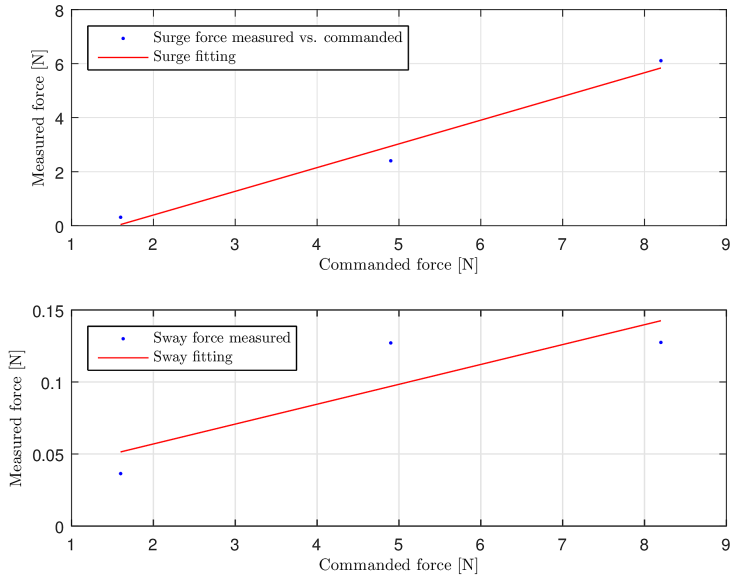

Figure 7.5: Forces measured in surge and sway while commanding positive surge force to the vessel.

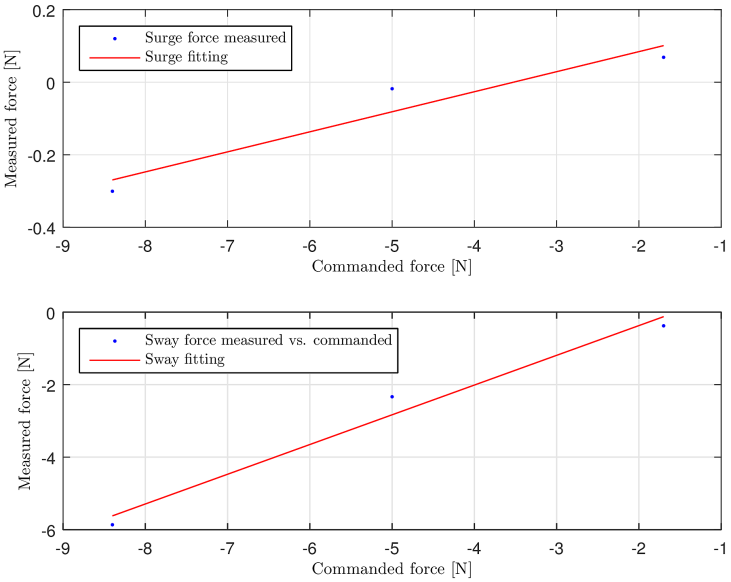

Figure 7.6: Forces measured in surge and sway while commanding negative sway force to the vessel.

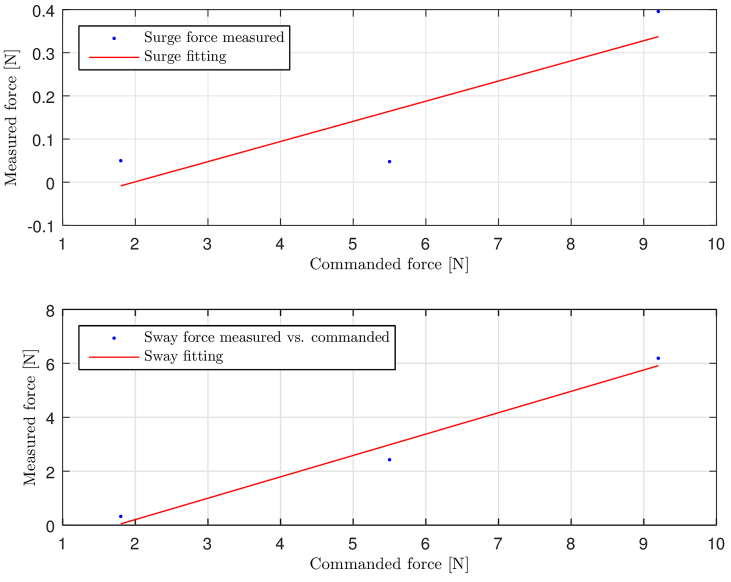

Figure 7.7: Forces measured in surge and sway while commanding positive sway force to the vessel.

Part IV

System Identification and Simulation

Chapter 8

Dynamics

The dynamic equations for a surface vessel are in this chapter divided into three main parts. The rigid-body kinetics of the vessel, the hydrostatics and the hydrodynamics. The motions of the rigid-body, along with the hydrostatics and the hydrodynamics can be used to create a dynamic model for the vessel which is used for vessel control in maneuvering and seakeeping and to simulate the vessel in HIL testing.

The work presented in this chapter is partially based on previous work [Idland, 2014].

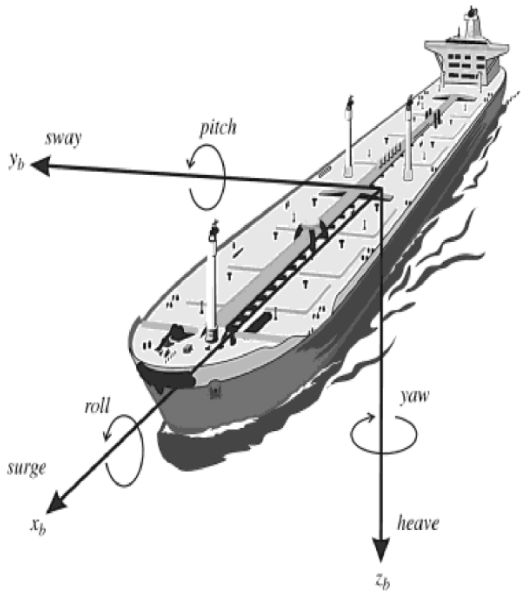

Figure 8.1: The six degrees of motion of a vessel [Fossen, 2011, p. 16].

Figure 8.1 shows the six possible motions defined in the body coordinate system$\{b\}$ that is fixed to the vessel. These motions and their corresponding forces, moments, velocities and positions are defined according to the SNAME-notation in Table 8.1.

	Forces and moments	**Linear and angular velocities**	**Positions and Euler angles**
Motions in surge	X	u	x
Motions in sway	Y	v	y
Motions in heave	Z	w	z
Rotation about the x-axis(roll)	K	p	ϕ
Rotation about the y-axis(pitch)	M	q	θ
Rotation about the z-axis(yaw)	N	r	ψ

Table 8.1: SNAME-notation for motions in six degrees of freedom.

8.1 Rigid-Body Equations of Motion

The rigid-body kinetics of a vessel are described as follows, according to [Fossen, 2011].

$$M_{RB}\dot{\nu} + C_{RB} = \tau_{RB} \tag{8.1}$$

where M_{RB} is the rigid body mass matrix, C_{RB} is the rigid body coriolis and centripetal matrix. This matrix is due to the rotations of the body-fixed reference frame $\{b\}$, shown in Figure 8.1, around the inertial North-East-Down frame $\{n\}$. The reference frame $\{n\}$, as well as the body fixed reference frame $\{b\}$ and the Earth-centered Earth-fixed (ECEF) reference frame are shown in Figure 8.2.

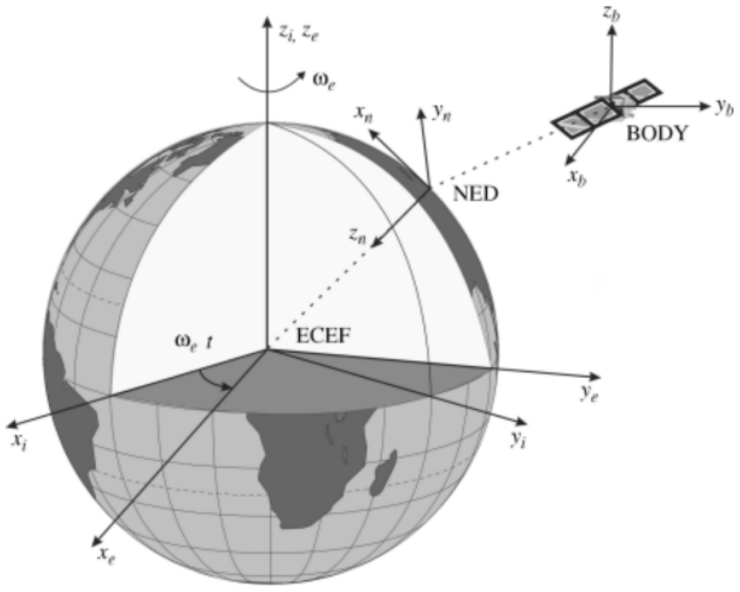

Figure 8.2: The Earth-centered Earth-fixed frame, the North-East-Down (NED) frame $\{n\}$, and the Body-fixed frame $\{b\}$, as visualized in [Fossen, 2011].

In (8.1), ν is the generalized velocity vector

$$\nu = [u, v, w, p, q, r]^T \tag{8.2}$$

expressed in $\{b\}$, and

$$\tau_{RB} = [X, Y, Z, K, M, N]^T \tag{8.3}$$

is the rigid-body forces and moments in the six degrees of freedom.

For a ship operating in the horizontal plane it is common to use three degrees of freedom (DOF). The motions in heave and roll are considered to be small enough to be negligible. This means that the motions in surge, sway, and yaw are the only ones considered. The state ν from (8.2) then reduces to

$$\nu = [u, v, r]^T$$

and the corresponding vector for τ_{RB} becomes

$$\tau_{RB} = [X, Y, N]^T$$

The rigid body mass matrix is derived by applying Newtonian mechanics as explained in [Fossen, 2011]. The relevant equations for the translational and rotational motions for a vessel in 3 DOF then become

$$m[\dot{u} - vr + wq - x_g(q^2 + r^2) + y_g(pq - \dot{r}) + z_g(pr + \dot{q})] = X \tag{8.4}$$

$$m[\dot{v} - wp + ur - y_g(r^2 + p^2) + z_g(qr - \dot{p}) + x_g(qp + \dot{r})] = Y \tag{8.5}$$

$$\begin{aligned} I_z\dot{r} + (I_y - I_x)pq - (\dot{q} + rp)I_{yz} + (q^2 - p^2)I_{xy} + (rq - \dot{p})I_{zx} \\ +m[x_g(\dot{v} - wp + ur) - y_g(\dot{u} - vr + wq)] = N \end{aligned} \tag{8.6}$$

Because a 3 DOF system is modeled, $q = p = w = 0$. The equations (8.4) - (8.6) can now be expressed as $M_{RB}\dot{\nu}$ with the following M_{RB} matrix

$$M_{RB} = \begin{bmatrix} m & 0 & 0 \\ 0 & m & mx_g \\ 0 & mx_g & I_z \end{bmatrix} \tag{8.7}$$

The matrix $C_{RB}(\nu)$ for a vessel operating i 3 DOF is, as seen in [Fossen, 2011], expressed as

$$C_{RB}(\nu) = \begin{bmatrix} 0 & 0 & -m(x_g r + v) \\ 0 & 0 & mu \\ m(x_g r + v) & -mu & 0 \end{bmatrix} \tag{8.8}$$

8.2 Hydrodynamic forces

The rigid body forces and moments τ_{RB} are divided into several parts as seen in (8.9).

$$\tau_{RB} = \tau_{hyd} + \tau_{hs} + \tau_{wind} + \tau_{wave} + \tau \tag{8.9}$$

The hydrodynamic forces acting on the vessel can be adequately approximated as a mass-damper system and expressed, according to [Fossen, 2011], as

$$\tau_{hyd} = -M_A \dot{\nu} - C_A(\nu)\nu - D(\nu)\nu \tag{8.10}$$

where M_A is an added mass matrix and $C_A(\nu)$ is the added coriolis and centripetal forces.

The hydrodynamic damping matrix $D(\nu)$ consists of the linear damping D and the non-linear part $D_n(\nu)$ as seen in (8.11).

$$D(\nu) = D + D_n(\nu) \tag{8.11}$$

As seen in [Skjetne et al., 2004, p. 129], D can be defined as (8.12), assuming that the surge motion is decoupled and that the vessel is symmetric around the xz plane. Both these assumptions are valid for the CS Saucer.

$$D = -\begin{bmatrix} X_u & 0 & 0 \\ 0 & Y_v & Y_r \\ 0 & N_v & N_r \end{bmatrix} \tag{8.12}$$

The non linear damping matrix $D_n(\nu)$ can be modeled in several different ways. Using second order modulus functions to describe the non linear damping, as described in [Fossen, 2011], results in (8.13).

$$D_n(\nu) = -\begin{bmatrix} X_{|u|u}|u| & 0 & 0 \\ 0 & Y_{|v|v}|v| + Y_{|r|v}|r| & Y_{|v|r}|v| + Y_{|r|r}|r| \\ 0 & N_{|v|v}|v| + N_{|r|v}|r| & N_{|v|r}|v| + N_{|r|r}|r| \end{bmatrix} \tag{8.13}$$

The added mass matrices M_A and $C_A(\nu)$ are defined as

$$M_A = \begin{bmatrix} X_{\dot{u}} & 0 & 0 \\ 0 & Y_{\dot{v}} & Y_{\dot{r}} \\ 0 & Y_{\dot{r}} & N_{\dot{r}} \end{bmatrix} \tag{8.14}$$

$$C_A(\nu) = \begin{bmatrix} 0 & 0 & Y_{\dot{v}}v + Y_{\dot{r}}r \\ 0 & 0 & X_{\dot{u}}u \\ -Y_{\dot{v}}v - Y_{\dot{r}}r & X_{\dot{u}}u & 0 \end{bmatrix} \tag{8.15}$$

Chapter 9

Moment of Inertia

The vessel consist of 4 main parts all centered around one point. The bottom plate of the vessel is a disc and it's moment of inertia is therefore calculated as

$$I_b = \frac{M_b R_b^2}{2}$$

where M_b is the mass and R_b is the radius of the bottom plate. The mass of the plate is calculated using the density of the MDF material and the volume of the plate. The mass M_b is then

$$\begin{aligned} M_b &= V_b \cdot 800 \frac{kg}{m^3} && (9.1)\\ &= \pi\ 0.199^2 \cdot 0.003 \cdot 800 && (9.2)\\ &= 0.298\ kg && (9.3) \end{aligned}$$

The moment of inertia for the bottom plate I_b is then calculated as

$$\begin{aligned} I_b &= \frac{M_b R_b^2}{2} && (9.4)\\ &= \frac{0.298 \cdot 0.199^2}{2} && (9.5)\\ &= 0.006 && (9.6) \end{aligned}$$

The plexi glass lid of the vessel is also a disc and it's moment of inertia is therefore calculated in the same way as the bottom plate.

$$I_l = \frac{M_l R_l^2}{2}$$

where M_l is the mass and R_l is the radius of the lid. The density of the plexi glass used on CS Saucer is $1190\frac{kg}{m_3}$. The radius of the lid is $R_l = 274\ mm$. The mass of the lid is calculated as

$$\begin{aligned} M_l &= \pi \cdot (0.274\ m)^2 \cdot 0.004 \\ &= 1.12\ kg \end{aligned}$$

The moment of inertia for the plexi glass lid can then be calculated numerically as

$$\begin{aligned} I_l &= \frac{M_l R_l^2}{2} \\ &= \frac{1.12 \cdot 0.274^2}{2} \\ &= 0.042 \end{aligned}$$

The top ring and the foam ring can be simplified to a single cylinder with inner radius r_1, outer radius r_2 and height h. Although the foam ring is not a perfect cylinder, the inaccuracies from this simplification are acceptably small. The moment of inertia for the cylinder is calculated as

$$I_c = \frac{1}{2} M_c (r_1^2 + r_2^2)$$

where M_c is the mass of the cylinder. The density of Divinycell H60 is $60\frac{kg}{m^3}$. From the 3D model the volume of the foam ring is known to be $V_c = 0.0070111055 m^3$. Using the density and volume of the foam ring, the exact mass can be calculated as

$$\begin{aligned} M_c &= 60\ \frac{kg}{m^3} \cdot 0.007\ m^3 + 0.1\ kg \\ &= 0.420\ kg + 0.1\ kg \\ &= 0.520\ kg \end{aligned}$$

where the mass of the top ring $M_t = 0.1\ kg$ is added to the mass of the foam ring. With $r_1 = 244\ mm$ and $r_2 = 274\ mm$ the moment of inertia for the simplified foam ring is calculated as

$$\begin{aligned} I_c &= \frac{1}{2} M_c (r_1^2 + r_2^2) \\ &= \frac{0.520(0.244^2 + 0.274^2)}{2} \\ &= 0.035\ kg \cdot m^2 \end{aligned}$$

The the three motors mounted on the bottom plate can be modeled as point masses around the center of the plate. The moment of inertia for all three motors with respect to the center of the bottom plate is calculated as

$$\begin{aligned} I_m &= 3 M_m r^2 \\ &= 3 \cdot 0.595\ kg \cdot (0.135\ m)^2 \end{aligned}$$

where r is the distance from the center of the plate to the point mass. the total moment of inertia for the vessel is calculated by adding all the previous parts together.

$$\begin{aligned} I_{total} &= I_b + I_l + I_c + I_m \\ &= 0.006 + 0.042 + 0.035 + 0.033 \\ &= 0.116\ kgm^2 \end{aligned}$$

Chapter 10

Added Mass Estimation

The added mass coefficients from the hull of a marine vessel can be approximated using different techniques. As explained in [Lewandowski, 2004, sect. 3.2.1] either strip theory or the "equivalent ellipsoid" method are well suited. For the CS Saucer, the "equivalent ellipsoid" method has been used. This method assumes that the added mass coefficient can be approximated using the coefficients of a spheroid with the same waterline measurements as the vessel in question. This fits nicely with the bowl shape of the CS Saucer.

From [Lewandowski, 2004, sec. 3.2.1] the following equations are used to calculate approximated values for $A_{11} = -X_{\dot{u}}$ and $A_{22} = -Y_{\dot{v}}$.

$$A_{11} = \rho \nabla k_1 \tag{10.1}$$
$$A_{22} = \rho \nabla k_2 \tag{10.2}$$
$$A_{66} = I_{yyDF} k' + x_B^2 A_{22} \tag{10.3}$$

Where k_1, k_2 and k' are Lamb's inertia coefficients. As is illustrated in Figure 10.1 the value of the inertia coefficients are dependent on the relationship between the length and the diameter of the ellipsoid. For the symmetric CS Saucer this relationship is $\frac{L}{b} = 1$ as they are equal. It is therefore seen from Figure 10.1 that $k_1 = k_2 \approx 0.5$ and $k' \approx 0$. The distance to the center of buoyancy x_B is equal to zero for the CS Saucer. This means that the added mass coefficient in yaw can be assumed to be zero because of the spherical shape of the vessel.

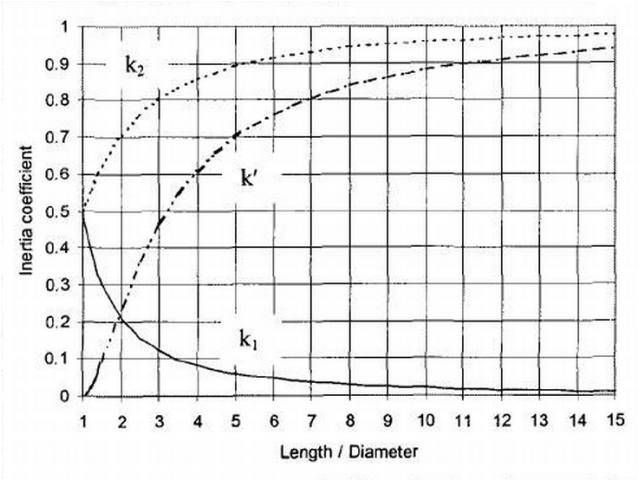

Figure 10.1: Lamb's inertia coefficients for ellipsoids, as seen in [Lewandowski, 2004, p. 42].

The coefficients can now be calculated as

$$A_{11} = A_{22} = \frac{\rho \nabla}{2} \tag{10.4}$$

$$A_{66} = 0 \tag{10.5}$$

The displaced volume ∇ is exported from the 3D model of the vessel with a draft d measured to be 4.0 cm and a density $\rho = 1000 \frac{\text{kg}}{\text{m}^3}$. The numerical values for the coefficients follows as

$$A_{11} = A_{22} = \frac{1000 \frac{\text{kg}}{\text{m}^3} \cdot 0.007 \text{m}^3}{2} \tag{10.6}$$

$$= 3.5 \text{ kg} \tag{10.7}$$

$$A_{66} = 0 \tag{10.8}$$

Chapter 11

Drag Coefficients

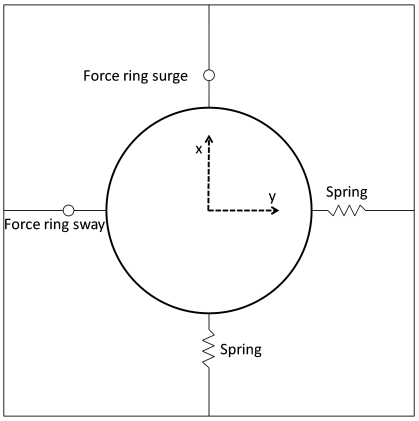

Figure 11.1: Setup for towing tests and thruster measurements of CS Saucer.

In order to estimate the hydrodynamic properties of the vessel several tests have been performed in the MC Lab at the Marine Technical center at NTNU. The test setup is illustrated in Figure 11.1. Two force rings have been fitted to the bow and the port side of the vessel. Springs are fitted to the stern and port side of the vessel in order to eliminate oscillations and keep the vessel straight when subjecting it to forces in surge and sway.

The post processing the resulting data series has been performed in MATLAB. The MATLAB script used for this is a modified version of the script

applied to the test data of CS Enterprise I. The original script was developed by Jostein Follestad. The curve fitting process has been performed with the Curve fitting app in MATLAB where a sample curve fitting has been performed and the generated code has been used to automate the process for all the test cases in this thesis that require curve fitting.

Figure 11.2 shows the drag resistance measured while towing the vessel in surge with towing speeds from 0.05 m/s to 1.00 m/s. The test was performed with all thrusters directed straight along the x axis of the body coordinate system. The propellers were removed from the thrusters in order to isolate the resistance forces created by only the hull and the thruster shafts and tunnels. The second degree polynomial curve fitting is used to identify the linear and nonlinear drag coefficients in the dynamic model of the vessel. The assumption has been made that the resistance forces in sway motion are equal to those found in surge motion. This assumption is made based on the symmetrical shape of the vessel and the fixed thrust configuration explained in Chapter 7.1.

The linear and nonlinear drag coefficients for CS Saucer in surge and sway motion are defined based on the fitted curve in Figure 11.2. The resulting coefficients are listed in Table 11.1.

Coefficient	Numerical value
X_u	-1.9599
$X_{\|u\|u}$	7.0948
Y_v	-1.9599
$Y_{\|v\|v}$	7.0948

Table 11.1: Drag coefficients in surge and sway based on test results.

The same test has been performed with all thrusters set to $\alpha = 90^o$. The thrusters are all directed perpendicular to the towing direction. Theoretically, this setting should produce the highest possible drag resistance as the maximum area of the thrusters are facing the water flow as the vessel is towed. The results from this test is shown in figure 11.4 and 11.5 with a nonlinear curve fitting based on the measurements. As expected the measured drag resistance in surge is larger than the resistance measured with $\alpha = 0^o$. The coefficients derived from the results shown in 11.2 will therefore

be precise only for a thrust configuration with $\alpha = 0^o$, a configuration that is not realistic for the CS Saucer as it would cause under actuation in the sway motion. However, the coefficients derived from the configuration $\alpha = 0^o$ are still considered to be sufficiently accurate to use in a simulation of the vessel.

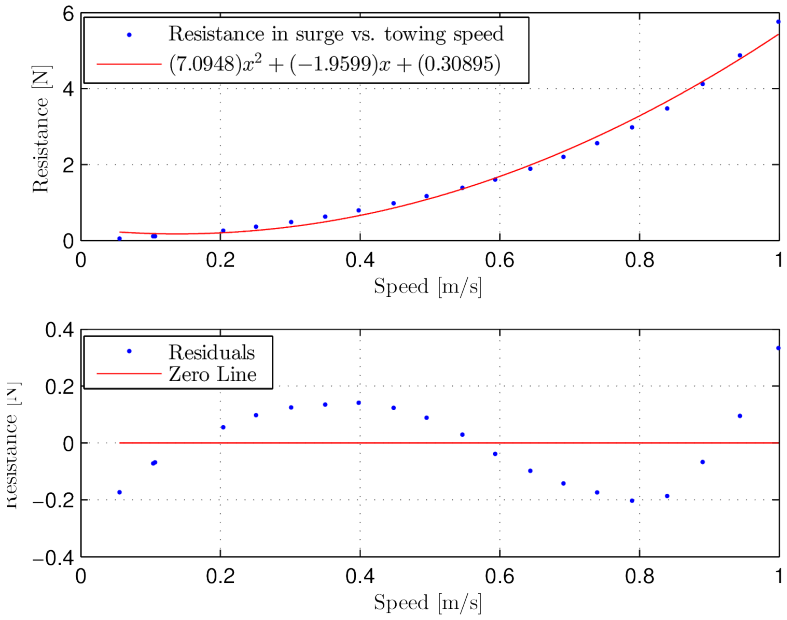

Figure 11.2: Drag forces acting on CS Saucer in surge with all thrusters set to $\alpha = 0$.

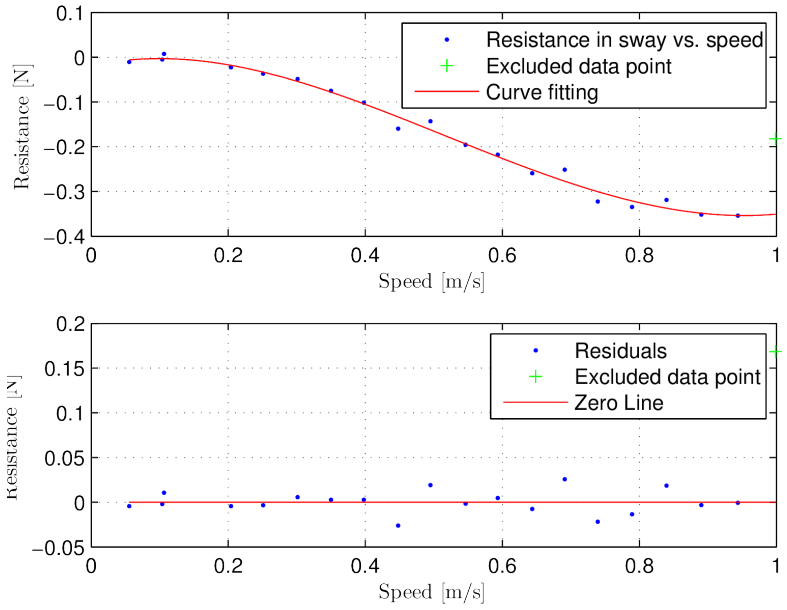

Figure 11.3: Drag forces acting on CS Saucer in sway with all thrusters set to $\alpha = 0$.

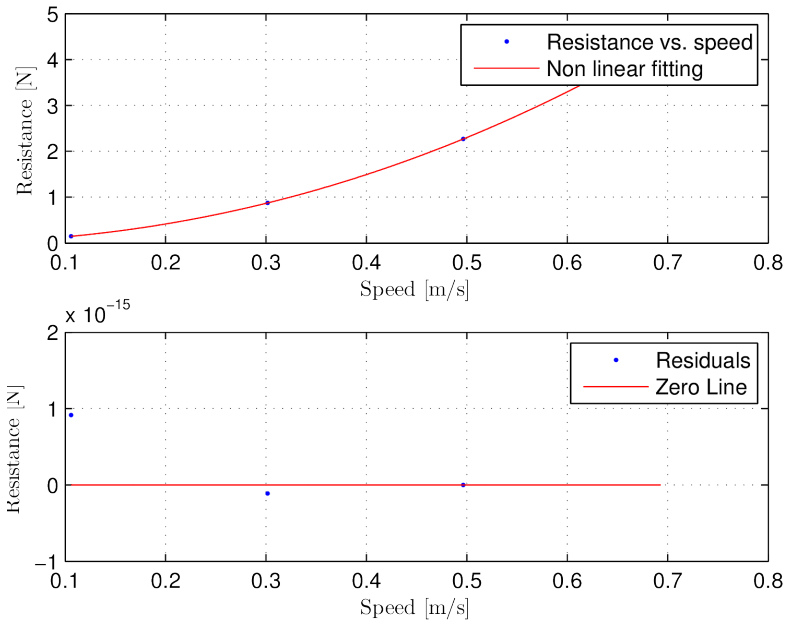

Figure 11.4: Drag forces acting on CS Saucer in surge with all thrusters set to $\alpha = \frac{\pi}{2}$.

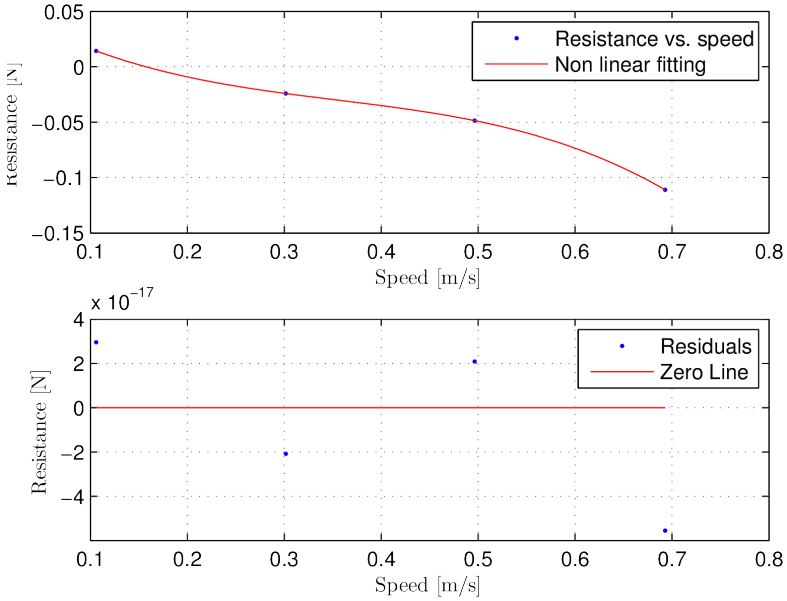

Figure 11.5: Drag forces acting on CS Saucer in sway with all thrusters set to $\alpha = \frac{\pi}{2}$.

11.1 Drag effects of alternative payloads

Towing tests with alternative payloads have been performed on the vessel. These aim to serve as a guide for future projects that require a different payload than the current payload with myRIO. The CS Saucer is designed to be able to hold a compactRIO. Using this embedded controller will result in a heavier payload than the one originally tested. Two alternative payloads have been tested and the results from these tests are presented in this section.

11.1.1 Case 1: 1 kg Additional Mass

Figure 11.6 and 11.7 shows the surge and sway forces measured with a non linear curve fitting applied to the resulting data. Compared to the results in Figure 11.2 and 11.5, the drag forces are not significantly larger. The results indicate that one can expect similar performance from the vessel with this increased payload.

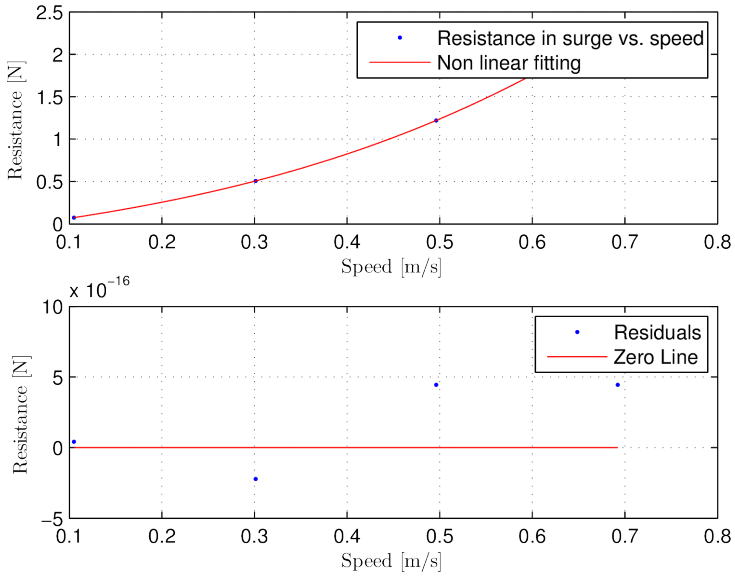

Figure 11.6: Drag forces acting on CS Saucer in surge with all thrusters set to $\alpha = 0$ and 1 kg mass added to the vessel.

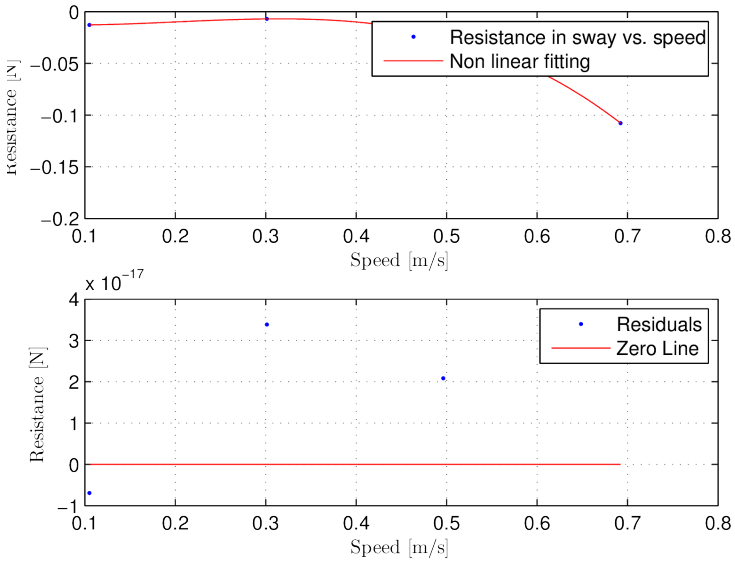

Figure 11.7: Drag forces acting on CS Saucer in sway with all thrusters set to $\alpha = 0$ and 1 kg mass added to the vessel.

11.1.2 Case 2: 3 kg Additional Mass

Figure 11.8 and 11.9 shows the surge and sway forces measured with a non linear curve fitting applied to the resulting data. As expected the drag forces measured are higher here than in the previous case. However, they are considered to be low enough to also classify this case as a viable option in future projects.

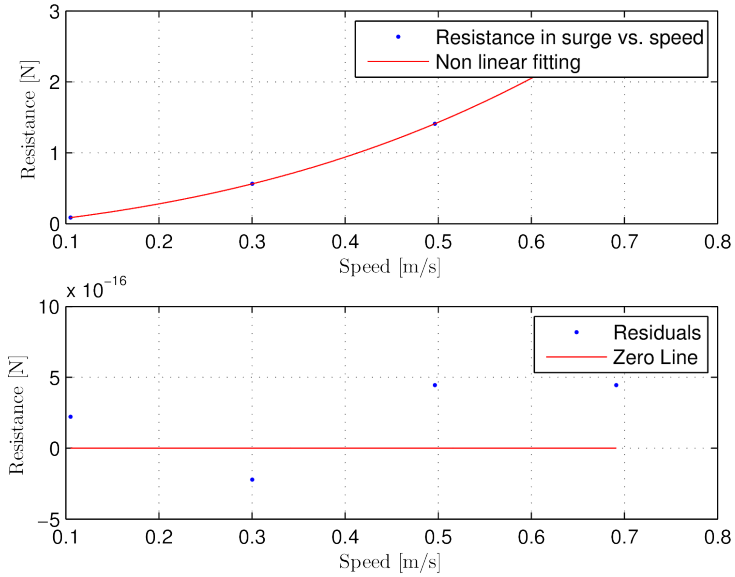

Figure 11.8: Drag forces acting on CS Saucer in surge with all thrusters set to $\alpha = 0$ and 3 kg mass added to the vessel.

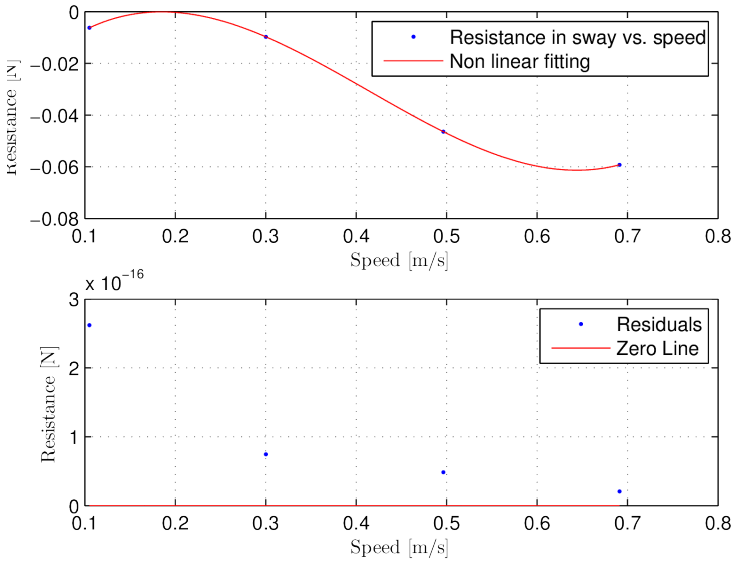

Figure 11.9: Drag forces acting on CS Saucer in sway with all thrusters set to $\alpha = 0$ and 3 kg mass added to the vessel.

Chapter 12

Thruster Force Mapping

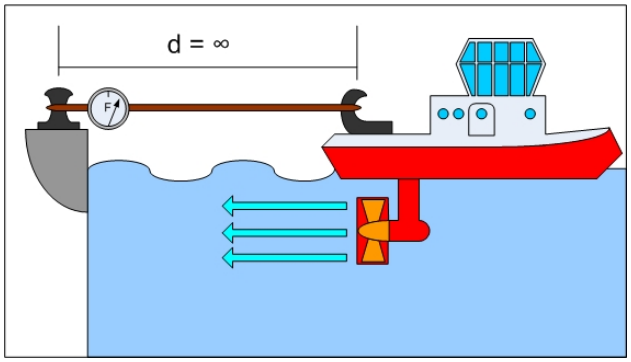

Figure 12.1: Bollard Pull test in ideal conditions [Himbeerkuchen, 2007].

In order to map the thrust forces produced by the vessel in surge and sway, an extended Bollard Test was performed. For this test the thruster angles were set according to the thrust allocation described in Chapter 7.1. All three thrusters were measured individually in surge and sway for positive and negative thrust. The resulting linear curve fittings shown in Figures 12.2, 12.3, 12.4, 12.5, 12.6, 12.7, 12.8, 12.9, 12.10 and 12.11 are used as the thrust force mapping in the thrust allocation in the Dynamic Positioning system. Because this is a linear approximation, the mapping will not yield perfect results in testing. The results will be best at higher force commands. This assumption is confirmed by the validation test discussed in 7.1, where the resulting plots show a measured thrust in the motion not commanded that decreases as the commanded thrust increases.

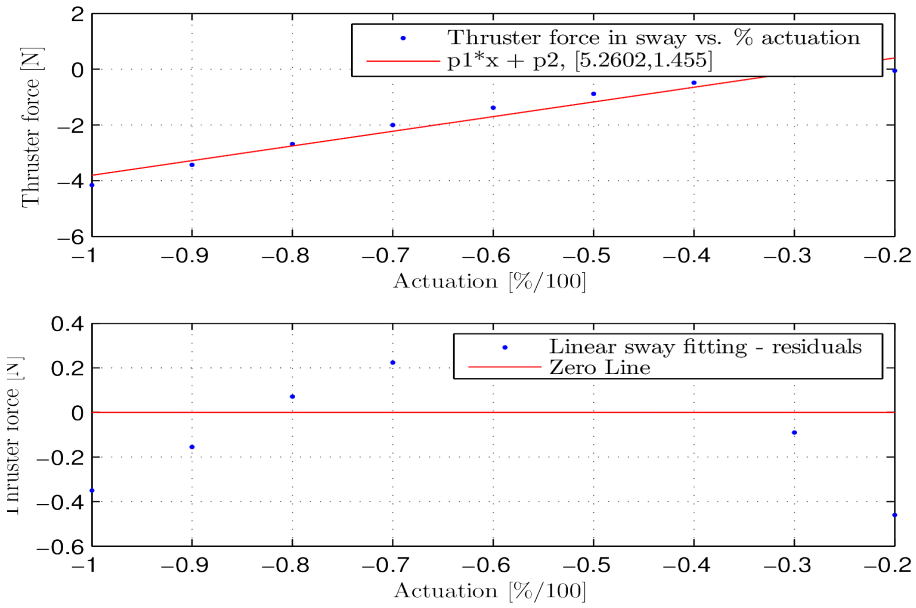

Figure 12.2: Force test in negative sway for thruster 0.

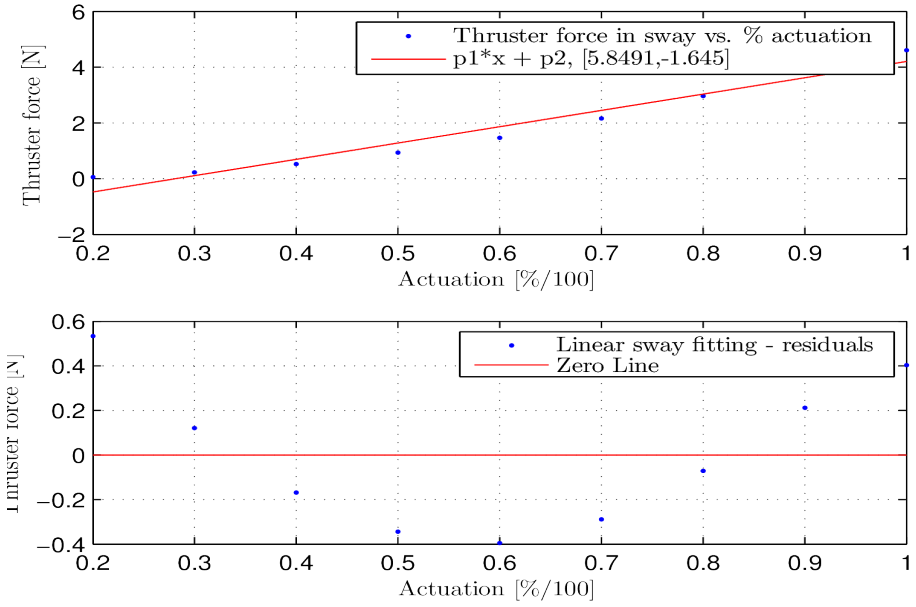

Figure 12.3: Force test in positive sway for thruster 0.

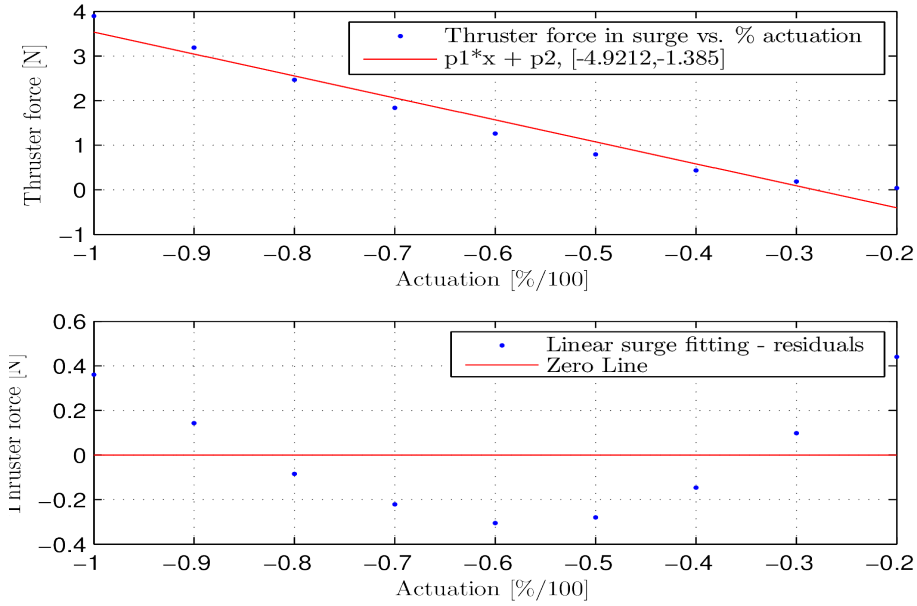

Figure 12.4: Force test in negative surge for thruster 1.

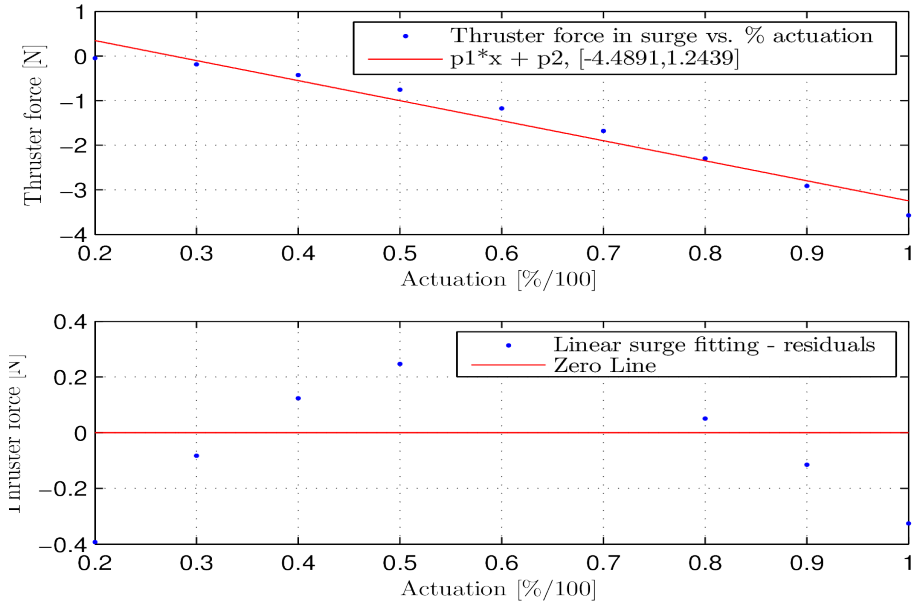

Figure 12.5: Force test in positive surge for thruster 1.

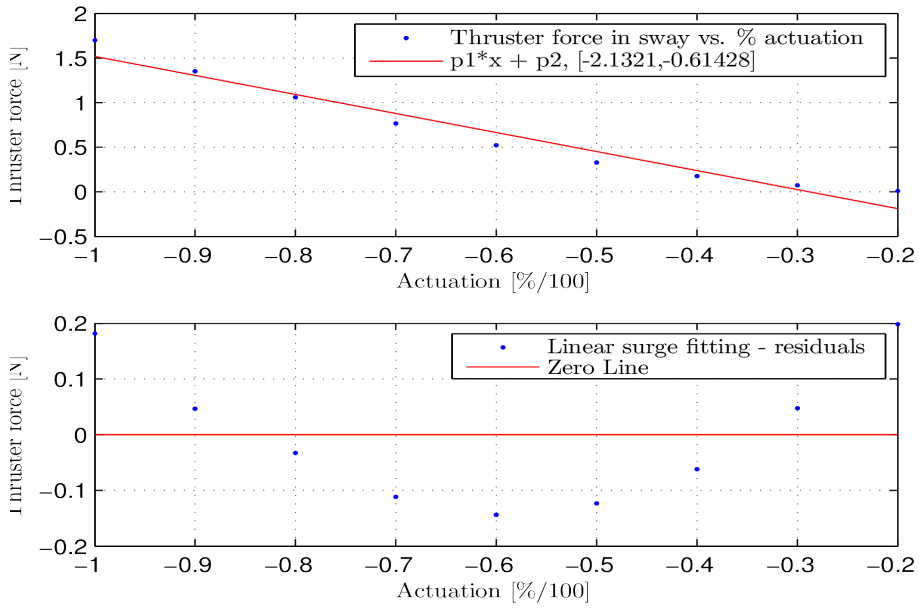

Figure 12.6: Force test in negative sway for thruster 1.

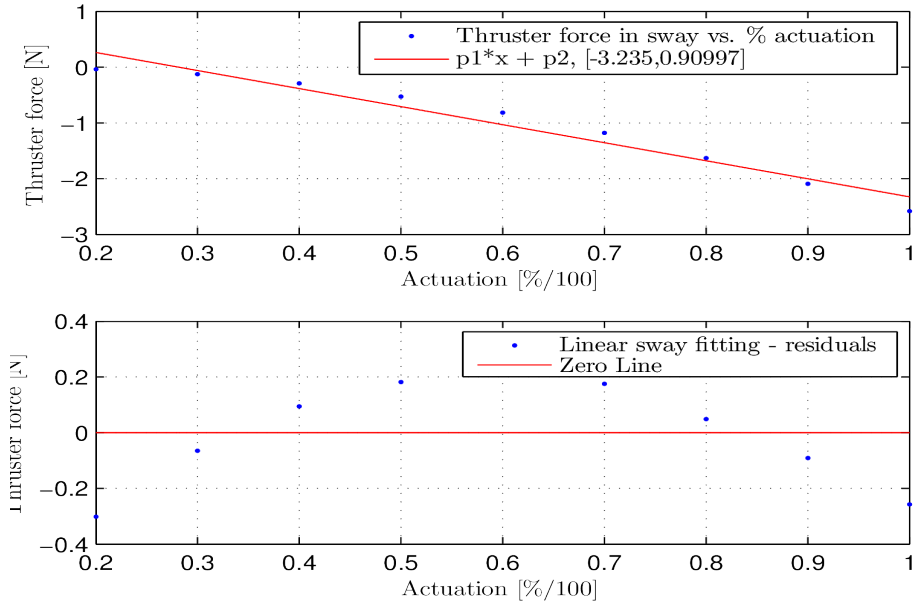

Figure 12.7: Force test in positive sway for thruster 1.

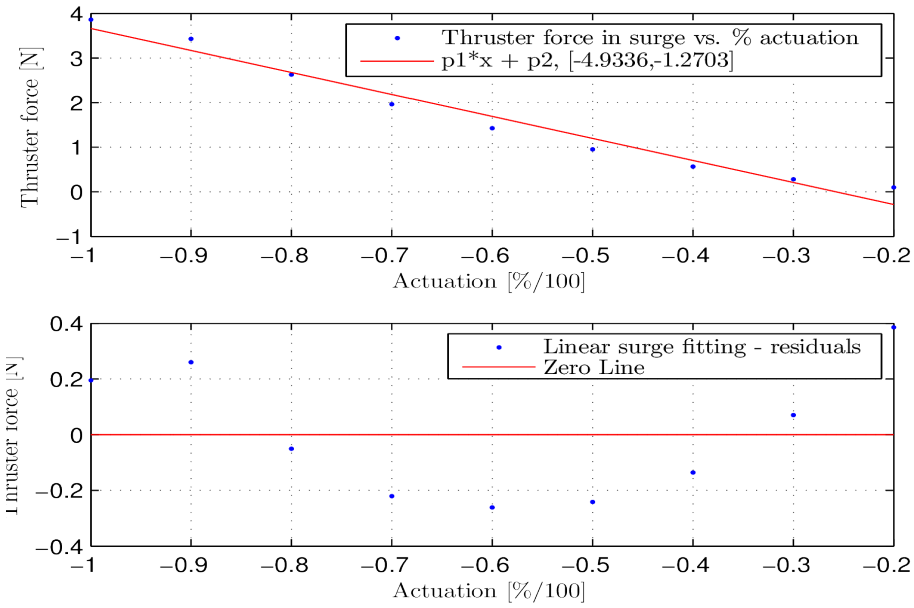

Figure 12.8: Force test in negative surge for thruster 2.

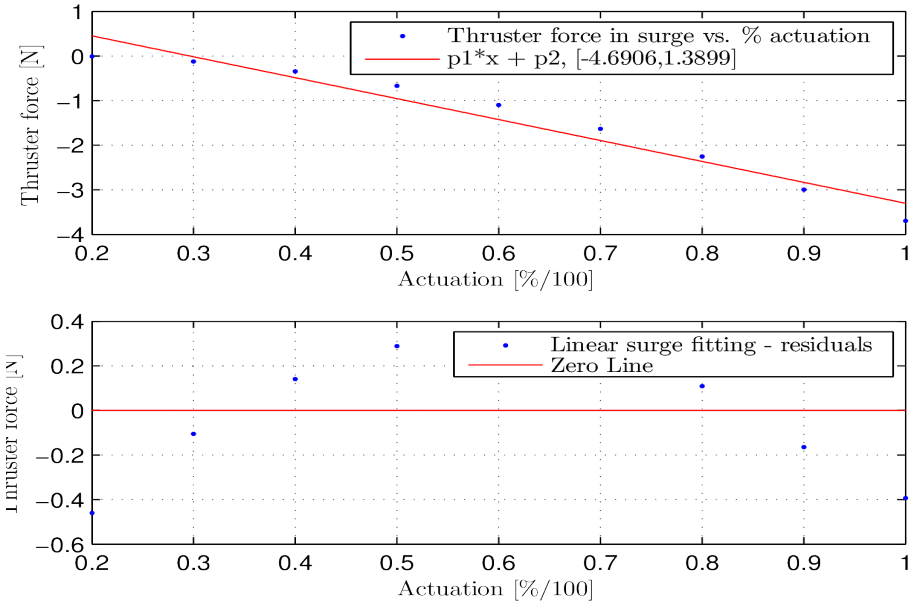

Figure 12.9: Force test in positive surge for thruster 2.

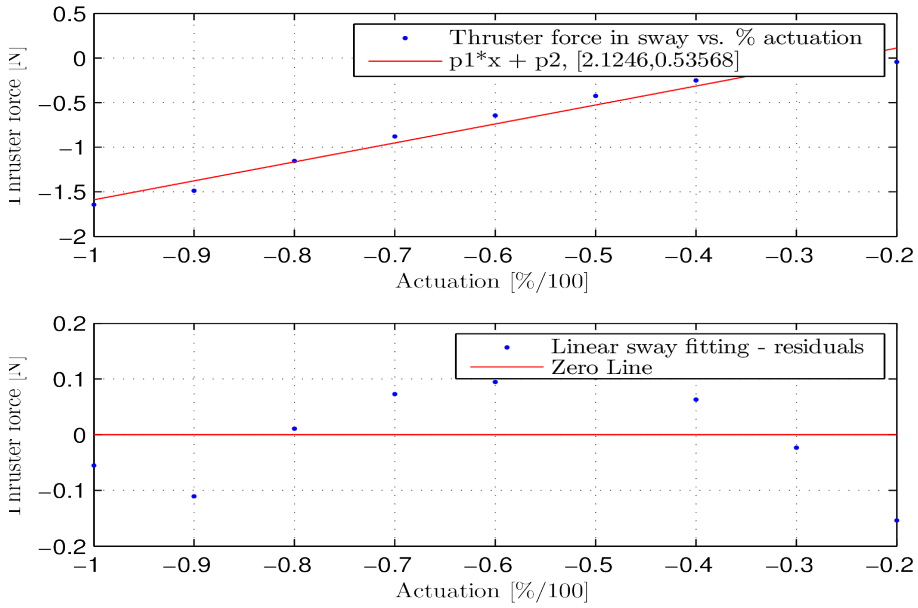

Figure 12.10: Force test in negative sway for thruster 2.

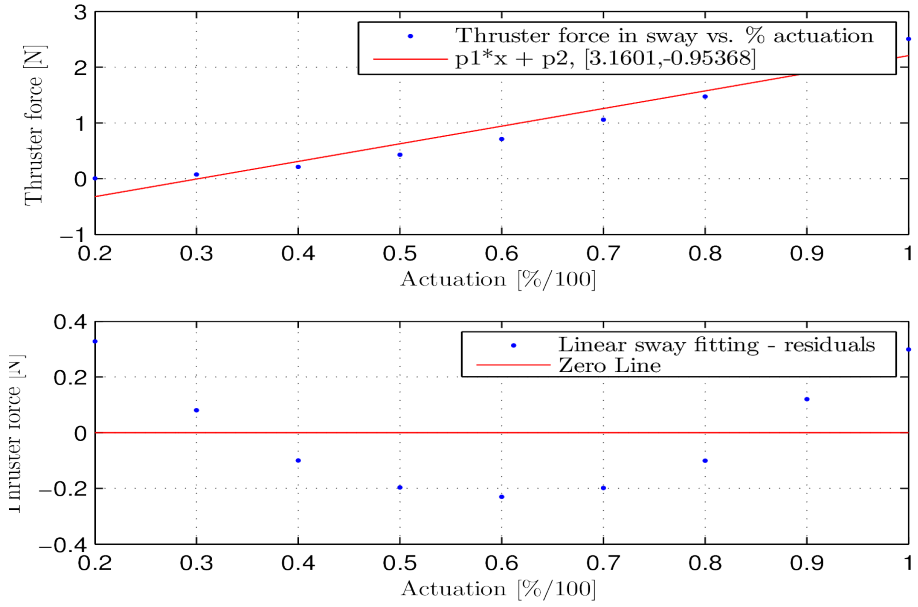

Figure 12.11: Force test in positive sway for thruster 2.

Chapter 13

Hardware-in-the-Loop Testing

Hardware-in-the-loop (HIL) is a testing method that is widely used in the marine industry, with established standards and procedures [Det Norske Veritas AS, 2011]. HIL testing allows testing of hardware and software without the vessel itself in motion. By simulating the responses of the vessel, the stability of a vessel and all its control systems can be ensured prior to a physical test.

Using the dynamic model suggested in Chapter 8, the HIL model for the CS Saucer can be defined as

$$(M_{RB} + M_A)\dot{\nu} + (C_{RB}(\nu) + C_A(\nu) + D + D_n(\nu))\nu = \tau \tag{13.1}$$

$$M\dot{\nu} + (C(\nu) + D(\nu))\nu = \tau \tag{13.2}$$

$$\tag{13.3}$$

where

$$M = \begin{bmatrix} m - X_{\dot{u}} & 0 & 0 \\ 0 & m - Y_{\dot{v}} & mx_g - Y_{\dot{r}} \\ 0 & mx_g - Y_{\dot{r}} & I_z - N_{\dot{r}} \end{bmatrix}$$

$$C(\nu) = \begin{bmatrix} 0 & 0 & -m(x_g r + v) \\ 0 & 0 & mu \\ m(x_g r + v) & -mu & 0 \end{bmatrix} + \begin{bmatrix} 0 & 0 & Y_{\dot{v}} v + Y_{\dot{r}} r \\ 0 & 0 & X_{\dot{u}} u \\ -Y_{\dot{v}} v - Y_{\dot{r}} r & X_{\dot{u}} u & 0 \end{bmatrix}$$

$$= \begin{bmatrix} 0 & 0 & (Y_{\dot{v}} - m)v + (Y_{\dot{r}} - mx_g)r \\ 0 & 0 & (X_{\dot{u}} + m)u \\ (m - Y_{\dot{v}})v + (mx_g - Y_{\dot{r}})r & (X_{\dot{u}} - m)u & 0 \end{bmatrix}$$

$$D(\nu) = \begin{bmatrix} X_u & 0 & 0 \\ 0 & Y_v & Y_r \\ 0 & N_v & N_r \end{bmatrix} + \begin{bmatrix} X_{|u|u}|u| & 0 & 0 \\ 0 & Y_{|v|v}|v| + Y_{|r|v}|r| & Y_{|v|r}|v| + Y_{|r|r}|r| \\ 0 & N_{|v|v}|v| + N_{|r|v}|r| & N_{|v|r}|v| + N_{|r|r}|r| \end{bmatrix}$$

and the thrust allocation with fixed angles from Chapter 7.1 is used for τ. The numerical values for the parameters in the matrices M, $C(\nu)$ and $D(\nu)$ are listed in Table 13.1. The process of estimating and calculating the numerical values of these parameters are discussed in Chapter 9, 10 and 11.

Parameter	Numerical value
m	6.3400 kg
x_g	0.0000 m
$-X_{\dot{u}}$	3.5000 kg
$-Y_{\dot{v}}$	3.5000 kg
$-N_{\dot{r}}$	0.0000
X_u	-1.9599
$X_{\|u\|u}$	7.0948
Y_v	-1.9599
$Y_{\|v\|v}$	7.0948
I_z	0.035 kgm^2

Table 13.1: Numerical values for the system parameters.

When HIL simulation is activated on CS Saucer, the control signals are fed back through the HIL sub VI as shown in Figure 17.1 instead of out to the

thruster motors and servo motors. The control signals are converted back to the force and moments vector τ and applied to the model (13.2).

The necessary preparations have been performed for a HIL simulation

- A dynamic model for the system has been proposed.
- The parameters of the dynamic model have been identified.
- The software on the embedded controller have been prepared for HIL implementation as described in Chapter 17.

The steps remaining in order to run a HIL simulation on the embedded controller myRIO are

- Implementation of dynamic model.
- Testing and validation.

Part V

High Level Control

The simplest form of automatic control of marine vessels was introduced with the gyro compass which made heading control possible [Skjetne, 2003]. As the number of possible available measurements has increased over the years, so has the number of control possibilities.

The modern control of marine vessels can be divided into the two categories seakeeping and stationkeeping. The term seakeeping is often used for vessels in transit traveling from one port to another. This type of control normally requires a constant speed that will optimize fuel and time consumption and heading control in order to navigate according to a predetermined path. Stationkeeping is used for low speed and higher precision control. Dynamic positioning systems on offshore vessels that want to hold a position either relative to another moving object or to a fixed point fall into this category.

Chapter 14

Dynamic Positioning

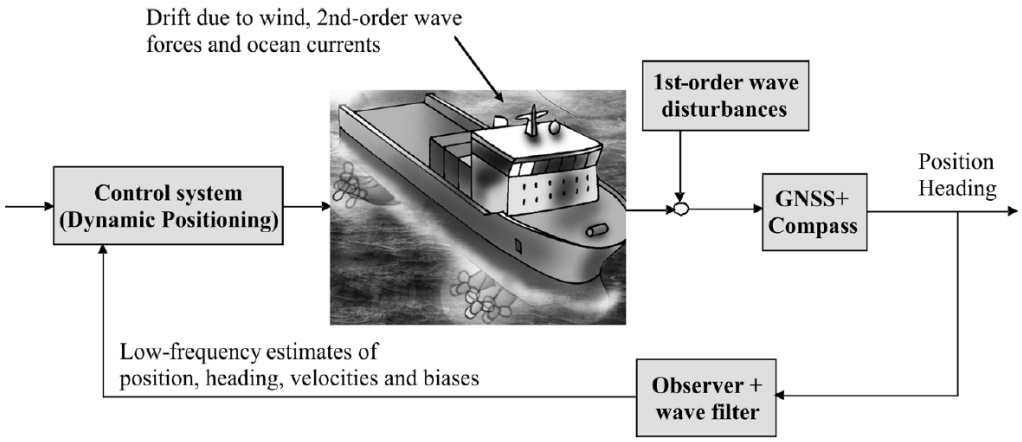

Figure 14.1: The main components and data flow of a dynamic positioning system [Fossen, 2011, p. 394].

A dynamic positioning (DP) system is generally used in low speed or station keeping operations. A fully actuated vessel is able to produce thrust in all the degrees of freedom of its configuration space. The configuration space of the surface vessel CS Saucer is defined to be the three degrees of freedom; surge, sway and yaw. A fully actuated vessel will therefore be able to control its states with thrust forces alone. The general structure of a dynamic positioning system is seen in Figure 14.1.

14.1 Dynamic Positioning Controller

The DP system implemented on CS Saucer is a straight forward state control solution, without an observer or a wave filter. This is a simplified system for use in the controlled conditions of the MC Lab. Not having an observer will lead to undesired behavior if the position signals is lost. It is therefore common to implement a dead reckoning system on real life systems where loss of measurements can lead to critical losses. A dead reckoning system will use the estimated data from the observer instead of using the measurements directly.

14.1.1 Reference Model

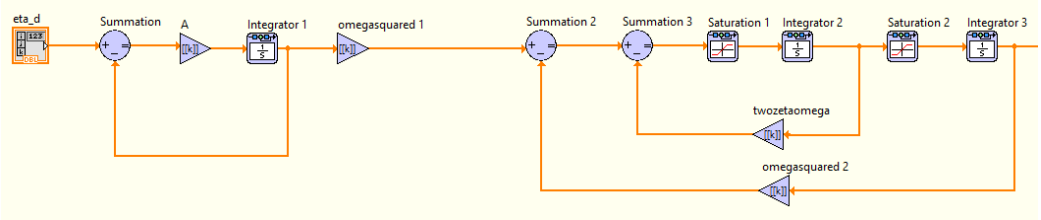

Figure 14.2: Reference model consisting of a low pass filter and a mass spring damper system.

The state vector of the system $\eta = [x\ y\ \psi]^T$ is controlled using the native PID controller VI in LabVIEW. The controller gain is calculated as

$$u(t) = K_c \left(\eta_e + \frac{1}{T_i} \int_0^t \eta_e \, dt + T_d \dot{\eta}_e \right) \tag{14.1}$$

where T_i is the integral time gain and T_d is the derivative time gain, both in minutes [National Instruments, 2008, ch. 2]. The error η_e in (14.1) is

$$\eta_e = R(\psi)(\eta_r - \eta) \tag{14.2}$$

where the reference η_r is generated by a third order reference model with a low pass filter combined with a mass-spring-damper system. The error vector

η_e is rotated to the body frame $\{b\}$ with the rotation matrix (14.3).

$$R(\psi) = \begin{bmatrix} \cos(\psi) & \sin(\psi) & 0 \\ -\sin(\psi) & \sin(\psi) & 0 \\ 0 & 0 & 1 \end{bmatrix} \tag{14.3}$$

The reference model is implemented as shown in Figure 14.2. This implementation is based on the position and attitude reference model proposed in [Fossen, 2011, p. 251]. The saturation blocks saturate the velocity and acceleration of the reference signal. This ensures that the reference does not "run away" from the state of the vessel in the event of a jump in the desired state η_d which is fed into the reference model. As explained in [Fossen, 2011], the saturation blocks should be tuned to the physical limitations of the vessel so that the error η_e can converge to zero. The parameters used for the implemented reference model are shown in Table 14.1.

LabVIEW block	Gain matrix/Saturation vector
A	diag([0.8, 0.8, 1.1])
omegasquared 1	diag([0.8, 0.8, 1.1])
omegasquared 2	diag([0.8, 0.8, 1.1])
twozetaomega	diag([1.7889, 1.7889, 2.0976])
Saturation 1	$[-0.13, -0.13, -0.26]^T$, $[0.13, 0.13, 0.26]^T$
Saturation 2	$[-0.28, -0.28, -0.56]^T$, $[0.28, 0.28, 0.56]^T$

Table 14.1: The gain matrices and saturation vectors for the implementation of the reference model in DP on CS Saucer.

When the DP controller is activated, ideally the reference should be initialized as $\eta_r = \eta$. However, this was not successfully implemented in LabVIEW. The DP controller will therefore receive a large error η_e unless the vessel is positioned very close to the position and attitude $\eta_{zero} = [0, 0, 0]^T$. This large error will lead to a high initial thrust force and an unstable performance from the vessel at best. This initialization problem has been solved by setting the PID gains to zero and feeding the current position η into the reference model for the first twenty seconds of the run time. This time is sufficient for the reference model to catch up to any current position that the vessel might have. After the initialization is completed the user will be alerted by an

indicator in the user interface, the PID gains will be switched back to the ones selected by the user and the desired position η_d defined by the user will be fed into the reference model. This solution has proved to be robust and the vessel responds smoothly to the reference signal after the initialization is complete.

14.1.2 Heading Error

In order to keep the heading of the vessel stable a wrap-around fix of the error ψ_e has been implemented with the code shown in Listing 14.1. With this fix the error is turned in the opposite direction if the original error is $|\psi_e| > \pi$. The wrap-around fix is illustrated in Figure 14.3.

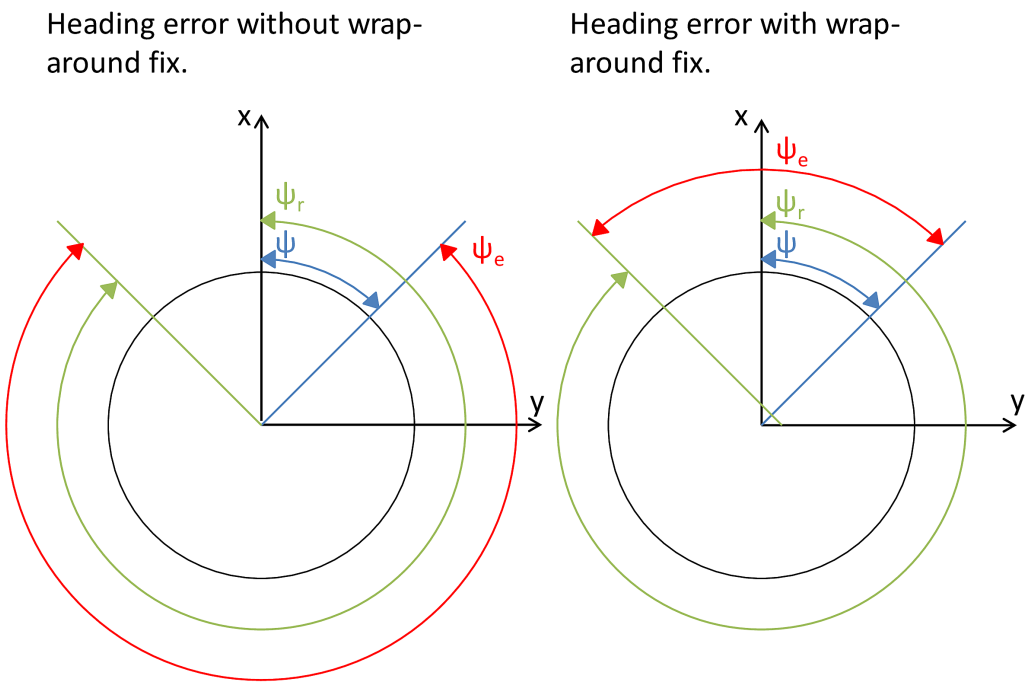

Figure 14.3: Wrap-around heading error on CS Saucer.

Listing 14.1: Calculate heading error with wrap-around.

```
function err = calculateError(psi_r, psi)
  err = psi_r - psi;
  if err > pi
    err =  err - 2*pi;
  elseif err < -pi
    err = err + 2*pi;
  end
end
```

14.1.3 Thrust Saturation

A saturation on the commanded force τ has been implemented in the DP control system. This solution allows the user to tune the DP controller aggressively and at the same time specify an upper limit to the forces commanded in the three degrees of freedom. The saturation logic saturates the total thrust force in surge and sway $F = \sqrt{X^2 + Y^2}$ and the moment N in yaw. The moment N is simply saturated to a fixed value specified by the user. The total thrust force in surge and sway F is saturated so that the relationship between X and Y remains the same. The implemented logic for this solution is shown in Listing 14.2.

Listing 14.2: Saturation of the total commanded thrust force in surge and sway.

```
function [Xout, Yout] = saturateF(X, Y)
Fmax = 3.7;
theta = atan(Y/X);
signX = sign(X);
signY = sign(Y);
Xout = X;
Yout = Y;
F = sqrt(X^2 + Y^2);
if (F > Fmax)
    Xout = cos(theta)*Fmax*signX;
    Yout = sin(theta)*Fmax*signY;
end
```

14.2 Test Case: Change of Stepping

In this test case, the desired state vector has been altered while running DP. This causes step changes in the desired value of all three states, as can be seen in Figure 14.4.

Figure 14.4 and 14.5 shows the state of the system and the position of the vessel, respectively. The states x and y follow their references x_r and y_r with some delay. However it is clear from the figure that both states converge to their references. The controller gains can be increased in order to get the two states to follow their references more closely. This would increase the small overshoot that can be seen in the figure and a larger derivative gain would therefore be recommended to counteract this issue. The third state in Figure 14.4, ψ, converges to its reference ψ_r quite rapidly. The vessel is very responsive in yaw motion and a lower proportional gain than for the previous states is necessary to get the state to follow its reference. The derivative gain is critical in this state as a pure proportional controller would result in large overshoots and possibly a non stable system.

As seen in Figure 14.4 the reference state $\eta_r = [x_r, y_r, \psi_r]$ smooths out the step signal generated by the desired state $\eta_r = [x_d, y_d, \psi_d]$. The acceleration and the speed of the reference models are sufficiently low so that the actual state can converge to the desired state.

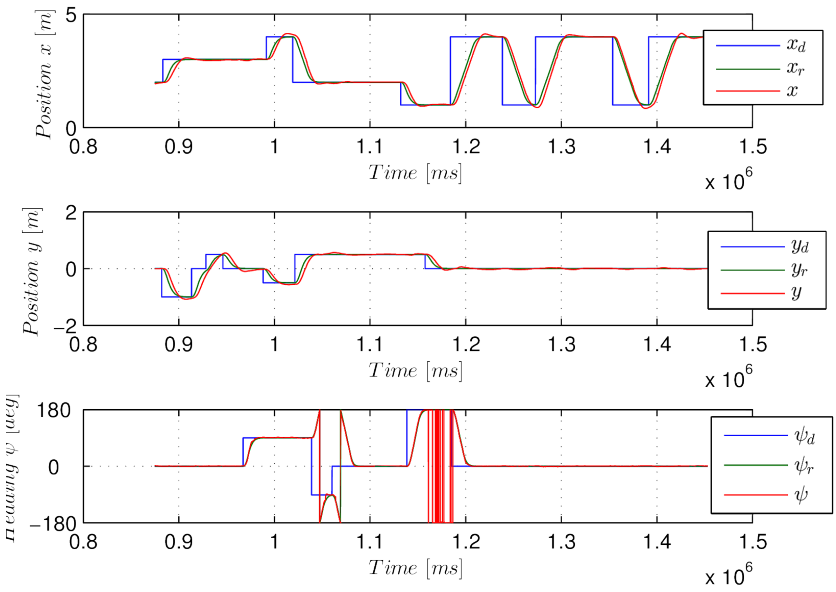

Figure 14.4: System state vs reference state and desired state in dynamic positioning.

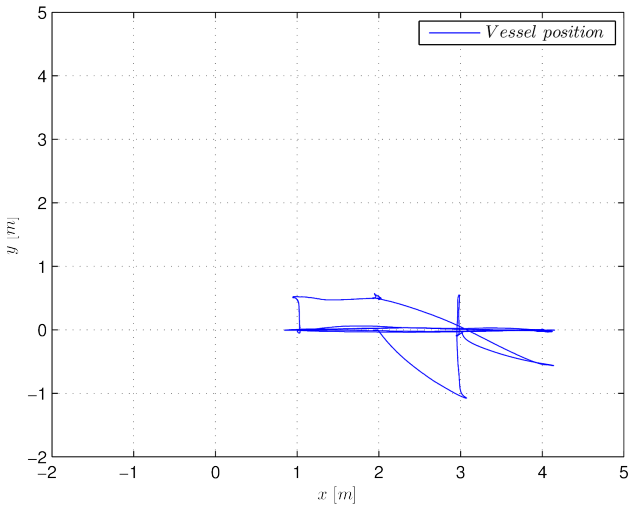

Figure 14.5: Vessel position in dynamic positioning.

Chapter 15

Path following

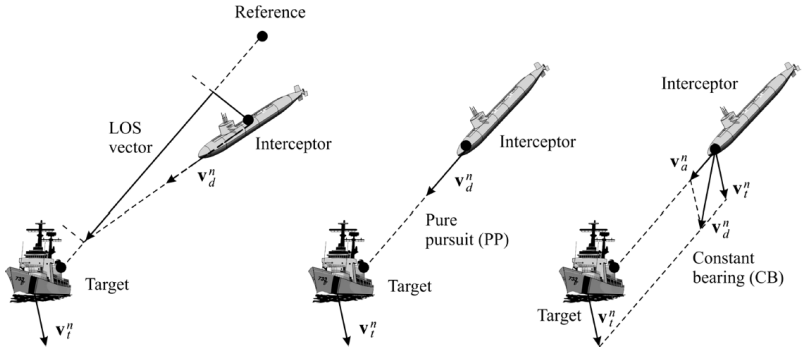

Figure 15.1: The three guidance strategies "Line-of-Sight", "Pure Pursuit" and "Constant Bearing" [Fossen, 2011, p. 243].

When tracking a target, the three guidance strategies "Line-of-Sight", "Pure pursuit" and "Constant Bearing" are considered to be the fundamental strategies [Breivik et al., 2008].

Line-of-sight (LOS) Guidance is a three point guidance system with the LOS vector directed from the typically stationary reference point to the target. The tracking entity, defined as the interceptor [Fossen, 2011, p. 242], is guided by the LOS vector towards the target. Pure pursuit guidance is a two point guidance strategy where the interceptor tracks the target directly by

aligning its course directly towards the target. As insinuated by its name, this strategy usually leads to the interceptor tailing the target. Constant bearing guidance is a two point guidance strategy where the interceptor approaches the target with a constant bearing so that the interceptor remains on a direct collision course with the target. These three guidance strategies are visualized in Figure 15.1.

15.1 Path Following Controller

In this thesis, path following is implemented with a version of Pure Pursuit guidance where the vessel tracks the next waypoint in the waypoint array (15.2) by controlling the heading of the vessel so that

$$\psi = \psi_{wp} \tag{15.1}$$

where ψ_{wp} is the angle of the current waypoint in the inertial coordinate system.

$$p_{wp} = [(x_1, y_1),\ ...,\ (x_n, y_n)] \tag{15.2}$$

15.1.1 Proximity to Waypoint

The proximity check to the current waypoint is implemented as shown in Listing 15.1. The proximity to the current waypoint is calculated as

$$e = \sqrt{(x_{wp} - x)^2 + (y_{wp} - y)^2} \tag{15.3}$$

The acceptance radius, which is defined as acceptanceradius = 0.3 in Listing 15.1, forms a circle of acceptance around the current waypoint. Once the vessel is inside this circle the current waypoint will change to the next waypoint in the array of waypoints. The acceptance radius can be tuned to modify the behavior of the vessel near waypoints. A acceptance radius that is too low could led to the vessel circling the target multiple times before the proximity check is positive. The circle of acceptance must therefore be designed with the precision of the controller in mind. In Listing 15.1, the

boolean variable *nextWP* will update the index of the current waypoint in the array of waypoints in the event of a positive proximity check.

Listing 15.1: Proximity of CS Saucer to the current waypoint.

```
function [x, y, nextWP] = proximitycheck(psi_r, psi)
  acceptanceradius = 0.3;
  nextWP = false;
  e = real(sqrt(e_x^2 + e_y^2));
  if e < acceptanceradius
    nextWP = true;
  end
end
```

15.1.2 Rudder model

A simplified thrust configuration has been chosen for path following. The bow thruster is fixed along the positive x-axis of the body fixed coordinate system while the rear port and starboard thrusters rotate based on the desired heading. The two rear thrusters will always be aligned parallel to each other, effectively acting as a single rudder situated at the x axis between the two thrusters.

The three thruster are actuated by constant control signals similar to a vessel in transit with constant speed. To prevent the two rear thrusters from dominating the bow thruster, the bow thrusters should not produce a combined thrust force that is larger than the thrust force created by the bow thruster. With this solution the bow thruster should dominate the two rear thrusters and help straighten the vessel to a stable course when the rudder is set to zero degrees. Course stability is an issue for unorthodoxly shaped vessels like the CS Saucer. The very low drag resistance of the vessel in the yaw motion reduces the vessels ability to stabilize to a course when the rudder model is set to zero degrees. Because of the relatively small area of operation in the MC Lab, the thrust forces are set relatively low so that the vessel is able to follow the desired waypoints without drifting out of the area covered by the positioning system.

With a constant thrust command, the rudder angle is controlled to minimize the heading error $\psi_e = \psi_d - \psi$. The desired rudder angle δ_d is obtained by

applying a proportional heading error as defined in (15.4).

$$\delta_d = K_p \psi_e \tag{15.4}$$

The desired rudder angle is saturated to $(-30^o,\ 30^o)$.

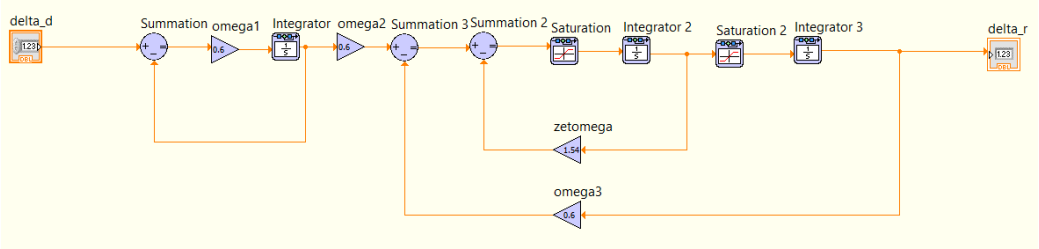

Figure 15.2: Reference model for the rudder angle consisting of a low pass filter and a mass spring damper system.

Figure 15.2 shows the reference model implemented for the rudder angle reference δ_r. However, since the servo motors controlling the angle of the thrusters are highly responsive, such a reference model for the rudder angle is not neccessary as the thrusters can handle the direct step reference $\delta_r = \delta_d$. The desired heading angle ψ_d is obtained by calculating the position error $\tilde{p}(t)$ (15.5).

$$\tilde{p}(t) = p_d - p(t) \tag{15.5}$$

where the position vector with respect to time is $\tilde{p}(t) = [x,\ y]^T$ and the desired position is the coordinates to the current waypoint $p_d = [x_d,\ y_d]^T$. The desired heading angle is then calculated as seen in Listing 15.2.

Listing 15.2: Calculate the desired heading to the current waypoint.

```
function psi_d = getPsi_d(x_e, y_e)
  psi_d = atan2(e_y, e_x);
  if(psi_d < 0)
    psi_d = 2*pi - abs(psi_d);
  end
end
```

The desired heading ψ_d is fed in to the wrap-around function seen in Listing 14.1 before it is applied to (15.4).

15.2 Test Case: Rudder Model

The results from the rudder model implementation reveal quite a severe course instability in the CS Saucer. The vessel showed a bias to the port side which could not be compensated for by the rudder. The vessel therefore turned in large counter-clockwise circles around the current waypoint without converging to a more stable path. Manual testing of the course stability was performed to rectify this issue. After extensive testing the angle of the fixed thruster was adjusted to $\alpha_0 = 1.255^o$. The control forces applied to the thrusters were also tuned to obtain a more stable course. The adjusted control inputs to the thrusters can be seen in Table 15.1.

Thruster id	Control input
u_0	0.21
u_1	0.07
u_2	0.12

Table 15.1: Adjusted control inputs to the thrusters in rudder path following mode.

The results from testing of path following with the rudder model are shown in Figure 15.3, 15.4 and 15.5. As seen in Figure 15.3 the position of the vessel $p(t) = [x, y]$ does not converge to the position of the current waypoint. The position of the vessel oscillates around the desired position. This phenomenon can also be observed in Figure 15.4 where the the vessel clearly circles the current waypoint $p_{wp} = [4.097, 0.673]$. Figure 15.5 shows the rudder angle and the heading of the vessel versus the desired heading. It is clear from these results that the proportional control law is not sufficient to make the heading converge to the desired heading.

The manual tuning of the bow thruster angle α_0 and the control inputs yielded little to no improvement in the results. Due to the bowl shape of CS Saucer, the vessel is highly sensitive to both the rudder angles and drag forces in the yaw motion. The manual tuning straightened the course marginally, however after about two meters the vessel still veered of to either the starboard or the port side. The vessel ends up in a constant circular motion with a constant heading error $\psi_e = \psi_d - \psi$.

Saturating the rudder angle at $(-10^o,\ 10^o)$ yielded no significant improvement to the vessel response. A possible solution to the course instability is to add integral action to (15.4) so that ψ_e will converge to zero. It is concluded that a more complex control theory must be designed in order to keep the vessel course stable. A control law with proportional and integral action can be defined as

$$\delta_d = K_p \psi_e + \int_0^t \psi_e \, dt \tag{15.6}$$

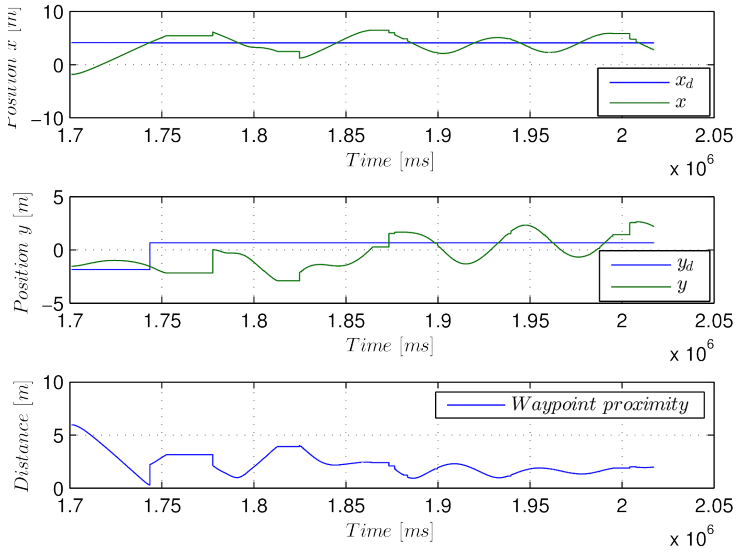

Figure 15.3: Position and proximity to waypoint, path following with rudder model.

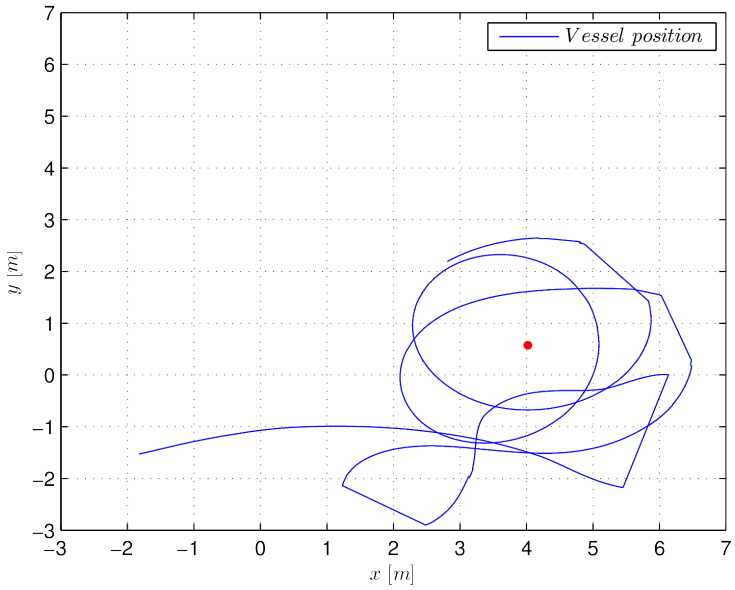

Figure 15.4: Position plot, path following with rudder model.

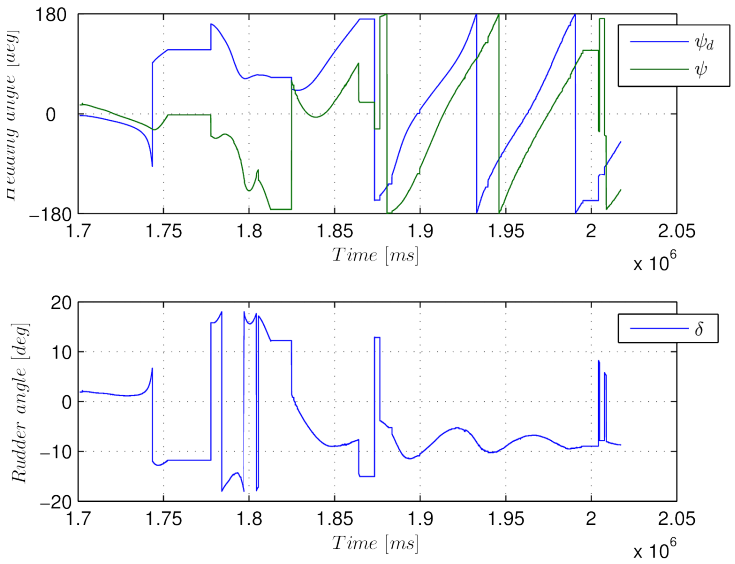

Figure 15.5: Rudder angle and heading vs desired heading, path following with rudder model.

15.3 Test Case: DP model

As a proof of concept for the waypoint logic, the DP controller described in Chapter 14 has been implemented with the waypoint array and the proximity check described earlier in this chapter. With the DP controller, the vessel does not simulate transit operation as with the rudder model. The desired heading can be set to the current waypoint as in the rudder model implementation. However, with the DP controller the desired heading is arbitrary as the position is controlled independent of the heading. This implementation therefore serves as a quality test for the waypoint array implementation and the embedded switching logic.

The results for path following with the DP model are shown in Figure 15.6 and 15.7. As in the results in Chapter 14 the actual position of the vessel converges to the desired position. Figure 15.6 also shows that the change in desired position from one waypoint to the next works satisfactory.

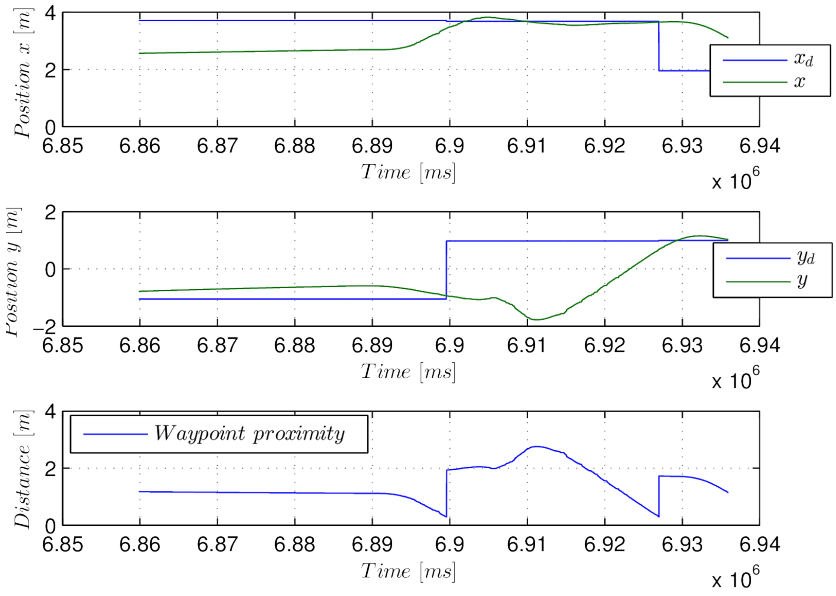

Figure 15.6: Position and proximity to waypoint, path following with DP model.

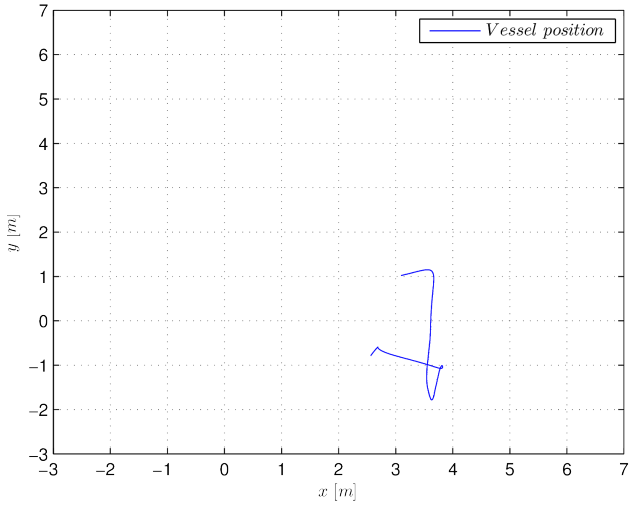

Figure 15.7: Position plot, path following with DP model.

Part VI

Software Development and Implementation

The software developed in this thesis is saved in the LabVIEW myRIO project "CyberShip Saucer". The software runs on the 2014 edition of the LabVIEW software. The additional modules required to run the software are listed in Table 15.2. As seen in Figure 15.8 the host and the target are both shown in the project explorer, where the target is the NI myRIO and the host is the computer running the project. The host "My Computer" runs the user interface which sends controls to the target and monitors simultaneously. The host and the target communicate over a local area network via shared variable nodes created in LabView. A more detailed explanation of the software implementation is given throughout this part.

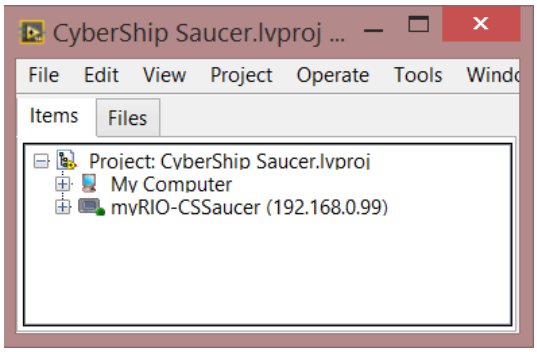

Figure 15.8: Project explorer for the project "CyberShip Saucer" in LabVIEW.

Software Module
LabVIEW 2014 myRIO Toolkit
LabVIEW 2014 Real-Time Module
LabVIEW Control Design and Simulation Module

Table 15.2: NI LabVIEW software modules required to run the project "CyberShip Saucer".

Chapter 16

Host VI

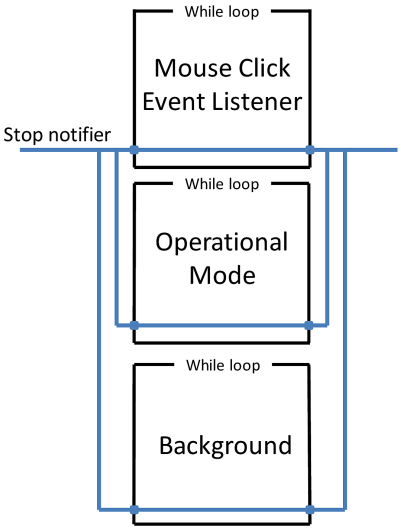

Figure 16.1: Parallel while loop structure in Host.vi.

The host application is run from the file "mainHost.vi". This application incorporates several subVIs that are located in the "subVIHost" folder. Graphical programming can very quickly become messy with wires running everywhere on the screen. SubVIs help structure code into modules so that the application remains structured as its complexity increases [National Instruments, 2015*b*].

The host application provides simultaneous monitoring of the vessel and user interaction. This is obtained by running several while loops in parallel, creating a multi threaded application that can preform tasks asynchronously. Stop handling is crucial when running multiple loops in parallel. A notifier is therefore implemented that connects the while loops together and passes a notification in the event of a stop command [National Instruments, 2014*b*]. The multi threaded structure of the host application is shown in Figure 16.1. The event listener loop enables the user to manually set waypoints or create an ellipse directly in a graph in the interface.

The operational mode loop handles the active operational mode selected at all times. The background loop receives all monitoring data from the target via shared variables and this target is visualized in the user interface. The Background loop also broadcasts shared variables to the target.

16.1 Vessel Position Plot

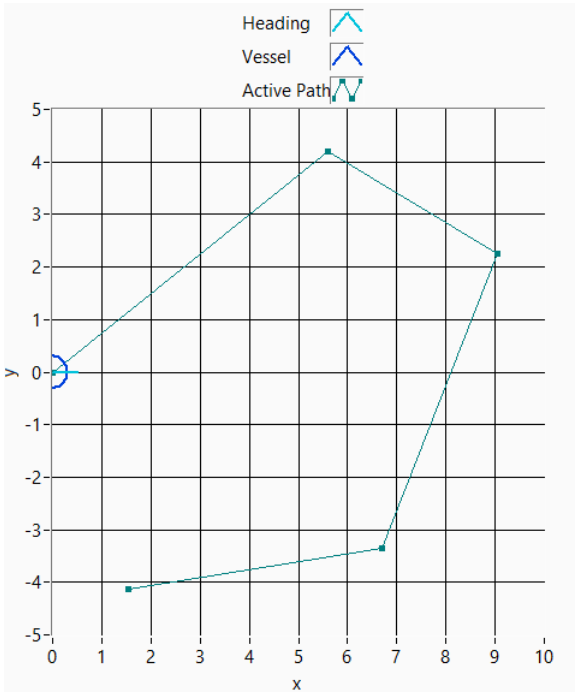

Figure 16.2: XY Graph showing the position, heading and desired path of CS Saucer.

The right hand side of the user interface displays real time data on the position and heading of the vessel in a XY Graph. When operated in one of the path following control modes this graph will also display the selected path for the vessel to follow. This feature is shown in Figure 16.2. The position of the vessel can also be monitored via the Dashboard app, where the position of the vessel is broadcasted directly from the myRIO to the device. This feature is shown in Figure 16.3.

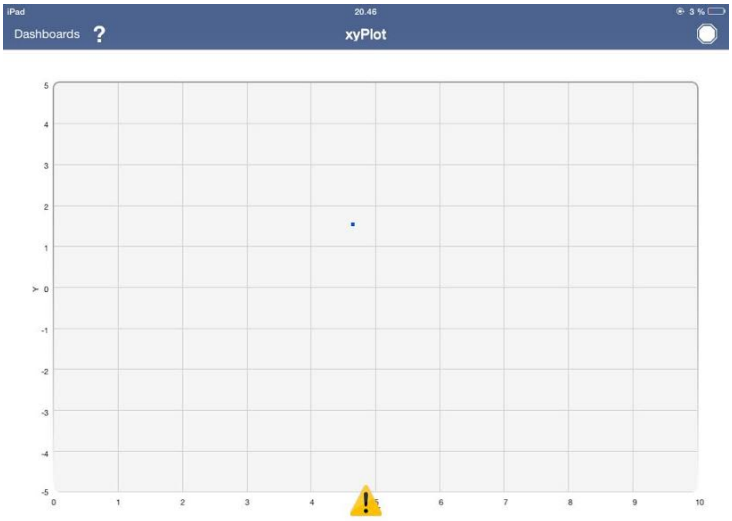

Figure 16.3: iPad Dashboard interface with an XY Graph showing the position of the vessel.

16.2 Thruster Force Visualization

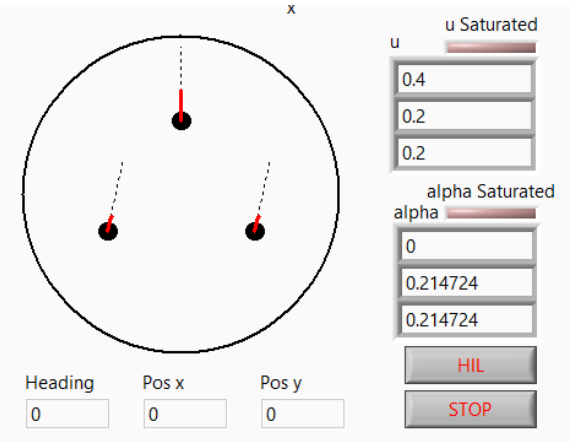

Figure 16.4: 2D drawing visualizing the current commanded thrust command signals u and thruster angles α.

In addition to position and heading data, the commanded force signal to each thruster $u = [u_0, u_1, u_2]^T$ and the thruster angles $\alpha = [\alpha_0, \alpha_1, \alpha_2]^T$ are updated in real time and visualized in a 2D pixel drawing. An indicator is located by the values to alert the user in the event of a saturation of the signals. This feature is shown in Figure 16.4.

16.3 Control Mode Tabs

The switching between control modes is implemented with Tab controls in LabVIEW. The Tab control is generally implemented using a case structure in the block diagram where each tab correspond to a case. However, for this application an event structure was used for the mouse click features in the "Path following" tab. An event structure is necessary to implement mouse click interaction between the user and the interface. However event cases for other events, such as a value change for the "Stop" button were also added to the event structure. These added event cases adds robustness to the application.

16.3.1 Manual Thruster Control

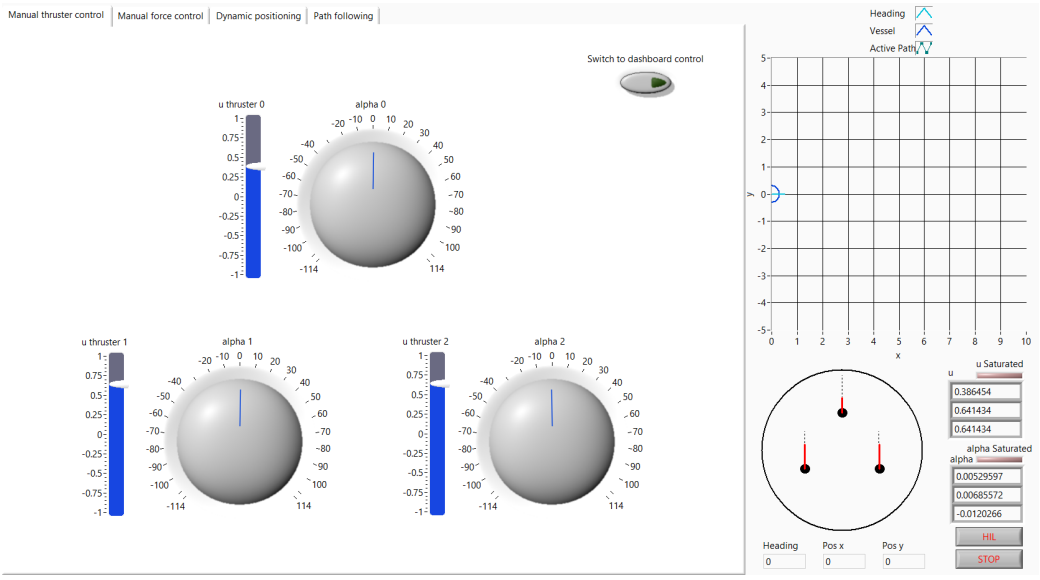

Figure 16.5: User interface in Manual Thruster Control mode.

Figure 16.5 shows the user interface for the "Manual thruster control" operational mode. The control signals to the individual thrusters are sent to the target via shared variables over the local area network. By activating dashboard control, the target can be controlled directly from an Android or iOS device using the NI Dashboard app [National Instruments, 2014*a*].

16.3.2 Manual Force Control

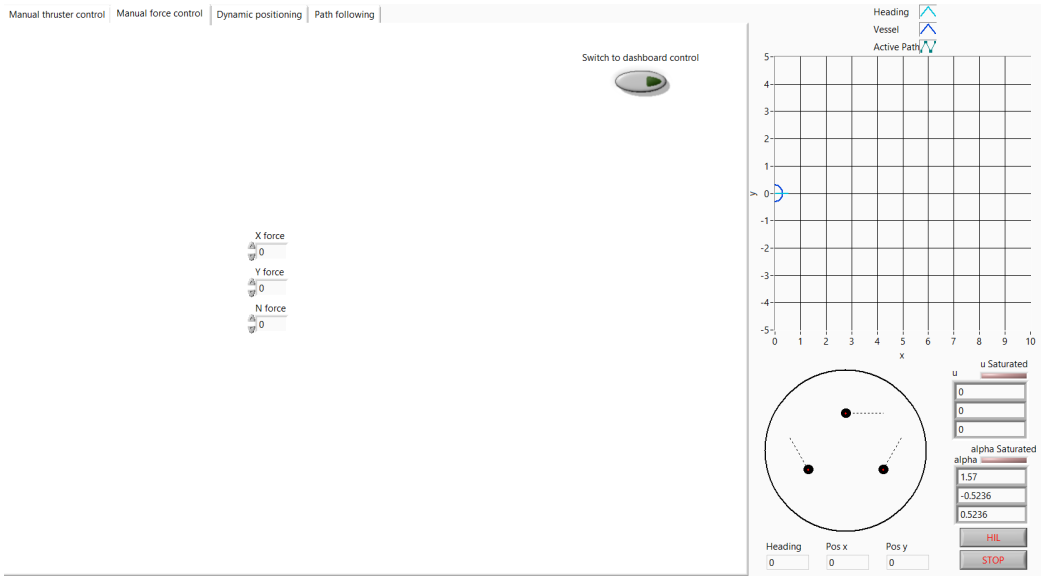

Figure 16.6: User interface in Manual Force Control mode.

Figure 16.6 shows the user interface for the "Manual force control" operational mode, where the force commands in surge, sway and yaw are sent to the target via shared variables. Like the "Manual thruster control" mode, the "Manual force control" mode can also be operated from the NI Dashboard app. This feature is shown in Figure 16.7.

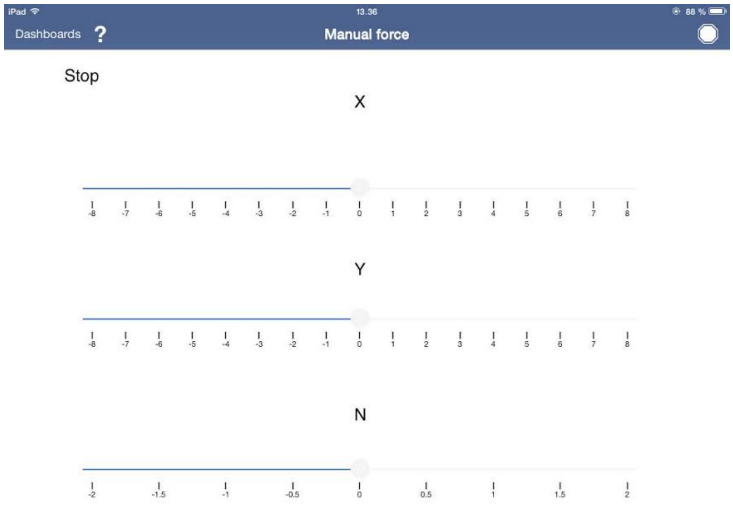

Figure 16.7: iPad Dashboard user interface in Manual Force Control mode.

16.3.3 Path Following

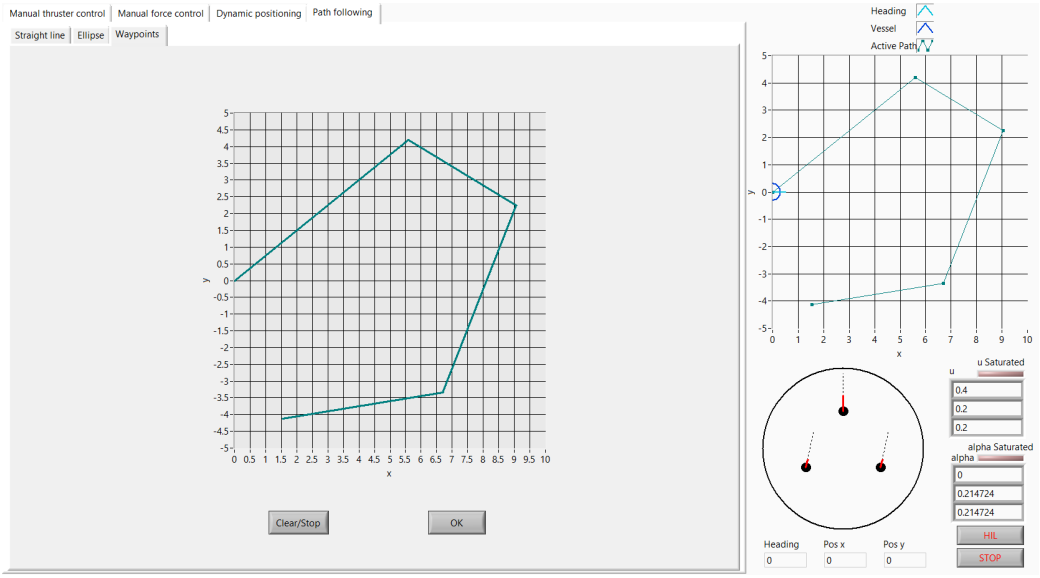

Figure 16.8: User interface in Waypoint Path Following Control mode.

Figure 16.8 shows on of the three possible ways of generating a waypoint array in the user interface. The path following mode is deployed when the user presses the "Ok" button, and can be aborted at any time by pressing the "Clear/Stop" button. The two XY plots in the tab control of the "Straight line" and "Waypoint" modes are linked to their own mouse click event case, which populates the waypoint array as the user clicks. The "Ellipse" waypoint array is created by selecting the foci and the roundness of the desired ellipse.

Chapter 17

Target VI

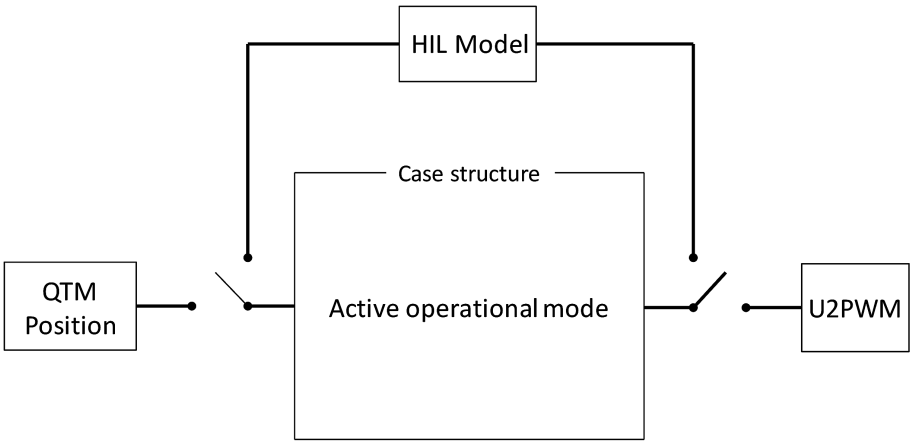

Figure 17.1: Visualization of data flow through the target main VI.

As seen in Figure 17.1, the main data flow of the target application goes through a case structure with one case for each of the operational modes available.

17.1 Shared Variable Nodes

The host and the the target communicate via shared variable nodes. The shared variable nodes are stored on the target in libraries corresponding to the function they serve. Each operational mode has a library with the shared variable nodes used specifically for that mode. The monitoring variables used by the host VI to display real-time information on the vessel is also stored in a separate library.

17.2 Measurements

The current position of the vessel is fed in to the case structure and the control signals to the motors and the servo motors is fed out from the case structure. The position and heading of the vessel is read from the Qualisys Track Manager (QTM) custom module that has been imported to the myRIO controller. This module is initialized on startup and reads the position at every ten milliseconds, the same frequency that the application runs at. The information read by the QTM module is converted to SI units with the "QTM2SI" subVI. The available measurements of the vessel are $\eta = [x, y, z, \psi, \theta, \psi]$.

17.3 Custom Controls

In order to create a shared variable for more complex data types, a custom control with a type definition must be created [National Instruments, 2011*a*]. The waypoint arrays used in the application are in reality arrays of clusters of two double precision numbers. A custom control must be developed graphically in LabVIEW and saved as a ".ctl" file. With the custom control created, a shared variable can be assigned this data type by selecting the custom control instead of the standard data types when creating a new shared variable node.

17.4 Battery Voltage Monitoring

Outside of the operational mode case structure, the voltage of one of the cells of the LiPo battery is monitored. Assuming all three cells of the battery are balanced, which is reasonable when the battery is functioning normally, checking one of the cells is sufficient to decide if the total voltage of the battery is too low. When the voltage of the battery is lower than the specified limit, a dialog box with instructions to charge the battery will appear on the host computer. Clicking "OK" in this dialog box will automatically stop the target VI, ensuring that the battery is not drained past its limit.

17.5 Controllers and HIL Simulation

The controllers for each of the control modes are developed in sub VIs that are placed in the appropriate case in the main VI. The active case corresponds to the case id that is fed into the case structure. This case id is transmitted from the host VI. All control subVIs produce control signals for the three motors and servo motors which are sent out of the operational mode case structure and to either the HIL model or to the "U2PWM" sub VI which in turn drives the motors and servo motors. The "U2PWM" module is explained in Chapter 6.3. The PWM signals are sent out through the pinouts listed in Table 5.1 through the myRIO PWM Express VIs native to the myRIO toolkit.

As seen in Figure 17.1, by activating the HIL mode, the control signals will feed through the HIL model instead of out to the hardware of the vessel. The state vector that feeds in to the operational mode case structure will be from the HIL model instead of the QTM module. The HIL mode is activated with a boolean shared variable node that is controlled from a button in the host application.

17.6 Data Logging

Continuous data logging has been implemented in the main target application. On initialization, a ".csv" file is created for each of the control modes.

The log file for a control mode will only be populated when that particular control mode is active. Each log file is created with a control mode identifier and a time stamp, e.g. "dp114700". The log file format ".csv" (comma separated values) is highly compatible with MATLAB and enables easy import and post processing of the data in MATLAB. The import code in the script is easily created using MATLAB's import file wizard which generates code for the import of a specific file. Data is logged at 100 Hz, using the LabVIEW Base packace function "Write to Text File" [National Instruments, 2011*b*]. A detailed instruction in the log file extraction process can be found in Appendix B.

Part VII

Conclusions and Further Work

Chapter 18

Conclusions

The marine cybernetics vessel CS Saucer has been designed, constructed and assembled to an operational vessel. The vessel has a shallow draft and is highly maneuverable in all directions. The vessel's three azimuth thrusters are powered by three Torpedo 800 motors and three Graupner DS8311 servos. The embedded controller is run by a National Instruments myRIO, which feeds PWM signals to the servos and to the motors via three ESCs. Manual thruster control, manual force control, dynamic positioning and a tentative path following control has been implemented on CS Saucer.

The vessel was constructed according to plan, however the weight of the hull turned out to be heavier than the initial estimates. The final weight of the vessel with the lid on is 6.43 kg. This gives a draft of approximately 4 cm, a draft that is larger than desired for the payload configuration with the myRIO controller. The weight of the hull alone is about 3 kg. Much of the extra weight is believed to come from the multiple layers of epoxy that was applied to ensure a good finish and a watertight hull. Estimates for the weight of the added epoxy was not considered in the initial estimates

System identification shows that the vessel has very little drag resistance. This is something that was anticipated due to the saucer shape of the hull. However, highly maneuverable shape of the hull introduces some new issues. The vessel is not course stable, something that complicates the implementation of path following control.

A linear approximation of the thrust forces has been used to implement the

thrust allocation. The thrust allocation works well with dynamic positioning and is generally considered precise enough for the control applications currently implemented on the vessel. However, manual force control in surge, sway and yaw shows some lack in course stability. The vessel response is more precise for higher control inputs to the thrusters, as the linear approximation is at its most precise for high inputs. This can be seen from the thrust force mapping results discussed in Chapter 12.

The software and hardware combination from National Instruments has proved to be both reliable and easy to use. The graphical programming language in LabVIEW, although sometimes a bit visually confusing, is very well documented with many articles and tutorials for first time users. The embedded controller myRIO has performed very well during this thesis and is easy to program and configure through LabVIEW and other National Instruments software.

Chapter 19

Further Work

19.1 Construction and Components

During the course of this thesis the realization has been made that the switching voltage converters that feed power to the servo motors may be unnecessary. The ESCs used to drive the propellers provide a 5V current that can be used to drive the servo motors. This should be investigated further and tested. Eliminating unnecessary components will lead to a more power efficient, stable and clean system. To test this theory, the red power wires from servo and ESC should be connected through a circuit board while the PWM signal wires and the ground wires remain connected as before.

In order to reduce the draft of the vessel, a new top lid should be made. The current lid made of plexi glass is unnecessarily thick at 4 mm. A thinner plexi glass lid or a lid made from another waterproof material will reduce the total weight of the vessel.

19.2 Low Level Control

19.2.1 Thrust Allocation

A complete thrust allocation for CS Saucer with azimuth angles α should be developed. In thesis the thrust allocation has been simplified with fixed thruster angles. However, the groundwork for a complete thrust allocation has been laid in Chapter 7.

19.2.2 Manual Control via Bluetooth

Manual control of the CS Saucer is currently only available through the host application and the Dashboard app for Android and iOS devices. In the future a manual control via bluetooth should be implemented for the vessel. Bluetooth support on the myRIO will make it possible to control the vessel via a joystick such as the Playstation 3 controller. A joystick control solution via bluetooth will make it easier to control the vessel manually in addition to serving as a failsafe in case of network error. Support for direct connection of the Playstation 3 controller via usb is currently possible with the use of the "Control Design and Simulation" module in NI LabVIEW [National Instruments, 2015*a*]. The use of a usb bluetooth dongle is, as of may 2015, not straight forward on the myRIO as it lacks support in the kernel of the NI Linux Real-Time OS running on the myRIO [National Instruments, 2014*c*]. A USB bluetooth dongle has been purchased for the CS Saucer with this use in mind.

To reduce stress on the thrusters and motors in CS Saucer a low pass filter should be implemented on the control signals sent to the ESCs. This will prevent rapid switching between positive and negative thrust force, something that can occur in DP control systems and causes stress to the motors and thrusters.

19.2.3 Components Monitoring

The Real-Time battery monitoring currently implemented on CS Saucer only monitors on of the three cells in the LiPo battery that powers the system.

A future monitoring solution should monitor all three cells as unbalanced voltage in the cells of a LiPo battery can lead to battery failure and damage to the vessel and its components.

The Marine 30 ESC has integrated cooling ribs on either side. The ESCs can still overheat something that can lead to component failure and be costly in the long run. By fitting a temperature sensor to the ESCs, a solution can be implemented where the system will shut down in the event of one of the ESCs overheating.

19.3 Course Stability

The vessel will need to be course stable in order to successfully implement path following control. Discussion and suggestions for further work on this topic can be found in Chapter 15.1.2.

19.4 HIL Testing

The embedded controller has been prepared for HIL simulation as explained in Chapter 17. A model for simulation has been proposed in Chapter 13. In order to run tests with HIL simulations, this model or some other model must be implemented on the myRIO embedded controller.

Bibliography

Bjørneset, S. [2014], Modelling and control of thruster assisted position mooring system for a rig, Master's thesis, NTNU.
URL: *https://daim.idi.ntnu.no/masteroppgaver/011/11351/masteroppgave.pdf*

Breivik, M., Hovstein, V. E. and Fossen, T. I. [2008], 'Straight-line target tracking for unmanned surface vehicles', *Modeling, Identification and Control* **29**(4), 131–149.

Det Norske Veritas AS, D. [2011], 'Standard for certification: Hardware in the loop testing (HIL)'. Viewed 2015-06-16.
URL: *https://exchange.dnv.com/publishing/stdcert/2011-07/Standard2-24.pdf*

Dong, N. T. [2005], Design of Hybrid Marine Control Systems for Dynamic Positioning, PhD thesis.
URL: *http://www.marin.ntnu.no/ãssor/PhD%20Thesis/Thesis_Dong.pdf*

Fossen, T. I. [2011], *Handbook of marine craft hydrodynamics and motion control*, John Wiley & Sons.

Himbeerkuchen [2007], 'File:bollard pull idealized.jpg'.
URL: *http://commons.wikimedia.org/wiki/File:Bollard_pull_idealized.jpg*

Idland, T. K. [2014], Autopilot control design for a fully-actuated offshore vessel, Technical report, NTNU.

Idland, T. K. [2015], 'Marine cybernetics vessel CS Saucer: Design, construction and control'. Visited: 2015-06-17.
URL: *https://vimeo.com/130998926*

Lewandowski, E. M. [2004], 'The dynamics of marine craft', *Training* **2015**, 08–17.

National Instruments, N. [2008], 'PID control toolkit user manual'. Viewed 2015-06-06.
URL: *http://home.hit.no/ hansha/training/labview/controlandsimulation/documents/PID%20Control%20in%20LabVIEW.pdf*

National Instruments, N. [2011*a*], 'Creating custom controls, indicators, and type definitions'. Viewed 2015-06-15.
URL: *http://zone.ni.com/reference/en-XX/help/371361H-01/lvconcepts/custom_cont_ind_type/*

National Instruments, N. [2011*b*], 'Write to text file function'. Visited: 2015-06-17.
URL: *http://zone.ni.com/reference/en-XX/help/371361H-01/glang/write_characters_to_file/*

National Instruments, N. [2014*a*], 'Getting started with data dashboard for labview'. Viewed 2015-05-31.
URL: *http://www.ni.com/tutorial/13757/en/*

National Instruments, N. [2014*b*], 'Stopping parallel while loops in LabVIEW with one stop button'. Viewed 2015-05-31.
URL: *http://digital.ni.com/public.nsf/allkb/267704CDE91156D186256F6D00711AAE*

National Instruments, N. [2014*c*], 'USB Devices tested on NI Linux RT (myRIO/cRIO-9068)'. Viewed 2015-06-13.
URL: *https://decibel.ni.com/content/docs/DOC-37389*

National Instruments, N. [2015*a*], 'Labview control design and simulation module'. Viewed 2015-06-13.
URL: *http://www.ni.com/labview/cd-sim/*

National Instruments, N. [2015*b*], 'Tutorial: SubVIs'. Viewed 2015-06-09.
URL: *http://www.ni.com/white-paper/7593/en/*

NTNU [2015], 'Handbook of marine HIL simulation and marine cybernetics laboratories'. Viewed 2015-06-16.
URL: *http://www.ntnu.no/imt/lab/cybernetics*

Skåtun, H. [2011], Development of a DP system for CS Enterprise I with Voith Schneider thrusters, Master's thesis, Norwegian University of Science and Technology, Norway.

Skjetne, R. [2003], 'Ship maneuvering: The past, the present and the future', *Sea Technology* **44**(3), 33–37.
URL: *https://www.researchgate.net/publication/237063048_Ship_Maneuvering_The_past_the_present_*

Skjetne, R., Smogeli, Ø. and Fossen, T. I. [2004], Modeling, identification, and adaptive maneuvering of cybership II: A complete design with experiments, *in* 'Proc. IFAC Conf. on Control Applications in Marine Systems', pp. 203–208.

Valle, E. [2015], Marine telepresence system, Master's thesis, NTNU.

Wee, A. [2012], 'Omnidirectional marine vehicle with Voith-Schneider propellers'. Viewed 2015-06-12.
URL: *https://www.youtube.com/watch?v=60_WNS5POw*

Appendix A

Component Data Sheets

A.1 Mtroniks toi Marine 30 ESC

INSTRUCTION SHEET AND WARRANTY

PLEASE READ & FULLY UNDERSTAND THE INSTRUCTIONS & WARRANTY BEFORE USE

INSTALLING YOUR ESC

Positioning of your ESC in the model

Mount the ESC as far away as possible from the receiver, using double sided tape or velcro.
Keep the thick power wires away from the antenna and other thin wires to avoid interference problems *(See Fig.1 for example install)*.
The antenna should come straight out of the receiver into the antenna tube and up out of the model. Do not attempt to use any part of the model as an antenna!
The ESC should be positioned to allow cooling air to pass over the heatsink, this reduces the risk of over-temperature shutdown.
Make sure your motor is fitted with two (2) motor capacitors (0.1uF) - one from the negative terminal to the can and one from the positive terminal to the can.

Wiring up of your ESC in model *(See Fig.1)*

The ESCs are supplied with Tamiya style plug and bullet connectors at the factory.
Colour coding for the wires is as follows:
Black=Batt -ve, Red=Batt +ve, Blue=Mot -ve, Yellow=Mot +ve

ALWAYS DISCONNECT FROM THE BATTERY PACK WHEN NOT SUPERVISED!

Receiver Lead Connections

The receiver lead on the ESC is the JR type, see chart below. For some receivers you may need to swap the red and brown wires in the plug.

	SIGNAL	+VE	-VE
RECEIVER TYPE	POSITION 1	POSITION 2	POSITION 3
FUTABA, SANWA, KO	White/Blue	Red	Black
HI-TEC	Yellow	Red	Black
JR, GRAUPNER, KYOSHO	White/Orange	Red	Brown
ACOMS	Yellow	Red	Black
AIRTRONICS	White/Orange	Black	Red

CAUTION! If using an external receiver battery, you must remove the red wire from the ESC's receiver lead first. If using more than one ESC in your model with an external receiver battery you must disconnect the red wire from ALL ESC's. If using more than one ESC in your model without an external receiver battery ensure that only one of the ESC's has the red wire connected.

All ESCs are fitted with 1.5A BEC unless otherwise stated.

SET-UP

Before beginning set-up you need to connect up your ESC as in Fig.1.(When plugging the ESC's receiver lead into the receiver make sure that the signal wire - orange - is facing inwards).

Calibrating the ESC to your transmitter

1. Switch on your transmitter ensuring the throttle control and throttle trim are in the neutral position.
NOTE: If you have removed the factory fitted battery connector, (see warranty) ensure polarity is correct.
2. Plug your ESC into your battery pack and turn the ESC on with the on/off switch. The red, green and blue *LED's* will flash for 2 seconds *(This is the set-up window, if you press the button once whilst the LED's are flashing you enter set-up, if you let the LED's flash for 2 seconds then stop, the ESC will operate with previously set values)*
3. With the LED's flashing, press the set button once, this will set your neutral position, the green LED will light.
4. Push the throttle control to the full forward position, then return to the neutral position, *(This has set maximum forward speed point, the red LED will light)*.
5. With the red LED lit, pull the throttle control to the full reverse position, then return to the neutral position. *(This has set the maximum reverse point)*. The ESC will light the LEDs to show it is in the neutral position.
The ESC is now ready to use.

Calibration is complete and the ESC will power the motor!

Failsafe mode

In failsafe mode the controller returns to the neutral position, this is shown by the Red LED flashing.
Failsafe mode is activated if there is a loss of signal due to being out of range or not receiving a correct receiver signal.

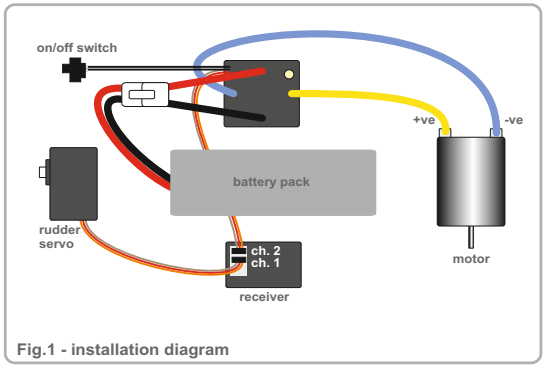

Fig.1 - installation diagram

Battery type selection

The ESC is NiCAD/NIMH and Lipo compatible.
To switch between **auto NiCAD/NIMH** cut off and **auto Lipo cutoff** you must press and hold the set button **before** switching the ESC on. With the set button pressed, switch on the ESC using the on/off switch, the LED's will cycle between blue and green, to use NiCAD/NIMH cells release the set button when the green LED is lit, to use Lipo cells release the set button when the blue LED is lit. The ESC will flash all 3 LED's then return to the neutral position. The Blue LED will be on solid all the time whilst being used in auto Lipo mode.

Reverse mode selection

The Marine ESC has 2 reverse modes, 'on' and 'off'. On mode gives full brakes until the motor has stopped then engages reverse. Off mode removes the reverse function completely allowing the ESC to operate as a forwards and brake only ESC.
To switch between '**on mode**' and '**off mode**', at any time when the ESC is in the neutral position, press and hold the set button. The red LED will cycle between on and off, to use the ESC in reversing mode, release the set button when the red LED is off. To use the ESC in brake only mode, release the set button when the red LED is lit. The ESC is ready to use.

What do the LED's mean?

Blue & Green LED's cycling - Battery type selection window.
Red LED cycling - Reverse mode selection window.
Red & Green & Blue LED's flashing for 2 seconds - Calibration window.
Red LED flashing - Failsafe mode.

Red & Green LED's on solid - Neutral position in NiCAD/NiMH mode.
Green LED lit solid - Full forwards position in NiCAD/NiMH mode.
Red LED lit solid - Full brake/Reverse position in NiCAD/NiMH mode.

Red, Green & Blue LED's on solid - Neutral position in Lipo mode.
Green & Blue LED's lit solid - Full forwards position in Lipo mode.
Red & Blue LED's lit solid - Full brake/Reverse position in Lipo mode.

A.2 Graupner DS8311 Servo

Product Sections

- **Whats New!**
- **Radio Control Model Boat Kits**
  - Aerokits
  - Aeronaut
  - Aquacraft
  - Billing Boats Suitable for RC
  - Caldercraft Scale Model Boats
  - Dragon RC Boats
  - Dumas
  - Dumas Chris-Craft
  - Graupner RC Boats
  - Graupner Premium Line
  - Joysway
  - Krick Kits Suitable for Electric Power
  - Krick Steam Launches
  - Mantua & Panart Suitable for RC
  - New Maquettes
  - Osborn Model Kits
  - Precedent Model Boats
  - Pro Boat
  - Racing Boats
  - Robbe RC Boats
  - Sailing Yachts
  - Tamiya
  - Thunder Tiger
  - Walterstons
- **Static Display Model Boat Kits**
  - Aeronaut Static Display Kits
  - Amati America's Cup Yachts
  - Amati Static Display Kits
  - Amati Specialist Kits (Non-Boat)
  - Artesania Latina Kits
  - Artesania Specialist Kits (Non Boat)
  - Billing Boats Static Display Kits
  - Caldercraft Heritage Series
  - Caldercraft Nelsons Navy
  - Constructo Kits
  - Corel Static Display Kits
  - Dumas Static Display Kits
  - Euromodel Como Static Display Kits
  - Krick Static Display Kits
  - Mamoli Static Display Kits
  - Mamoli "Mini Mamoli"
  - Mantua Static Display Kits
  - Mantua RMS Titanic
  - Mantua "Silhouette Line"
  - Mantua Specialist Kits (Non-Boat)
  - Matchstick Kits
  - Modellers Shipyard
  - Model Shipways Static Kits
  - Model Expo Specialist Kits (Non-Boat)
  - Occre Static Display Kits
  - Occre Specialist Kits (Non Boat)
  - Osborn Model Kits
  - Panart Static Display Kits
  - Panart Amerigo Vespucci Multi Part Kit
  - Sergal Static Display Kits
  - Soclaine (MGS)
  - Tasma
  - Victory Models

Graupner DS8311 Hi Performance BB MG Servo (G5164)

Cornwall Model Boats | Radio Control Equipment | Servos | Graupner Servos | Graupner DS8311 Hi Performance BB MG Servo

Graupner DS8311 Hi Performance BB MG Servo

Double ballbearing supported hi-performance proportional servo with 5.5 mm wide drive gearwheels and featuring a powerful cobalt-samarium electric motor.
Though of diminutive size the servo comes up to the highest requirements as regards torque, power, resolution and operational reliability. Designed mainly for large models and other applications requiring maximum operating power. A long-life special potentiometer with sextuple wiper guarantees optimum resolution.

Specification
Torque at 4.8 V approx. 9.8 kg/cm
Torque at 6.0 V approx. 11.2 kg/cm
Holding moment at 4.8 V (Ncm) approx. 180
Holding moment at 6.0 V (Ncm) approx. 212
Transit speed at 4.8 V (sec. / 40°) approx. 0.15
Transit speed at 6.0 V (sec. / 40°) approx. 0.12
Weight g approx. 59
Gearbox PG MG
Bearings 2 x BB
Dimensions (LxWxH) approx. 39 x 19 x 39,5 mm
Part No: G5164

Price: £100.00 (Including VAT at 20%)
Euros: €133.99 (Inc VAT) / US Dollars: US$120.83 (Tax Free)

Quantity: 1

ADD TO CART

Customers who bought this item also bought:

1. MFA Torpedo 800 Marine Electric Motor (Ref: M1114/1)
2. Graupner Schottel Drive Unit II (2335) (Ref: G2335)
3. Plain Coupling Insert 1/4 (Ref: C8018)
4. Plain Coupling Insert 5mm (Ref: C8008)

Cornwall Model Boats | Radio Control Equipment | Servos | Graupner Servos | Graupner DS8311 Hi Performance BB MG Servo

<< Previous **Recently Viewed** Next >>

A.3 Graupner Schottel drive unit II

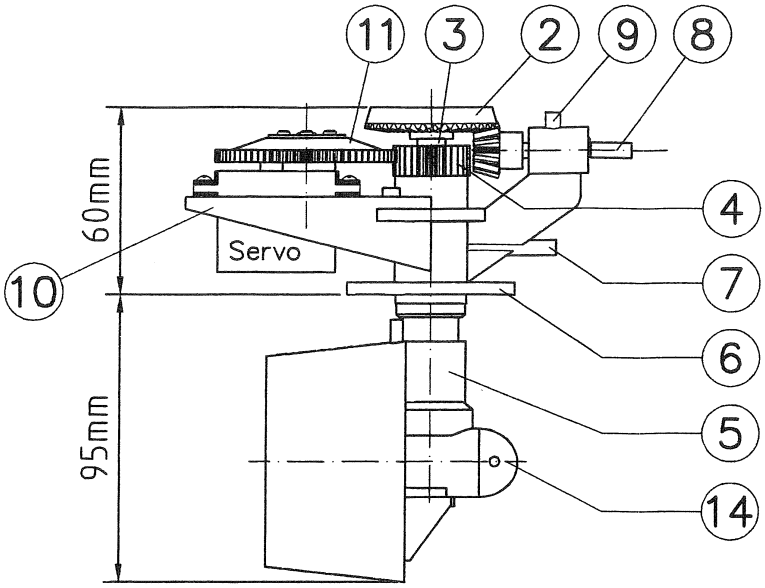

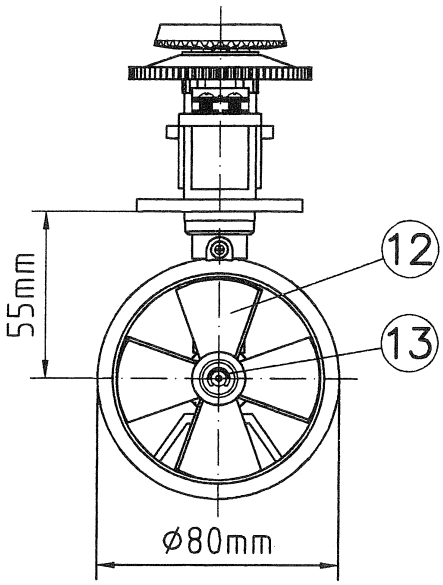

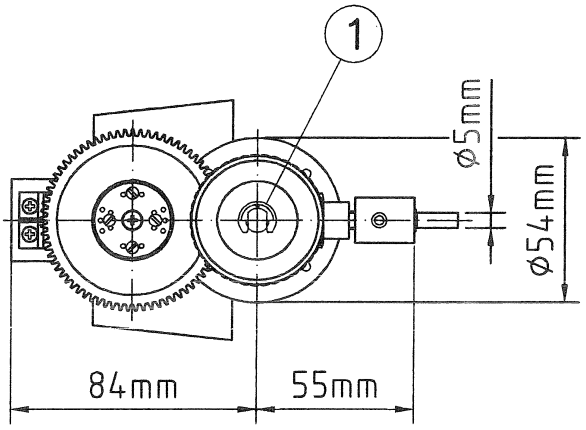

Gewicht ca. 215g

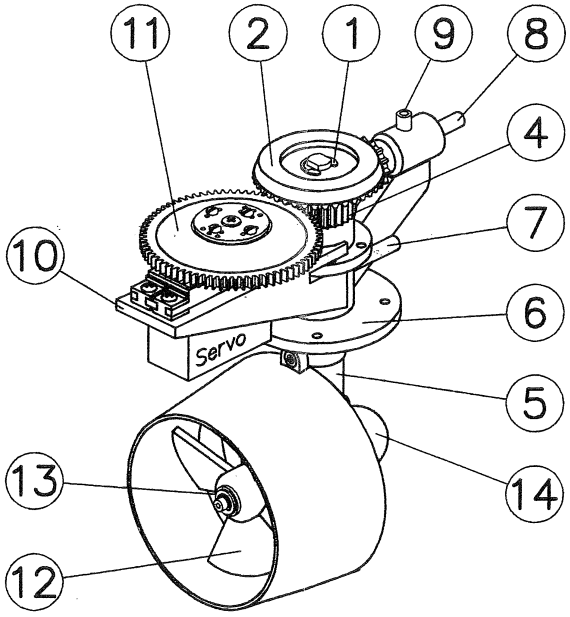

Graupner

Order No. 2335

Operating instructions for the Schottel drive unit II

Introduction:

The Schottel drive unit is a modern, powerful means of propulsion designed for working ships which require outstanding manoeuvrability as a basic characteristic.

The propeller is mounted in a power-enhancing Kort nozzle which can be swivelled to either side. The water flow from the propeller can therefore be directed accurately to steer the vessel, and a separate rudder is not required.

Used in conjunction with a powerful electric motor the Schottel drive unit II represents a potent system capable of powering quite large and heavy models. It is of extremely strong all-plastic construction. A special integral mount is provided to take a high-power servo for direct steering control. The swivel movement of the propeller is geared up 2:1 to increase its angular range, and maximum travel is about 180° depending on servo.

The swivel movement has no mechanical stops. Reverse running is possible by reversing the direction of rotation of the electric motor (requires a speed controller with reverse).

Safety notes:

- Never run the system out of water for longer than 1 minute.
- The power system should be run-in in water before being operated at full power.
- The power system must be installed in the boat's hull carefully in order to achieve a 100% watertight installation. Check this before you run the boat in the open (use a bath half-full of water).
- Be sure to disconnect the electric motor from the power supply before carrying out any work on the propulsion system.
- Never attempt to stop or slow the rotating propeller with your hand or fingers. Do not obstruct the propeller with any object.
- Do not forcibly swivel the Schottel drive unit by hand, as this could cause mechanical damage to the steering servo.
- Protect the system from shocks and other mechanical loads.
- Do not apply abrupt steering movements when the motor is at full power.

This propulsion system is designed for use by advanced modellers only, as it calls for experience and specialist knowledge in marine modelling. The power system is not a toy, and should not be used or handled by young persons under 16 years except under adult supervision.

Assembly and installation :

To install or remove the drive system is must first be partially dismantled. This is the procedure: remove the circlip (1) and lift out the top bevel gear (2). Remove the transverse pin. Using a flat broad-bladed screwdriver carefully lever out the sintered bush (3). The steering pinion (4) can now be removed by pulling the lower drive section (5) against the mounting flange (6). Reverse this procedure to re-assemble the unit. Take care not to damage the plastic parts.

Before re-assembling the components pack the grooves in the drive shaft with water-resistant grease. When the system is assembled you can top up the grease via the grease nipple (7). The twin-ballraced drive shaft (8) should also be greased, this time via the integral grease nipple (9). Otherwise the drive system is maintenance-free. The gears and sintered bushes require no lubrication.

The Schottel drive unit should be installed in the hull plano-parallel with the waterline, and the hull must be reinforced in the area of the drive unit (e.g. extra bulkheads) in order to absorb the considerable loads which arise at that point without suffering damage or distortion. Attach the flange (6) using the M3 countersunk screws supplied. To seal the joints we recommend silicone sealant (bathroom suppliers) or Marabu Fixogum, which is a releasable adhesive used in drawing offices. Apply the sealant to the whole of the flange and all round the screws before fitting them.

Fit the rubber grommets and metal sleeves in the steering servo and screw it in the servo mount (10).The servo mount can be attached to the shaft in any of five different positions to suit your installation.

Fix the 25 mm Ø servo output disc (supplied) to the steering gear (11) using four self-tapping screws. You will need to shorten the self-tapping screws by 1 mm using side-cutters.

The propeller (12) can be withdrawn from the shaft after removing the circlip (13).

If two power systems are to be installed in a model, remove the factory-fitted right-hand rotation propeller from one unit and replace it with the left-hand propeller also supplied.

Operating notes:

The power unit is designed for input speeds of up to 8000 rpm; higher rotational speeds will result in damage. The unit must only be run in water. If you have to operate the system "dry", do not run the motor for longer than 1 minute.

The power system may be rather stiff when brand-new. After a running-in period of about 15 - 20 minutes in water the unit should rotate freely, and it is then fully operational. If not it is possible to loosen the bottom shaft bearing in the bearing cap (14). To do this push metal pins into the lateral holes as far as they will go, and carefully open the bearing cap (14) by about 1/4-turn.

All steering commands should be smooth and gentle; under no circumstances apply sudden steering movements at full motor power. The load on the recommended C 4821 servo is considerable in this application, and for this reason we strongly recommend the use of a high-capacity 4-cell NC battery of at least 1.4 Ah. Alternatively you may prefer to provide a second, separate 4-cell NC pack for the steering servo in conjunction with an external adaptor (Order No. 3053), so that the servos's power supply is independent of the receiver. This arrangement also provides the maximum safety level.

Accessories:

Order No.	Description
6373	SPEED 900 BB Torque 12 V
3896	C 4821 steering servo
346	Shaft coupling
570	High-performance lubricating grease
Specialist supplier	Silicone sealant or Marabu Fixogum mounting adhesive (drawing office suppliers)

A.4 DC/DC Converter

Features

- Efficiency up to 95%,Non isolated, no need for heatsinks
- Pin-out compatible with LM78XX Linears
- Low profile(L*W*H=11.5*8.5*17.5mm)
- Wide input range.(4.75V ~ 18V)
- Short circuit protection, Thermal shutdown
- Non standard outputs available as specials between 1.5V ~ 6.5V
- Low ripple and noise
- "L" Version with 90° pins

INNOLINE
DC/DC-Converter

R-78Bxx-1.5(L) Series

1.5 AMP
SIP3
Single Output

Selection Guide

Part Number* SIP3	Input Range (V)	Output Voltage (V)	Output Current (A)	Efficiency Min. Vin (%)	Efficiency Max. Vin (%)
R-78B1.5-1.5	4.75 – 18	1.5	1.5	83	78
R-78B1.8-1.5	4.75 – 18	1.8	1.5	85	81
R-78B2.5-1.5	4.75 – 18	2.5	1.5	88	84
R-78B3.3-1.5	4.75 – 18	3.3	1.5	91	88
R-78B5.0-1.5	6.5 – 18	5.0	1.5	94	92
R-78B6.5-1.5	8.0 – 18	6.5	1.5	95	93

* add Suffix "L" for 90° bent pins, e.g. R-78B5.0-1.5L

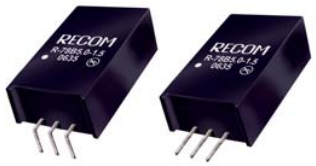

RECOM
INTERNATIONAL POWER

Description

The R-78Bxx-1.5 Series high efficiency switching regulators are ideally suited to replace 78xx linear regulators and are pin compatible. The efficiency of up to 95% means that very little energy is wasted as heat so there is no need for any heat sinks with their additional space and mounting costs. The L-Version with 90° pins allows direct replacement for laid-flat regulators where component height is at a premium.Low ripple and noise figures and a short circuit input current of typically only 10mA round off the specifications of this versatile converter series.

Derating-Graph
(Ambient Temperature)

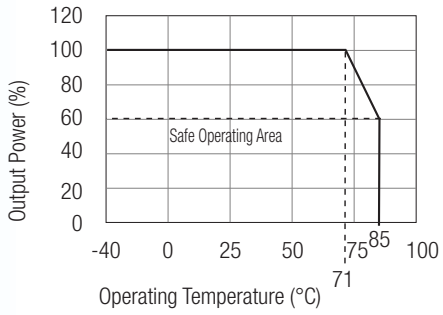

R-78Bxx-1.5 (L) Series

Specifications (refer to the standard application circuit, Ta: 25°C, minimum load = 10%)

Characteristics	Conditions	Min.	Typ.	Max.
Input Voltage Range	All Series, see Selection Guide	4.75		18.0V
Output Voltage Range (for customized parts)	All Series	1.5		6.5V
Output Current (see Note 1)	All Series	0		1500mA
Output Current Limit	All Series			5000mA
Short Circuit Input Current	All Series		60	80mA
Internal Power Dissipation				0.65W
Short Circuit Protection				Continuous, automatic recovery
Output Voltage Accuracy (At 100% Load)	All Series		±2	±3%
Line Voltage Reguölation (Vin = min. to max. at full load)	All Series		0.2	0.4%
Load Regulation (10% to 100% full load)	All Series		20	25mV
Dynamic Load Stability (with Output Capacitor=100µF)	100% <-> 50% load		±80	±120mV
	Transient Recovery Time		1.0	1.5ms
Ripple & Noise (10% to 100% full load)	All Series		15	30mVp-p
Temperature Coefficient	-40°C ~ +85°C ambient			0.015%/°C
Max capacitance Load				1000µF
Switching Frequency		300	340	380kHz
Quiescent Current	Vin = min. to max. at 0% load		7	9mA
Input Reflected Ripple Current	All Series		150	200mAp-p
Operating Temperature Range		-40°C		+85°C
Operating Case Temperature				+100°C
Storage Temperature Range		-55°C		+125°C
Case Thermal Impendance				60°C / W
Thermal Shutdown	Internal IC junction		+160°C	
Relative Humidity				95% RH
Case Material			Epoxy with Non-Conductive Plastic Case(UL94V-0)	
Package Weight				4g
MTBF (+25°C) *Detailed Information see Application Notes chapter "MTBF"*	using MIL-HDBK 217F			3250 x 10³ hours
. (+71°C)	using MIL-HDBK 217F			1059 x 10³ hours

Note 1: The converter requires a minimum load of 6mA to start up properly. Once started, the load can be reduced to 0%

Standard Application Circuit

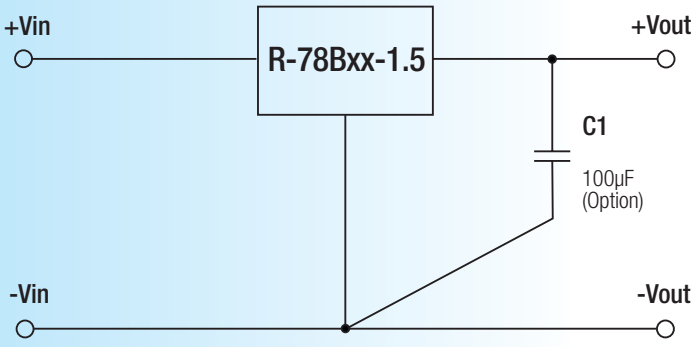

Add a blocking diode to Vout if current can flow backwards into the output, as this can damage the converter.

R-78Bxx-1.5 (L) Series

Characteristics

Efficiency

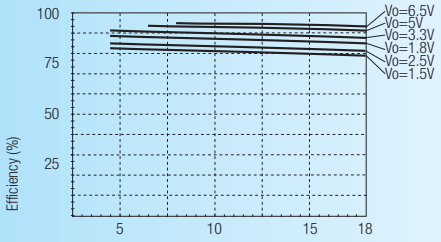

Efficiency Vs Vin (Full Load)

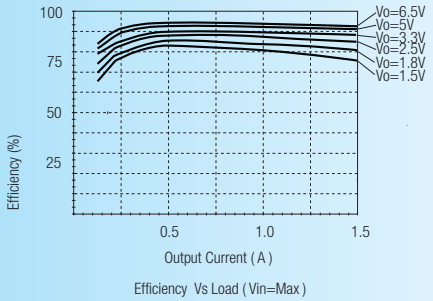

Efficiency Vs Load (Vin=Max)

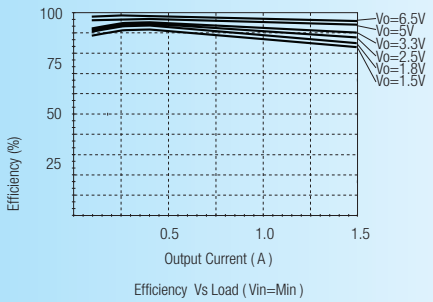

Efficiency Vs Load (Vin=Min)

Ripple

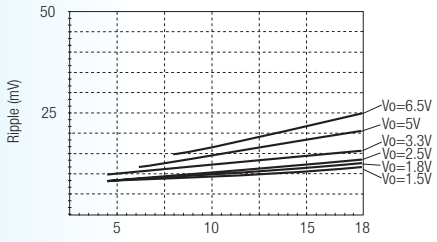

Ripple Vs Vin (Full Load)

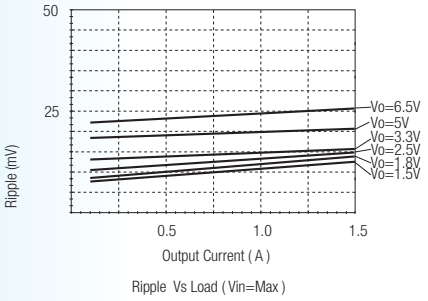

Ripple Vs Load (Vin=Max)

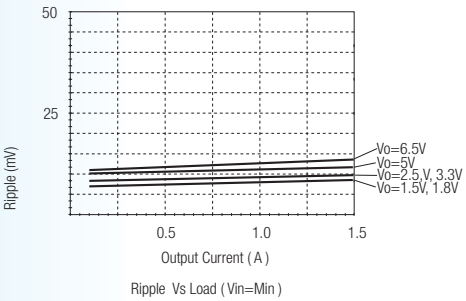

Ripple Vs Load (Vin=Min)

R-78Bxx-1.5 (L) Series

Application Examples

High efficiency multiple output

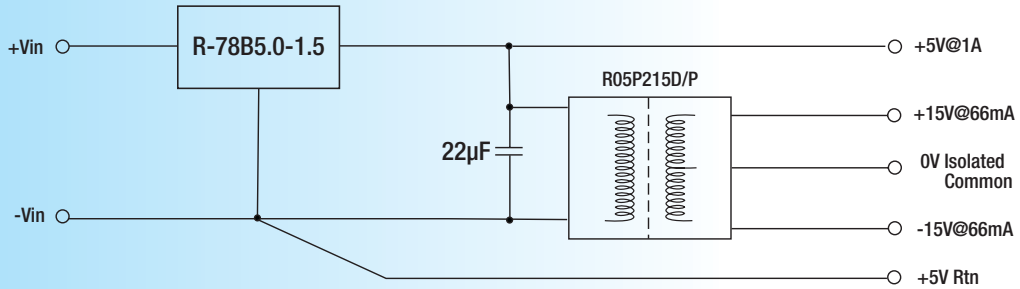

- Wide input range suits both 12V and 7.2V battery packs
- 5.2kV isolated short circuit protected outputs for analogue circuits, e.g. medical grade interface
- High efficiency +5V/1A protected output for digital circuits
- Further decoupling filtering may be necessary between the converters

Isolated, wide Input range, Distributed Power Architecture (Point of Load)

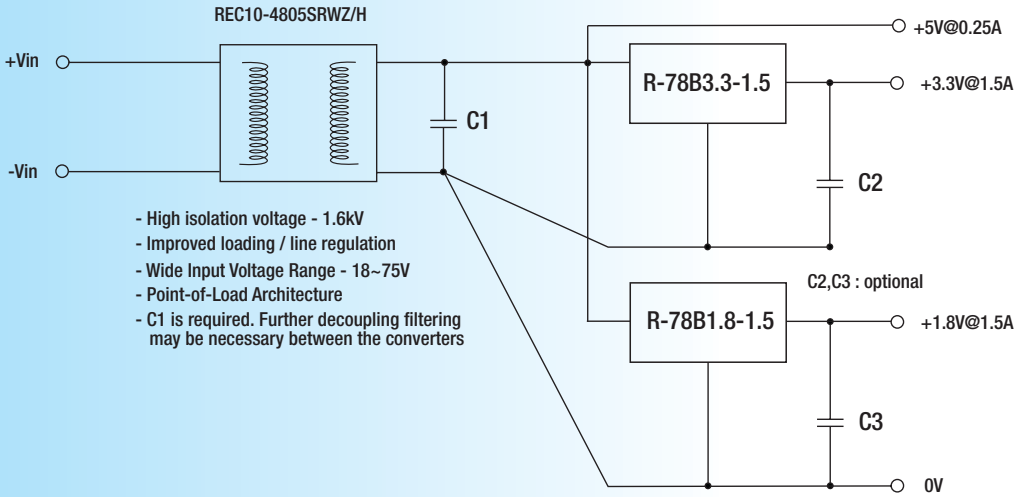

- High isolation voltage - 1.6kV
- Improved loading / line regulation
- Wide Input Voltage Range - 18~75V
- Point-of-Load Architecture
- C1 is required. Further decoupling filtering may be necessary between the converters

Package Style and Pinning (mm)

SIP3 PIN Package

3rd angle projection

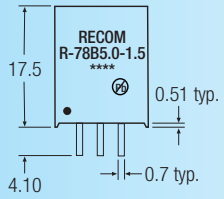

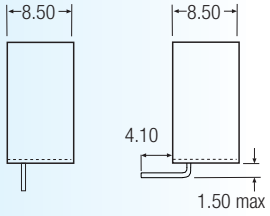

L - Version

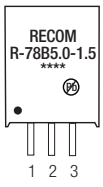

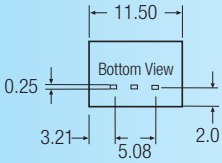

Recommended Footprint Details

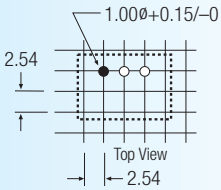

Pin Connections	
Pin #	
1	+Vin
2	GND
3	+Vout

xx.x ±0.5mm
xx.xx ±0.25mm

A.5 Aluminum Electrolyte Capacitor

PX SERIES

105℃ Standard

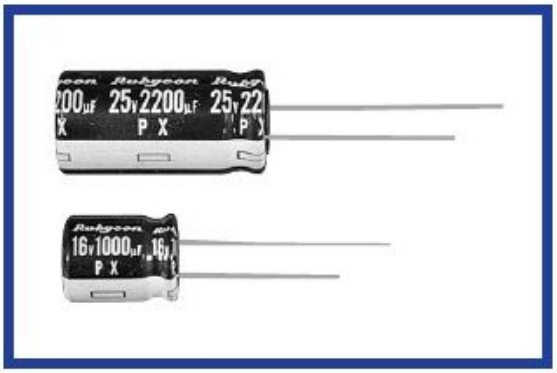

◆FEATURES

- RoHS compliance.

◆SPECIFICATIONS

Items	Characteristics		
Category Temperature Range	−55~+105℃	−40~+105℃	−25~+105℃
Rated Voltage Range	6.3~100V.DC	160~400V.DC	450V.DC
Capacitance Tolerance	±20%(20℃, 120Hz)		
Leakage Current(MAX)	6.3~100V.DC	160~450V.DC	
		CV≦1000	CV>1000
	I=0.01 CV or 3μA whichever is greater. (After 2 minutes application of rated voltage)	I=0.1CV+40μA (1minute) I=0.03CV+15μA (5minutes)	I=0.04CV+100μA (1minute) I=0.02CV+25μA (5minutes)
	I=(μA) Leakage Current C=(μF) Rated Capacitance V=(V) Rated Voltage		

(tanδ) Dissipation Factor(MAX) (20℃, 120Hz)

Rated Voltage	6.3	10	16	25	35	50	63	100	160	200	250	350	400	450
tanδ	0.28	0.24	0.20	0.16	0.14	0.12	0.10	0.08	0.20	0.20	0.20	0.25	0.25	0.25

When rated capacitance is over 1000μF, tanδ shall be added 0.02 to the listed value with increase of every 1000μF.

Endurance

After life test with rated ripple current at conditions stated in the table below, the capacitors shall meet the following requirements.

Capacitance Change	Within ±25% of the initial value.
Dissipation Factor	Not more than 200% of the specified value.
Leakage Current	Not more than the specified value.

Case Size	(hrs) Life Time
φD≦8	1000
φD≧10	2000

Low Temperature Stability Impedance Ratio(MAX) (120Hz)

Rated Voltage	6.3	10	16	25	35	50	63	100	160	200	250	350	400	450
Z(−25℃)/Z(20℃)	5	4	3	2	2	2	2	2	3	3	4	6	6	7
Z(−40℃)/Z(20℃)	10	8	6	4	3	3	3	3	4	4	8	8	10	–

◆MULTIPLIER FOR RIPPLE CURRENT

Frequency Coefficient

(Hz) Frequency		60(50)	120	500	1k	10k≦
Coefficient	0.47~1μF	0.50	1.00	1.20	1.30	1.50
	2.2~4.7μF	0.65	1.00	1.20	1.30	1.50
	10~47μF	0.80	1.00	1.20	1.30	1.50
	100~1000μF	0.80	1.00	1.10	1.15	1.20
	2200~33000μF	0.80	1.00	1.05	1.10	1.15

◆OPTION

	Code
PET Sleeve	EFC

◆DIMENSIONS (mm)

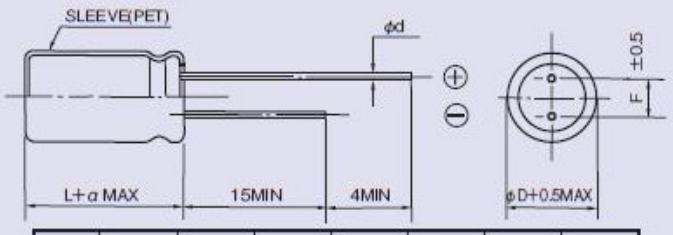

φD	5	6.3	8	10	12.5	16	18
φd	0.5		0.6			0.8	
F	2.0	2.5	3.5	5.0		7.5	
α	100V以下 WV≦100:1.5 160V以上 WV≧160:2.0					2.0	

◆PART NUMBER

□□□ Rated Voltage | PX Series | □□□□□ Rated Capacitance | M Capacitance Tolerance | □□□ Option | □□ Lead Forming | D×L Case Size

Rubycon

MINIATURE ALUMINUM ELECTROLYTIC CAPACITORS PX

◆STANDARD SIZE

Size φD×L(mm), Ripple Current (mA r.m.s./105℃, 120Hz)

WV (V.DC) / Cap(μF)	6.3 (0J)		10 (1A)		16 (1C)		25 (1E)		35 (1V)		50 (1H)		63 (1J)	
	Size	Ripple	Size	Ripple	Size	Ripple	Size	Ripple	Size	Ripple	Size	Ripple	Size	Ripple
0.47											5×11	7		
1											5×11	13		
2.2											5×11	20		
3.3											5×11	25		
4.7											5×11	32		
10											5×11	47	5×11	48
22									5×11	64	5×11	70	5×11	80
33							5×11	69	5×11	77	5×11	94	6.3×11	100
47					5×11	80	5×11	84	5×11	100	6.3×11	115	6.3×11	140
100	5×11	96	5×11	105	5×11	130	5×11	135	6.3×11	170	8×11.5	200	8×11.5	230
220	5×11	160	5×11	165	6.3×11	220	6.3×11	240	8×11.5	300	10×12.5	360	10×16	390
330	6.3×11	210	6.3×11	235	6.3×11	270	8×11.5	335	10×12.5	400	10×16	470	10×20	540
470	6.3×11	275	6.3×11	295	8×11.5	375	8×11.5	440	10×12.5	525	10×20	600	12.5×20	700
680	6.3×11	285	8×11.5	430	8×11.5	480	10×12.5	630	10×16	760	12.5×20	980	12.5×25	800
1000	8×11.5	460	8×11.5	500	10×12.5	640	10×16	740	10×20	865	12.5×25	1060	16×25	1200
2200	10×16	775	10×16	860	10×20	1050	12.5×20	1090	16×25	1370	16×31.5	1600	18×31.5	1400
3300	10×20	985	10×20	1100	12.5×20	1300	16×25	1500	16×25	1680	18×35.5	1780		
4700	12.5×20	1150	12.5×20	1350	12.5×25	1650	16×25	1800	16×35.5	1870				
6800	12.5×25	1480	16×25	1700	16×25	1900	16×35.5	1910	18×35.5	1920				
10000	16×25	1700	16×25	1950	16×31.5	1950	18×35.5	2050						
15000	16×31.5	2090	16×35.5	2090	18×35.5	2070								
22000	18×31.5	2280	18×35.5	2180										
33000	18×40	2350												

WV (V.DC) / Cap(μF)	100 (2A)		160 (2C)		200 (2D)		250 (2E)		350 (2V)		400 (2G)		450 (2W)	
	Size	Ripple	Size	Ripple	Size	Ripple	Size	Ripple	Size	Ripple	Size	Ripple	Size	Ripple
0.47	5×11	8					6.3×11	8	6.3×11	8				
1	5×11	15					6.3×11	16	6.3×11	16	6.3×11	16	6.3×11	15
2.2	5×11	21					6.3×11	30	6.3×11	25	8×11.5	31	8×11.5	20
3.3	5×11	30			6.3×11	36	6.3×11	30	8×11.5	30	8×11.5	34	10×12.5	33
4.7	5×11	35	6.3×11	43	6.3×11	40	8×11.5	45	8×11.5	45	10×12.5	42	10×12.5	35
10	5×11	60	8×11.5	77	8×11.5	57	10×12.5	90	10×16	95	10×16	64	10×20	37
22	6.3×11	98	10×12.5	92	10×16	105	10×16	105	12.5×20	175	12.5×20	140	12.5×25	100
33	8×11.5	140	10×16	125	10×20	140	10×20	140	12.5×25	220	16×25	170	16×25	125
47	8×11.5	185	10×20	150	10×20	195	12.5×20	190	16×25	260	16×25	200	16×31.5	155
100	10×16	290	12.5×25	320	16×25	340	16×25	310	18×31.5	370	18×35.5	310	18×40	200
220	12.5×20	560	16×31.5	410	16×35.5	580	18×35.5	485						
330	12.5×25	690	18×31.5	570	18×40	675								
470	16×25	880	18×40	855										
680	16×31.5	900												
1000	18×35.5	985												

Appendix B

Handbook for the CS Saucer

B.1 Required Software

Software
LabVIEW 2014
LabVIEW 2014 myRIO Toolkit
LabVIEW 2014 Real-Time Module
LabVIEW Control Design and Simulation Module

Table B.1: NI LabVIEW software required to run the project "CyberShip Saucer".

B.2 Deployment

When the power source is connected and the Wifi indicator lights up, the vessel is ready to deploy.

- Run the host application "mainHost.vi".
- Deploy the target application "main.vi".

The vessel is now operational.

B.3 NI Dashboard Manual Control

The CS Saucer can be controlled directly from an Android or a iOS device with the NI Dashboard app.

B.3.1 Manual Thruster Control

- Make sure that your device is connected to the local are network with a static ip adress.
- Create a new Dashboard with six slide controls, these will be the six control inputs u_0, u_1, u_2, α_0, α_1 and α_2.
- Configure the scale of the slide controls so that $u \in [-1, 1]$ and $\alpha \in [-114, 114]$
- Tap a control to connect it to its corresponding shared variable node on the myRIO. The ip adress for the myRIO-Saucer is: 192.168.0.99.
- The shared variable nodes for the manual thruster control are located in the library "libctrlMaualThruster". Be careful to only use the variables with the label "$_{\text{DSH}}$".
- Start the dashboard.

B.3.2 Manual Force Control

- Make sure that your device is connected to the local are network with a static ip adress.
- Create a new Dashboard with three slide controls, this will be the commanded force vector $\tau = [X, Y, N]^{\mathrm{T}}$.
- Configure the scale of the slide controls so that $X \in [-9, 9]$, $Y \in [-9, 9]$ and $N \in [-4, 4]$
- Tap a control to connect it to its corresponding shared variable node on the myRIO. The ip adress for the myRIO-Saucer is: 192.168.0.99.

- The shared variable nodes for the manual force control are located in the library "libctrlMaualForce". Be careful to only use the variables with the label "$_{\text{DSH}}$".
- Start the dashboard.

B.4 Data Logging

Continuous data logging has been implemented in the main target application. On initialization, a ".csv" file is created for each of the control modes. The log file for a control mode will only be populated when that particular control mode is active. Each log file is created with a control mode identifier and a time stamp, e.g. "dp114700". The log file format ".csv" (comma separated values) is highly compatible with MATLAB and enables easy import and post processing of the data in MATLAB. The import code in the script is easily created using MATLAB's import file wizard which generates code for file import for a specific file.

The log files on the myRIO are stored in the "files/tmp" folder which is a temporary folder that is cleared on reboot. Saving the log files in this directory ensures that the target does not use all of its storage memory to store old log files. A log file can be easily exported from the target by using the "Map network drive" feature in Windows. Simply map to the static ip of the target as shown in Figure B.1. Remember to check the "Connect using different credentials" box. When prompted for a password, type in "admin" as the user and leave the password blank as shown in Figure B.2. The "files/tmp" directory of the target is now available in the windows file explorer as seen in Figure B.3.

B.5 Charging the Traxxas LiPo Battery

Connect both the balancing plug and the main power plug to the charger before starting a charge. Then place the battery in the flame resistant bag. Ensure that the charger is set to LiPo mode before pressing start. The charging indicator will turn green when the battery is fully charged.

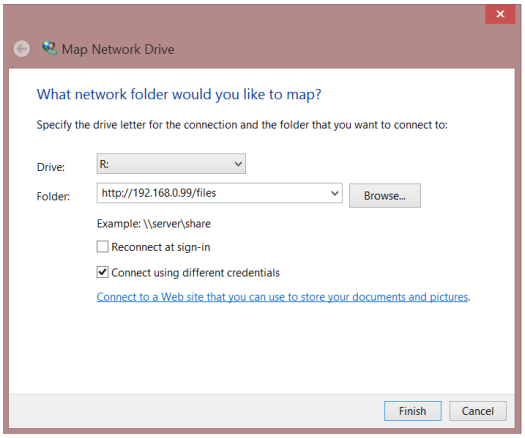

Figure B.1: Map network drive to the NI myRIO.

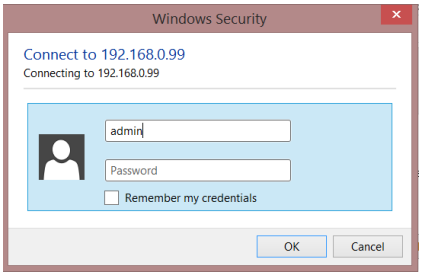

Figure B.2: Login credentials on the myRIO-Saucer. The password is blank.

Discharging the battery lower than 9V can destroy it or lead to reduced capacity and performance. It is therefore recommended that the battery should be charged when reaching a voltage of 11.1. The voltage of the battery can be measured with a voltmeter on the balancing plug. Using the ground wire in the balancing plug, the voltage of each of the cells can be measured from three remaining wires in the plug. If the LiPo battery is discharged below 9V it will not charge in LiPo mode. It is therefor wise to stay well above this limit. Should this happen, the battery can be charged in "NIMh" mode for maximum 10 seconds. This has proved to be effective for getting the voltage above 9V and able to charge in LiPo mode again. However it should be stressed that this measure be used with extremea caution and only as a last resort.

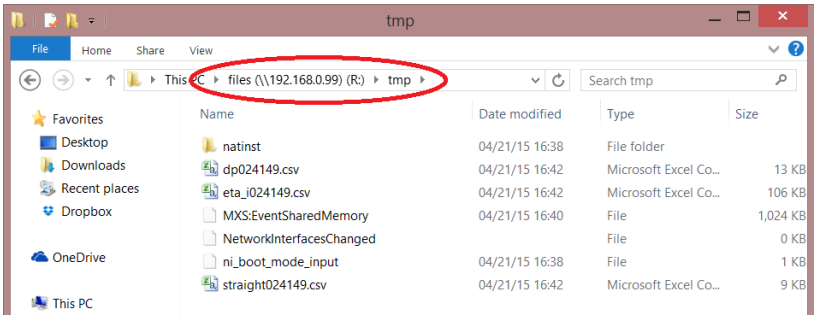

Figure B.3: The log files are saved in the tmp folder on the myRIO.

Appendix C

Digital Attachment

The digital attachment "delivery.zip" contains

- **CyberShip Saucer:** Folder with LabVIEW source code.
- **CS Saucer 3D-Model:** Folder with 3D model of the vessel.
- **Poster-TorKIdland.pdf:** Thesis poster.

Appendix D

3D Model Drawings

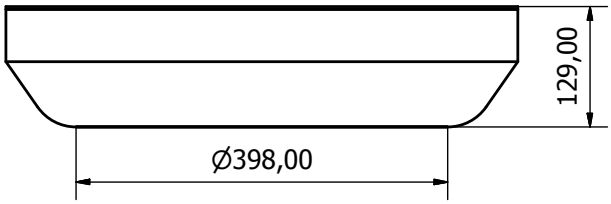

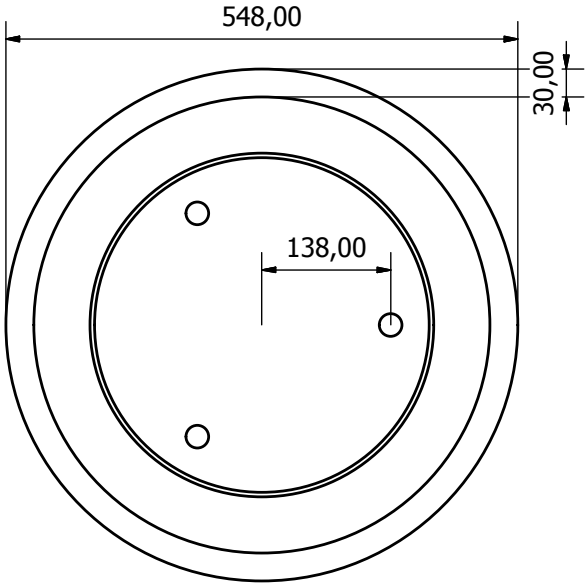

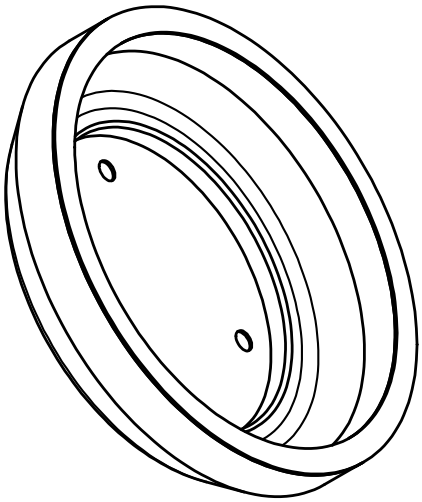

Designed by	Checked by	Approved by	Date	Date	
Jostein				24.02.2015	

saucerAssembly2	Edition	Sheet 1 / 4	

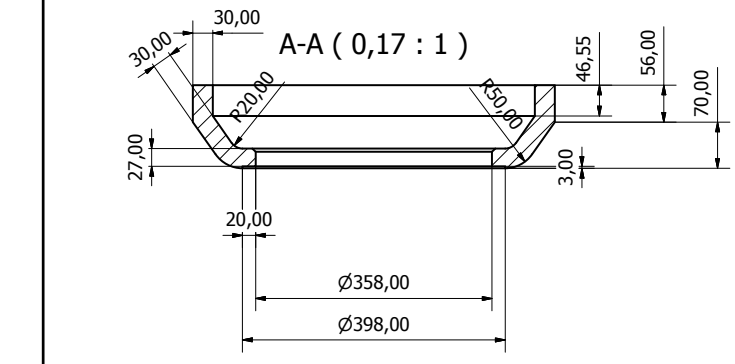

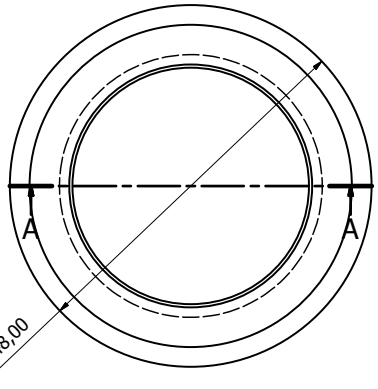

Designed by	Checked by	Approved by	Date	Date	
Jostein				24.02.2015	

	saucerAssembly2	Edition	Sheet
			2 / 4

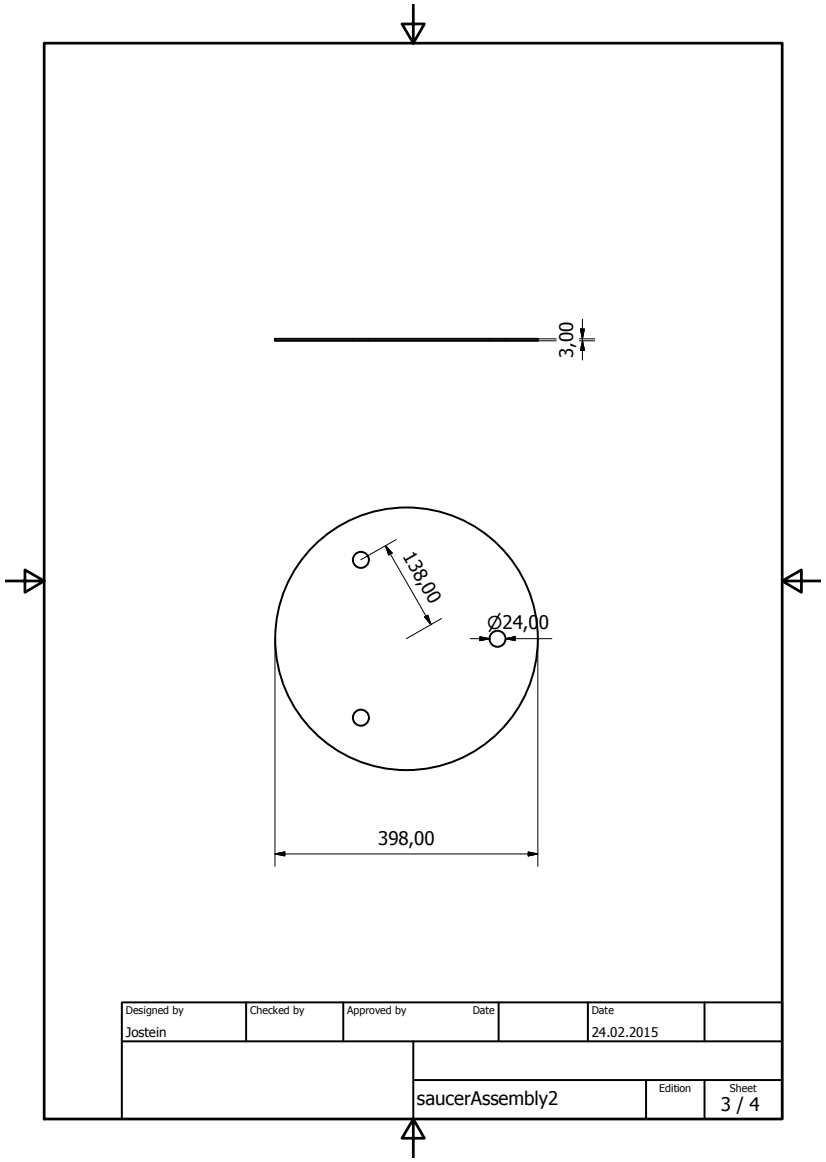

Designed by	Checked by	Approved by	Date	Date	
Jostein				24.02.2015	

saucerAssembly2	Edition	Sheet 3 / 4	

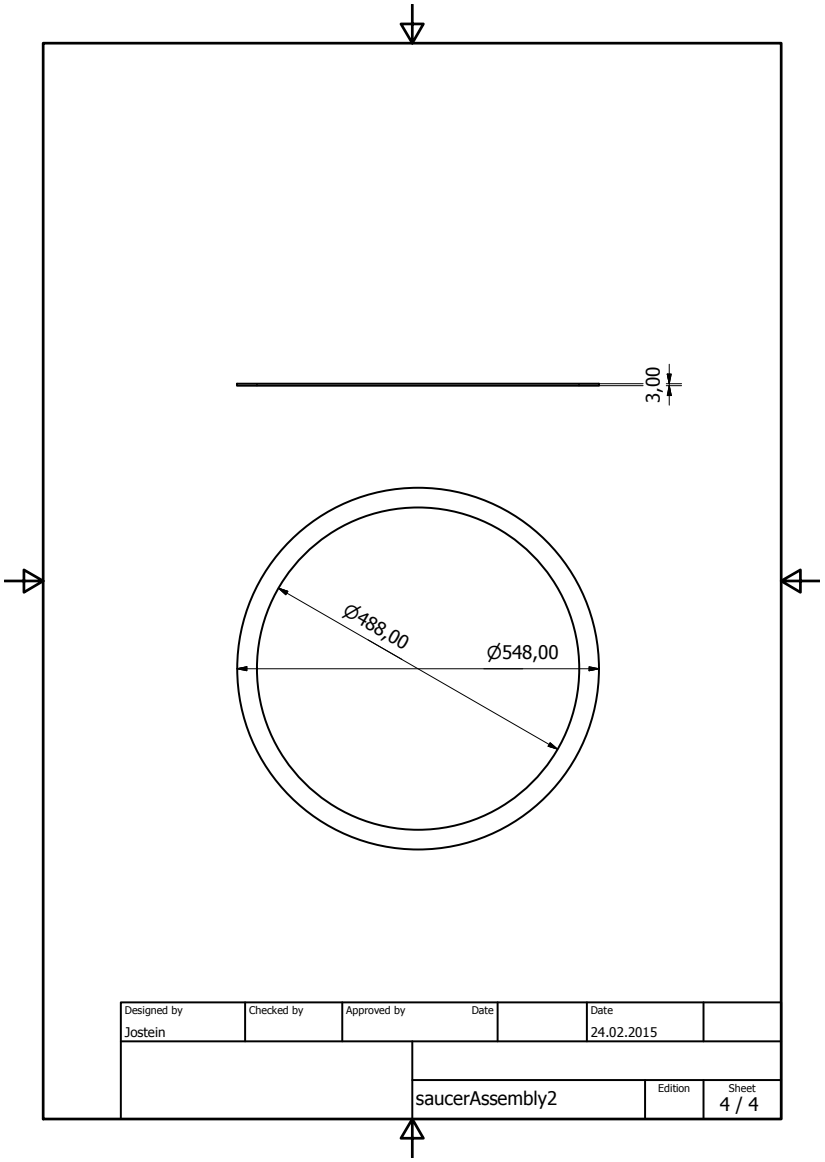

Designed by	Checked by	Approved by	Date	Date	
Jostein				24.02.2015	

saucerAssembly2	Edition	Sheet 4 / 4	